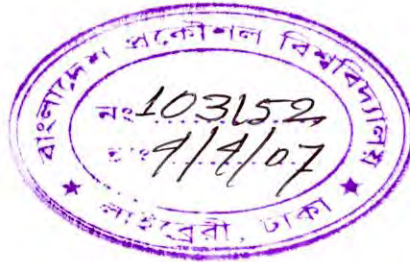


SOIL-STRUCTURE INTERACTION ANALYSES OF BURIED RIGID PIPES UNDER SURFACE LOAD



by

MD. AYNUL KABIR

A thesis submitted to the Department of Civil Engineering of Bangladesh University of Engineering & Technology, Dhaka in partial fulfillment of the requirement for the degree

of

MASTERS OF SCIENCE IN CIVIL ENGINEERING (GEOTECHNICAL)




November 2006

**BANGLADESH UNIVERSITY OF ENGINEERING AND TECHNOLOGY
DEPARTMENT OF CIVIL ENGINEERING**

The thesis titled “Soil-Structure Interaction Analyses of Buried Rigid Pipes under Surface Load” submitted by Md. Aynul Kabir, Roll No: 040404201, Session: April, 2004 has been accepted as satisfactory in partial fulfillment of the requirement for the degree of Master of Science in Civil Engineering (Geotechnical) on November 06, 2006.

BOARD OF EXAMINERS



Dr. Ashutosh Sutra Dhar
Associate Professor
Department of Civil Engineering
BUET, Dhaka.

Chairman
(Supervisor)



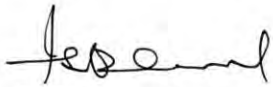
Dr. Md. Mazharul Hoque
Professor and Head
Department of Civil Engineering
BUET, Dhaka.

Member
(Ex- officio)



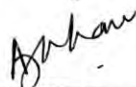
Dr. Abdul Muqtadir
Professor
Department of Civil Engineering
BUET, Dhaka.

Member



Dr. Ishtiaque Ahmed
Professor
Department of Civil Engineering
BUET, Dhaka.

Member



Dr. Ahsanul Jalil Khan
Geotechnical Consultant
Apt. B-2, House No. 45, Road No. 27,
Block A, Banani-1213.

Member
(External)

November 2006

TO
MY PARENTS

DECLARATION

I hereby certify that the research work reported in this thesis work has been performed by me and that this work has not been submitted elsewhere for any other purpose, except for publication.



(Md. Aynul Kabir)

November 2006

ACKNOWLEDGEMENT

The thesis was carried out under the supervision of Dr. Ashutosh Sutra Dhar, Associate Professor, Department of Civil Engineering, Bangladesh University of Engineering and Technology (BUET), Dhaka. I wish to express my deepest gratitude to him. In fact, it would have been impossible to complete the thesis without his continuous guidance, invaluable suggestions, affectionate encouragement as well as constant impetus at every stage of this thesis work. He, with his kindness and friendship, directed the research from its inception to the completion.

Special thanks should go to Dr. Munaz Ahmed Noor, Associate Professor, Department of Civil Engineering, BUET, for his encouragement and friendly cooperation. He was involved with Dr. Ashutosh Sutra Dhar and the author in a project funded by Committee for Advanced Studies and Research (CASR), BUET. Actually, that research originated the idea of necessities of this thesis work.

Above all, I acknowledge the blessings of almighty Allah, the most Beneficent, and the most Merciful, for enabling me to carry out such a valuable and important thesis on buried pipe design.

ABSTRACT

The effect of the surface live load on buried rigid pipe has been investigated based on soil-pipe interaction analysis. Two-dimensional and three-dimensional finite element analysis was performed to investigate the interaction between the pipe and soil under surface load.

For the finite element analysis, a mesh-sensitivity analysis was carried out to eliminate errors associated with the density of mesh as well as extent of the boundary taken into consideration. The analyses were performed using linear elastic and elastoplastic material models. A parametric study was conducted to understand the effects of pipe and soil modulus on the pipe responses (i.e. thrusts, moments on pipe wall) calculated from two dimensional and three dimensional analysis. The study indicates that 2D plane strain idealization is valid for pipe with low modulus while a three dimensional analysis will be required for concrete pipes or pipes with stiffer materials. Finite element results were compared with different design standards for shallow burial condition. It is observed that ASCE and AASHTO design standards provide 30 to 50 percent unconservative estimate with respect to finite element results due to the effects of live load in region near to crown.

The study revealed that the pattern of stress distributions, due to concentrated surface load, in longitudinal and transverse direction of the pipe at crown level is almost similar. The maximum stress was directly under the load, which decayed gradually away from the load. However, a tensile stress develops at the pipe-soil interface at some distance from the load in longitudinal direction when the pipe is buried at a depth less than 0.5 times the diameter. Stress distributions in longitudinal direction of the pipe showed that stresses decrease and become insignificant at a short distance (1.5 m) away from the pipe. Thus, stresses reaching to the pipe from any wheel load may not be affected by the stresses from the other wheel of the same axle if the wheels are located at a distance farther than 1.5 m. Pipe with greater stiffness appeared to attract greater surface load due to arching.

Three-dimensional finite element analysis appeared successful in predicting the observed response of full-scale test pipes under surface live load. The test, undertaken by Ontario Concrete Pipe Association in Canada, was modeled effectively using the FE method. The three-dimensional analysis was then used to develop influence lines for different stresses for various positions of the concentrated surface load with respect to the pipe axis. The influence lines for stresses on the pipe and the surrounding soil are found useful to calculate the ground stresses developing due to the live load.

CONTENTS

	Page Number
DECLARATION	iv
ACKNOWLEDGEMENT	vii
ABSTRACT	viii
CONTENTS	x
LIST OF FIGURES	xiii
LIST OF TABLES	xvi
LIST OF SYMBOLS	xvii
CHAPTER 1	1
INTRODUCTION	1
1.1 GENERAL	1
1.2 BRIEF HISTORY OF RIGID PIPE DESIGN	2
1.3 CURRENT STATE-OF-THE-ART FOR INCLUSION OF LIVE LOAD	3
1.4 NECESSITY FOR THIS STUDY	4
1.5 OBJECTIVES	4
1.6 METHODOLOGY	5
1.7 RESEARCH SCOPES AND LIMITATIONS	6
1.9 ORGANIZATION OF THE THESIS	6
CHAPTER 2	8
REVIEW OF PIPE ANALYSES AND DESIGN METHODS	8
2.1 INTRODUCTION	8
2.2 MARSTON-SPANGLER LOAD THEORY	9
2.3 SEMI-EMPIRICAL METHOD	11
2.4 ANALYTICAL SOLUTION	12
2.5 NUMERICAL SOLUTION	17
2.5.1 SPIDA Code	17
2.5.2 SOILCON Code	17
2.5.3 CANDE Code	19
2.6 OTHER FINITE ELEMENT MODELS FOR BURIED PIPE ANALYSIS	20
2.7 SUMMARY	21

CHAPTER 3	22
FINITE ELEMENT MODEL FOR SOIL-PIPE INTERACTION ANALYSIS	22
3.1 GENERAL	22
3.2 TWO-DIMENSIONAL FINITE ELEMENT MODEL	23
3.2.1 Geometry Formulation	23
3.2.2 Materials Used in FE Analyses	25
3.2.3 The Study of Boundary Effect	25
3.2.4 Effect of Mesh Refinement	28
3.2.5 Effect of Soil-Pipe Interaction	31
3.2.6 Evaluation Using Close-form Solution	31
3.3 THREE-DIMENSIONAL FINITE ELEMENT MODEL	33
3.3.1 Geometry Formulation	33
3.3.2 Tuning of Three-dimensional Mesh	34
3.4 PARAMETRIC STUDY	35
3.5 SUMMARY	39
CHAPTER 4	40
SOIL STRESSES DUE TO SURFACE LOAD	40
4.1 GENERAL	40
4.2 ACCOUNT FOR LIVE LOAD IN THE DESIGN CODES	41
4.2.1 ASCE 15-93 Code	41
4.2.2 Canadian Highway Bridge Design Code	47
4.2.3 AASHTO Design Code	49
4.3 FINITE ELEMENT ANALYSIS	53
4.3.1 Pipe Stresses from FE Analysis	54
4.3.2 Effect of Soil Cover on Pipe Stress	58
4.3.3 Ground Stresses from FE Analysis	60
4.3.4 Effect of Soil-Pipe Interaction	62
4.3.5 Effect of Cover Depth on Ground Stress	63
4.4 COMPARISON OF SOIL STRESS WITH DESIGN MODELS	65
4.5 LATERAL DISTRIBUTION OF THE STRESS	66
4.6 SUMMARY	71
CHAPTER 5	72
ANALYSIS AND INTERPRETATION OF FULL-SCALE TEST	72
5.1 GENERAL	72
5.2 LIVE LOAD TEST (PROGRAM AT UWO, CANADA)	73

5.2.1	Introduction	73
5.2.2	Test Bed Configuration	73
5.2.3	Test Procedure	76
5.2.4	General Vehicle Information	77
5.3	PRESSURE CELL RESPONSE	79
5.3.1	Crown Cells	79
5.3.2	Springline and Oblique Cells	82
5.4	COMMENTS ON FULL-SCALE TEST RESULTS	84
5.5	3-D FINITE ELEMENT MODELING OF FULL SCALE TESTS	85
5.5.1	Mesh	86
5.5.2	Material Models	86
5.5.3	Influence Line for Vertical Soil Stress at Pipe Crown	87
5.6	COMPARISON WITH MEASUREMENTS	89
5.7	SUMMARY	95
 CHAPTER 6		96
INCORPORATION OF SURFACE LOAD IN DESIGN CODE		96
6.1	INTRODUCTION	96
6.2	DEVELOPMENT OF INFLUENCE LINES	97
6.3	INFLUENCE LINES FOR SOIL STRESSES	99
6.4	CALCULATION OF STRESS USING INFLUENCE LINES	100
6.5	SUMMARY	102
 CHAPTER 7		103
CONCLUSIONS AND RECOMMENDATIONS		103
6.1	INTRODUCTION	103
6.2	CONCLUSIONS	103
6.3	RECOMMENDATIONS FOR FUTURE STUDY	105
 REFERENCES		106
 APPENDICES:		
APPENDIX A: STRESS CONTOURS		
APPENDIX B: ANSYS CODE USED IN THE ANALYSIS		

LIST OF FIGURES

	Page Number
Figure 2.1: Marston-Spangler Load Theory (Spanger and Handy, 1973)	10
Figure 2.2: Diagram for coefficient C_d for ditch conduits (Spangler and Handy, 1973)	11
Figure 2.3: Elastic Plate Theory	12
Figure 2.4: Uniform and non-uniform deformation of buried pipe (Moore, 2000)	14
Figure 3.1: Different Soil Zones in Finite Element Mesh	24
Figure 3.2: Effects at Crown due to uniform Surface Load	26
Figure 3.3: Effects at Springline due to uniform Surface Load	27
Figure 3.4: Effects at Invert due to uniform Surface Load	28
Figure 3.5: Vertical Stresses with Mesh Density (2D Model)	29
Figure 3.6: Crown Moment with Mesh Density	30
Figure 3.7: Finite Element Mesh (2D)	30
Figure 3.8: Thrust at Springline with Surface Load	32
Figure 3.9: Moment at Springline with Surface Load	32
Figure 3.10: 3-D Structural Solid Element (SOLID45 in ANSYS)	33
Figure 3.11: Finite Element Model Geometry (3D)	34
Figure 3.12: Vertical Stresses with Mesh Density (3D Model)	35
Figure 3.13: Crown Stresses in Different Pipe-Soil Modulus	37
Figure 3.14: Variation of Crown Stresses in 2D & 3D Model	37
Figure 3.15: Springline Stresses in Different Pipe-Soil Modulus	38
Figure 3.16: Variation of Springline Stresses in 2D & 3D Model	38

Figure 4.1: Standard Embankment Installations (ASCE, 1993)	42
Figure 4.2: Arching Coefficients and Heger Earth Pressure Distribution (Heger et al. 1985)	43
Figure 4.3: Effective Area of the Live Load (After ASCE, 1993)	44
Figure 4.4: Distributed Load Area Two HS 20 Trucks Passing	44
Figure 4.5: Distributed Load Area Alternative Loads in Passing Mode	45
Figure 4.6: Effective Supporting Length (after ASCE, 1993)	46
Figure 4.7: Earth Pressure Distribution for Standard Installations of Circular Concrete Pipes (Heger et al. 1985)	48
Figure 4.8: AASHTO (2002) Wheel Loads and Wheel Spacing	51
Figure 4.9: AASHTO (2002) Wheel Load Surface Contact Area (Foot Print)	52
Figure 4.10: Schematic View of Pipe x-section with Surrounding Soil	54
Figure 4.11: Circumferential Stress Distribution on Exterior Wall of Pipe ($E_p/E_s = 1000$)	55
Figure 4.12: Circumferential Stress Distribution on Interior Wall of Pipe ($E_p/E_s = 1000$)	57
Figure 4.13: Variation of Stresses with Cover Depth	59
Figure 4.14: Circumferential Stress Distribution on Soil ($E_p/E_s = 1000$)	61
Figure 4.15: Horizontal Stress Distribution on Soil at Crown Level ($E_p/E_s = 1000$)	62
Figure 4.16: Vertical Stresses on Soil at Pipe Springline Level	63
Figure 4.17: Variation of vertical soil stress with depth	64
Figure 4.18: Comparison of Finite Element Stresses with Design	65
Figure 4.19: Distribution of Vertical Stress in Transverse Direction	66
Figure 4.20: Distribution of Vertical Stress in Longitudinal Direction	68
Figure 4.21: Stresses along Longitudinal and Transverse Direction (Burial depth = 0.5D)	70
Figure 5.1: Plan View of the Pipe Bed at the Barrie Test Site (Wong, 2002)	74
Figure 5.2: Longitudinal Profile of the Approaching Ramp along with Test Pipes (Wong, 2002)	74
Figure 5.3: Trench Geometry (After Wong, 2002)	74
Figure 5.4: Location of Earth Pressure Cells	76
Figure 5.5: Axle Configuration for Vehicles A to F (Wong, 2002)	78

Figure 5.6: Crown Cell Response at the Barrie Site due to Truck A and F (After Wong, 2002)	79
Figure 5.7: Average Crown Stresses due to Truck A (After Wong, 2002)	80
Figure 5.8: Average Crown Stresses due to Truck F (After Wong, 2002)	80
Figure 5.9: Springline Cell Response at the Barrie Site due to Truck A and F (After Wong, 2002)	83
Figure 5.10: Oblique Cell Response at the Barrie Site due to Truck A and F (After Wong, 2002)	83
Figure 5.11: Finite Element Mesh	85
Figure 5.12: Location of Unit Surface Load for FE Analysis	87
Figure 5.13: Influence Line for Vertical Soil Stress at 100 mm above Pipe-Crown (Transverse Direction, Burial Depth = 2.2D)	88
Figure 5.14: Influence Line for Vertical Soil Stress at 100 mm above Pipe-Crown (Longitudinal Direction, Burial Depth = 2.2D)	89
Figure 5.15: Comparison of Crown Stresses due to Truck F	94
Figure 5.16: Comparison of Crown Stresses due to Truck A	94
Figure 6.1: Location of Unit Surface Load in Transverse Direction	97
Figure 6.2: Plotting of influence line for a quantity (Schematic)	98
Figure 6.3: Location of Unit Surface Load in Longitudinal Direction	98
Figure 6.4: Influence Line for Vertical Soil Stress at 100 mm above Pipe-Crown (Transverse Direction, Burial Depth = 2.2D)	99
Figure 6.5: Influence Line for Vertical Soil Stress at 100 mm above Pipe-Crown (Longitudinal Direction, Burial Depth = 2.2D)	100
Figure 6.6: Pipe Stress Calculation from Influence Line (one vehicle)	101
Figure 6.7: Pipe Stress Calculation from Influence Line (two vehicles)	101
Figure A-1: Contour of Horizontal Stress under Uniform Surface Load	A-2
Figure A-2: Contour of Vertical Stress under Uniform Surface Load	A-3
Figure A-3: Contour of Stress Intensity Developed on Pipe Wall	A-4
Figure A-4: Contour of Stress under Concentrated Surface Load (3-D Model)	A-5
Figure A-5: Contour of Horizontal Stress due to Concentrated Surface Load at Shallow Burial Condition	A-6

LIST OF TABLES

	Page Number
Table 2.1: Pipes Stiffness Classes (Moore, 2000)	15
Table 2.2: Recommended Hyperbolic Parameters for Compacted Soils (Selig, 1990)	19
Table 4.1: Standard Installation of concrete pipes and backfill Requirements (ASCE, 1993)	41
Table 4.2: Critical Live Loads and Spread Dimensions at the top of the Pipe (ASCE, 1993)	46
Table 4.3: Force Factors for Earth Loads (Heger et al. 1985)	49
Table 4.4: Earth Pressure Factors (Heger et al. 1985)	49
Table 4.5: Length Factors for Earth Pressures (Heger et al. 1985)	49
Table 5.1: Crown Cell Location and Designation at the Barrie Site (Wong, 2002)	75
Table 5.2: General Information of the Tested Vehicles (Wong, 2002)	77
Table 5.3: Crown Stresses due to Axle Loads (Truck A & F) (After Wong, 2002)	82
Table 5.4: Springline and Oblique Stresses due to Axle Loads (Truck A & F) (After Wong, 2002)	84
Table 5.5: Stress Matrix due to Unit Load ($E_p=20000$ Mpa, $E_s=20$ Mpa) (Truck F)	91
Table 5.6: Stress Matrix due to Unit Load ($E_p=15000$ Mpa, $E_s=30$ Mpa) (Truck F)	91
Table 5.7: Crown Stress Increase due to Axle Loads (Truck F)	92
Table 5.8: Stress Matrix due to Unit Load ($E_p=20000$ Mpa, $E_s=20$ Mpa) (Truck A)	92
Table 5.9: Stress Matrix due to Unit Load ($E_p=15000$ Mpa, $E_s=30$ Mpa) (Truck A)	93
Table 5.10: Crown Stress Increase due to Axle Loads (Truck A)	93

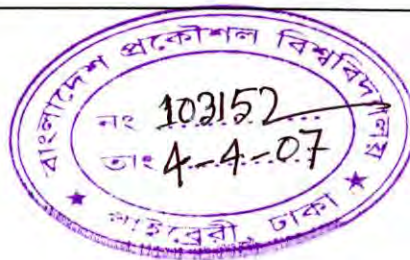
LIST OF SYMBOLS

Symbols	Meanings
A	: Area of the Pipe X-section
A_e	: Effective Area on Top of the Pipe
A_{LL}	: Distributed Live Load Area
$BCOVER$: Soil Cover below Pipe Invert
B_d	: Trench Width for Trench Installation
C	: Compressibility Ratio
C_d	: Load Coefficient
D	: Diameter of the Pipe
D_0	: Culvert Span for Embankment Installation
DS	: Soil cover beside Pipe Springline
E_p	: Modulus of Elasticity of Pipe Materials
E_s	: Modulus of Elasticity of Soils
F	: Flexibility Ratio
FEM	: Finite Element Method
H	: Height of Fill above Top of Conduit
I	: Moment of Inertia of Pipe X-section
IM	: Impact Factor
K	: Ratio of Active Lateral Unit Pressure to Vertical Unit Pressure
L_e	: Effective Length of the Buried Pipe
L_L	: Lane Loading
M_{cr}	: Moment at Pipe Crown
M_{inv}	: Moment at Pipe Invert
M_{sp}	: Moment at Pipe Springline
N_{cr}	: Thrust at Pipe Crown
N_{inv}	: Thrust at Pipe Invert
N_{sp}	: Thrust at Pipe Springline
P_{cr}	: Crown Pressure

P_L	: Live Load per Unit Length of the Pipe
P_W	: Wheel Load
R	: Radius of the Pipe
t	: Thickness of the Pipe
T_{COVER}	: Soil Cover above Pipe Crown
T_{sl}	: Springline Thrust
W	: Wheel Load Average Pressure Intensity
W_c	: Soil Weight per Unit Length Transmitted to the Pipe
W_{cr}	: Crack Load in the Three-Edge-Bearing Test
W_s	: Weight per Unit Length of Soil Prism above the Pipe
W_T	: Total Live Load
γ_s	: Average Unit Weight of the Soil
μ	: Coefficient of Friction between Backfill and Sides of Ditch.
σ_d	: Non-uniform Component of pressures in 2D Load System
σ_h	: Lateral Earth Pressure
σ_m	: Uniform Component of Pressures in 2D Load System
σ_v	: Vertical Earth Pressure

CHAPTER 1

INTRODUCTION



1.1 GENERAL

Underground pipes have served to improve people's standard of living since the dawn of civilization and so engineers and planners realize that the subsurface infrastructure is an absolute necessity to the modern community. The underground water systems serve as arteries to the cities, and the sewer systems serve as veins to carry off the waste. Despite a relatively long history that the field of pipe-soil interaction has experienced, some fundamental questions concerning the buried rigid pipe under surface load still remain unanswered. In this connection, computer modeling can be an important and economical tool for investigating the behavior of buried structures. The process of calibrating computer models with limited field test data and then using the models to investigate the behavior of structures with a much wider range of variables has proven an effective process for both research and design.

Pipes made from vitrified clay and concrete are rigid in nature. For the rigid pipes, as the name implies, deflection is negligible. Strength to resist wall stresses due to the combined effects of internal pressure and external load therefore govern the design of rigid pipes. Wall stress is the only performance limit for those pipes. The wall stress on the pipe is caused by the thrust and the bending moment due to external soil load, particularly for gravity flow pipes.

Clay and pre-cast concrete pipes have been used by the municipalities for storm and wastewater applications for many years. Majority of the sewer pipes in many countries are pre-cast concrete (Allouche and Freure, 2001), while other flexible piping systems are also gaining popularities. Municipalities in Bangladesh

predominately use concrete pipes. Concrete pipes are considered as the rigid pipes that have significant structural strength. Early design of such structures was based solely on destructive tests for the determination of their inherent strengths. While this method works reasonably well for small diameter pipes, an improved design method is needed for larger diameter concrete pipes. Heger et al. (1985) developed a more rational design method for rigid pipes using pipe-soil interaction analysis. However, the live load is assumed to be distributed uniformly on top of the pipe. While the assumption of uniformly distributed live load is reasonable for deeply buried pipe; this may not be true for pipes under shallow burial (Noor and Dhar, 2003). There is a need for a study of the structural performance of rigid pipe under surface live loads in order to develop a rational basis for design of such structures.

1.2 BRIEF HISTORY OF RIGID PIPE DESIGN

In early time, pipelines were installed applying local discretion with little consideration for design. The inceptive buried pipes were mostly manufactured from vitrified clay or concrete. The development of relatively rational buried pipe designs started when "Marston load theory" was developed in the early 1900's. Marston and Anderson (1913) developed the well-known load theory from the silo arching solution of Janssen (1895). The solution can be used to calculate vertical load reaching the crown of rigid pipes.

In fact, design of rigid pipes is still generally based on the traditional indirect method. In this design, earth load on top of the pipe is calculated using the Marston-Spangler theory (Spangler and Handy, 1973). Pipes are then designed to withstand the load in standard laboratory tests. A bedding factor is used to relate the field loading conditions with the laboratory test results. However, Standard Installation Direct Design (SIDD) method developed by Heger et al. (1985), using finite element analysis, has been revealed as a more rational design method of the buried rigid pipes. The method provides four different earth pressure distributions (called 'Heger Earth Pressure') around the pipe for four standard installation types. Details of 'Heger Earth Pressure' are discussed further in Chapter 4.

Different finite element codes have also been used for analysis of soil-pipe system. Modeling of the concrete arch culvert, particularly in North America, has been performed using the computer program CANDE (Culvert Analysis and Design) developed by Katona (1978). The Utah State University developed a FEA program called "PIPE" based on CANDE. Another computer program, SPIDA (Soil-pipe Interaction Design and Analysis), has been used for the design and analysis of buried concrete pipe (Heger et al. 1985). A brief overview of the computer codes is outlined further in Chapter 2.

1.3 CURRENT STATE-OF-THE-ART FOR INCLUSION OF LIVE LOAD

The live load in SIDD is considered as a uniformly distributed load on the top of the pipe, which is added to the earth load. The wheel load is assumed to produce a uniform pressure at the top level of the pipe over a rectangular area with its dimensions equal to the wheel footprint dimensions plus 1.75 times the depth of fill. In the case of overlapping of two or more areas, the total load is distributed over the combined effective area. The LRFD of AASHTO (1998) specification made a significant change in the procedure of calculating the live load distribution over buried pipes modifying the rate of load spreading to 1.15 to 1.75 times the depth, depending on the type of backfill conditions. The effects of pipe stiffness on the distribution of surface load are not incorporated in the AASHTO design method. Dhar et al. (2004) revealed from full-scale test of PVC pipes under quasi-live load that load-spreading rate of 1.15 worked reasonably well for calculation of pipe deflections. However, the effect of surface load on the behavior of rigid pipe has not been evaluated. Noor and Dhar (2003) revealed that pipe-soil interaction analysis would be required to determine the stresses around shallow buried rigid pipes while classical theory (Boussinesq, 1885) could be used to calculate the soil stresses for pipes under deep burial.

1.4 NECESSITY FOR THIS STUDY

The Standard Installation Direct Design (well known as SIDD) method, currently incorporated in various design codes, is considered as the most rational method of design for rigid pipe. In this method, the thrust and bending moment on pipe-wall are calculated based on the Heger Earth Pressure, which is used to estimate the pipe-wall stresses. However, calculation of the wall-thrust and bending moment from the complicated Heger Earth Pressure is not straightforward. Dhar et al (2005) presented an approach of developing simplified equations for calculation of wall-thrust and bending moment for deeply buried rigid pipes based on continuum theory solution and finite element analysis. The pipe under shallow burial condition and with localized non-uniform soil support was not considered in the simplified approach. Besides, the live load is considered in current design codes as an additional uniformly distributed load on top of the pipe, as discussed earlier. However, Noor and Dhar (2003) revealed that the assumption of uniformly distributed live load is not applicable for pipes under shallow burial condition. Pipe-soil interaction analysis, where the pipe and the soil are modeled together, would be necessary to account for the mechanism of load transfer between the pipe and soil during the application of surface live load. Therefore, research is needed to enhance the approach of incorporating the effects of surface load on pipe.

1.5 OBJECTIVES

The objective of this thesis is to investigate the behavior of shallow buried rigid pipes under surface load considering soil-structure interaction and to develop a better understanding about transfer of surface load around the pipes. Soil stress measured in full-scale tests (Allouche et al, 2003) is used to interpret the soil-pipe interaction behavior observed in the field tests. Specific objectives of the research are to:

- Review the numerical and analytical solutions for buried rigid pipe design.
- Study the performance of 2D and 3D Finite Element Modeling in simulating pipe behavior.

- Perform a parametric study to identify the parameters affecting pipe performance.
- Investigate the soil-pipe interaction behavior of shallow buried rigid pipes under surface load using the Finite Element Method.
- Investigate the effect of soil cover on transfer of surface load around the pipe.
- Interpret full-scale test observations of soil stresses around pipes under surface load.
- Develop a design method for rigid pipes by rationally incorporating the effects of surface load.

1.6 METHODOLOGY

Traditionally, soil and pipe are considered separately for analysis of the effect of live load on buried pipe, where the load reaching to the pipe is estimated as a uniformly distributed load at the pipe crown. In current research, Soil and pipe have been modeled together to evaluate the distribution of stress around the pipe considering the interaction between pipe and soil under a surface load. Both 2D and 3D finite element analyses were conducted for the soil-pipe interaction under the surface load for buried rigid pipe. Linear elastic material model was used for the rigid pipe in the finite element analysis while both elastic and elastic-perfectly plastic (Mohr-Coulomb) model were used for the soil. Rigidity of the pipe was ensured using a high modulus of pipe materials (as those of concrete). For the finite element analysis, a mesh-sensitivity analysis was carried out to eliminate errors associated with the density of mesh and the extent of the boundary. Results of the continuum theory solution were used to evaluate the two-dimensional and three-dimensional finite element solution. Three-dimensional analysis was then extended for investigation of pipe under different burial depths and subjected to concentrated live loads. The results of analysis were compared with the calculations using current design methods. Influence lines were then developed based on the FE analysis to calculate the soil stresses around the pipe for various position of concentrated surface live load.

1.7 RESEARCH SCOPES AND LIMITATIONS

The scopes of this research are as follows:

- Soil-pipe interaction analysis was performed using Finite Element method to study the effects of live load for rigid pipe under shallow burial. Three-dimensional finite element analysis was used to understand the three-dimensional phenomenon under concentrated live load.
- Soil stress measured in full-scale tests (Allouche et al, 2003) was analyzed using finite element method to interpret the observed behavior.
- Based on the finite element analysis, influence lines for stresses on the pipe were developed which were useful to understand the pattern of the ground stresses developing due to the live load. A design proposal was then made to incorporate the effect of live load using the influence lines.

The analysis was limited to pipes in uniform ground. Thus, the backfill and native soil is assumed to be the same. Large diameter concrete pipe with diameter to thickness ratio of 8 was emphasized. Besides, the principle of superposition was used for calculation of the effect of different wheel loads on the pipe responses. However, the superposition principle appeared reasonable in predicting the pipe response. The effect of non-linearity due to soil plasticity appeared insignificant on the pipe responses, indicating applicability of superposition principle. The pipe-soil interface was modeled using continuum element with elastic-perfectly plastic material model during the analysis. Continuum element with elasto-plastic material property was successfully used to model pipe-soil interface in Dhar and Moore (2004).

1.8 ORGANIZATION OF THE THESIS

Chapter 2 of this thesis reviews the current status of buried rigid pipe analysis and design methods. Analysis of numerical and analytical solution is discussed elaborately. Finite element methods used for analysis of pipe-soil interaction are also reviewed.

Chapter 3 describes finite element model developed for the analysis. Both two dimensional and three dimensional models are developed. The idealizations used in the finite element models and estimation of soil and pipe parameters is described in detail in this chapter. Finite element results are verified using analytical solution. A parametric study for the effects of soil and pipe stiffness is carried out and described in this chapter.

Chapter 4 examines the soil and pipe stresses due to concentrated surface load for different burial conditions. Comparisons of stresses from finite element analyses, current design codes and Boussinesq solution are presented in this chapter.

Chapter 5 interprets a full scale test observations of soil stresses around a concrete pipe, carried out in Ontario, Canada. The set-up of the full scale test is briefly discussed in this chapter. Influence lines for different soil stresses around pipe were developed for the test set-up using finite element analysis. Finite element results are then compared with the measured pipe responses.

The influence lines (developed based on the FE analysis) can effectively be used to calculate the soil stresses around the pipe for various position of surface load. Thus, a proposal for incorporating live load in rigid pipe design is made using the influence lines in Chapter 6.

Finally, Chapter 7 provides a list of conclusions that are drawn from this research. Recommendations are also made for future research.

CHAPTER 2

REVIEW OF PIPE ANALYSES AND DESIGN METHODS

2.1 INTRODUCTION

Municipalities in different countries have been using clay and pre-cast concrete pipes for storm and wastewater applications for many years. Concrete pipes have been used predominantly by the municipalities in Bangladesh. The piping system must be strong enough to withstand induced stresses, have relatively smooth walls for ease of water movement, have a tight joining system, and be somewhat chemically inert with respect to soil and water. In fact, the life of the pipe, after it is installed is not just a function of the pipe material, but is largely a function of the loading conditions and the environment to which it is subjected. It is design engineer's responsibility to assess all factors and formulate a design with a predicted design life. For this reason, the subject of soil-pipe interaction has been of engineering interest since the early 1900s.

In the past several decades various projects have been undertaken to improve rigid pipe design and numerous articles have been published on the same subject. A number of specialized ASCE and other conferences and symposia have been held. Many of the important design aspects for rigid pipe have been established. This chapter reviews the current status of analyses methods used to investigate the behavior of buried rigid pipe.

Design of rigid pipes is generally based on the traditional indirect method. In this method pipes are designed to withstand the expected equivalent earth load in standard laboratory tests (e.g. Three Edge Bearing Test). The earth load is calculated using the Marston-Spangler theory. A direct design method known as Standard Installation Direct Design method was also developed for rigid pipe based on extensive finite

element analysis (Heger et al. 1985). The Standard Installation Direct Design (SIDD) method provides four different earth pressure distributions around the pipe for four standard installation conditions. The earth pressure was then used to calculate the thrust and bending moment on pipe-wall. The live load is considered as an additional uniformly distributed load on the top of the pipe. A brief overview of the methods of analysis and design of rigid pipe is outlined the following sections.

2.2 MARSTON-SPANGLER LOAD THEORY

The load on the pipe can be estimated by the Marston-Spangler load theory (Spangler, 1941 and Spangler and Handy, 1973). This theory considers the amount of soil weight in the prism directly above the culvert that is carried by shearing resistance of the soil on the vertical sides of the prism as shown in Figure 2.1. The soil weight per unit length, W_c , transmitted to the pipe is calculated by:

$$W_c = C_d \gamma_s B^2 \quad (2.1)$$

Where, C_d is a dimensionless load coefficient, γ_s is the average unit weight of the soil, and B is equal to the culvert span D_0 for embankment installation, and equal to trench width B_d for trench installation. The load coefficient is a function of the soil-pipe system geometry and installation conditions. It is determined by:

$$C_d = \frac{1 - \exp\left[-2K\mu'\left(\frac{H}{B}\right)\right]}{2K\mu'} \quad (2.2)$$

Here,

K = ratio of active lateral unit pressure to vertical unit pressure.

H = height of fill above top of conduit, in feet.

$\mu' = \tan\phi$ = coefficient of friction between backfill and sides of ditch.

Using this theory, the magnitude of arching, A , is given by:

$$A = 1 - \frac{W_c}{W_s} \quad (2.3)$$

Where W_c is the soil weight per unit length transmitted to the pipe, and W_s is the weight per unit length of soil prism above the pipe (Figure 2.1).

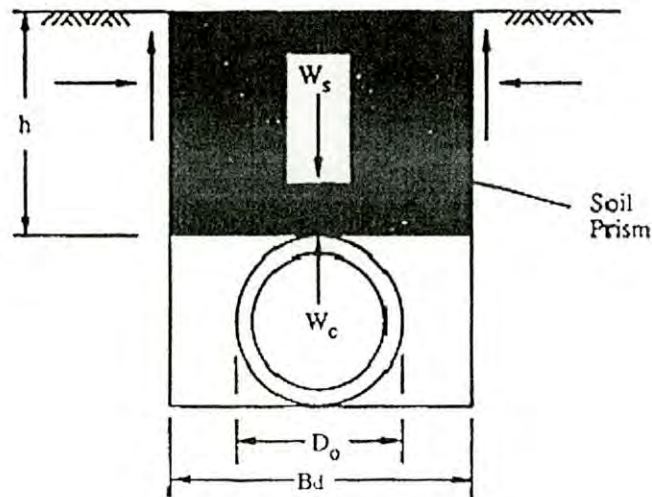


Figure 2.1: Marston-Spangler Load Theory (Spangler and Handy, 1973)

The springline thrust in the pipe wall, T_{sl} , is estimated by:

$$T_{sl} = \frac{W_c}{2} \quad (2.4)$$

And the crown pressure, P_{cr} , by:

$$P_{cr} = \frac{W_c}{D_o} \quad (2.5)$$

Evaluation of W_c is made easy by the use of the computation diagram in Figure 2.2 (Spangler and Handy, 1973) in which value of C_d for various values of H/B_d are plotted for several kinds of filling materials having different coefficients of internal friction.

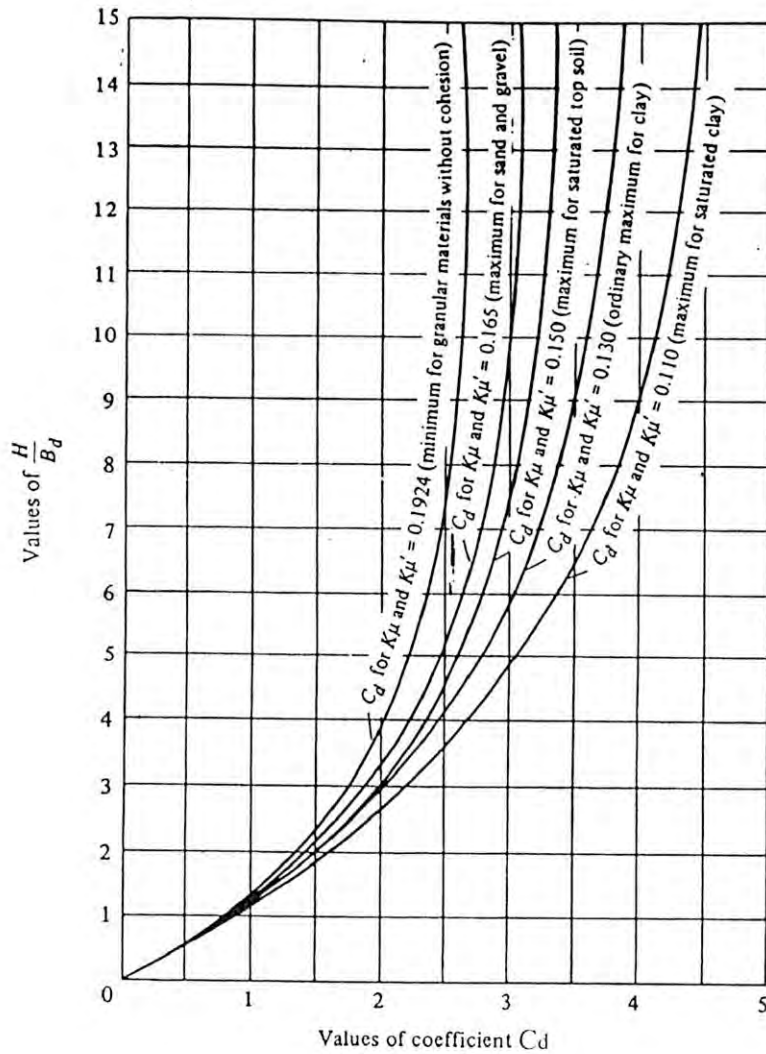


Figure 2.2: Diagram for coefficient C_d for ditch conduits (Spangler and Handy, 1973)

2.3 SEMI-EMPIRICAL METHOD

The direct design of rigid pipe focuses on determination of the pipe wall stresses that develop due to soil-pipe interaction. An earlier so-called 'direct design' of concrete pipe was reported in Moore (2000), where the springline bending moment from the three-edge bearing test is to be compared with the moment expected in the field. The springline moment associated with limiting crack load, W_{cr} , in the three-edge-bearing test was estimated assuming the pipe sample to respond as an elastic ring (Young and Trott, 1984):

$$M = W_{cr} \times r (\pi^1 - 0.5) \quad (2.6)$$

Where, r = Radius of the pipe.

The moment is then equated to the springline bending moment expected in the field. The expected springline bending moment can be calculated based on an assumed earth pressure distribution around the pipe. Paris (1921) and Olander (1950) proposed two different semi-empirical earth pressure distributions around concrete pipe.

2.4 ANALYTICAL SOLUTION

Burns and Richard (1964) developed the elasticity solution for the soil-structure interaction of a pipe buried in a homogeneous soil. They analyzed the interaction of an elastic circular cylindrical shell embedded in an elastic medium. The model is shown in Figure 2.3. The earth load and live load are applied as pressures on the boundary of the medium. The loaded surface is assumed at infinity in the derivation of the solution. The depth for which this theory is valid is determined by noting at what value of h the resulting stress and displacement distribution in the medium becomes the free-field distribution. This depth is equal to at least twice the cylinder diameter.

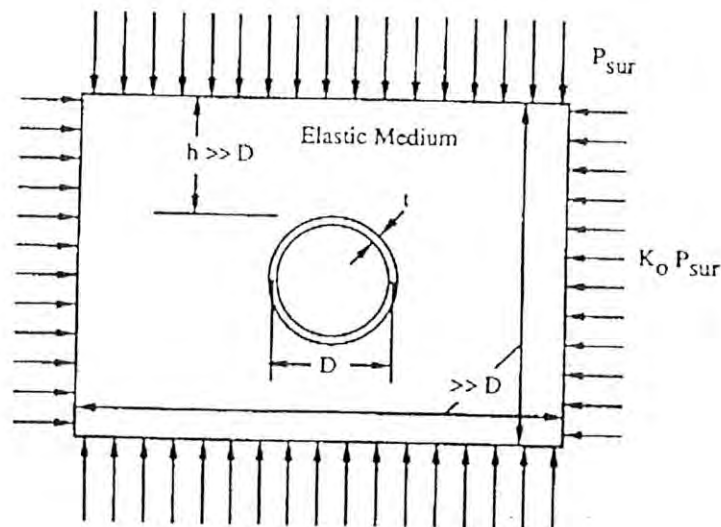


Figure 2.3: Elastic Plate Theory

The solutions are developed for plane-strain condition where no strain is allowed in the longitudinal direction of the cylinder. Free-field conditions exist at large distances from the cylinder. Thus, the lateral boundary condition is represented by the state of

stress shown in Figure 2.3. The soil and pipe are each represented by Young's modulus and Poisson's ratio. The soil is assumed to be homogeneous, isotropic, linear, elastic material. The cylinder of thickness, t , and diameter, D , is always in full contact with the surrounding medium and is installed under no-load. Either no-slip or full-slip (frictionless) conditions are assumed at the interface.

Both the soil and the pipe are assumed to be weightless. The vertical geostatic pressure and the live load pressure at the depth of the structure are represented by an equal pressure applied at the top surface of the medium. The results of the analysis are for these applied pressures only and are to be superimposed on the conditions existing prior to the application of these pressures caused by the installation of the pipe and placement of backfill to the crown of the pipe.

Burns and Richard (1964) elastic solution gives expressions for the normal and shear stresses between the shell and the soil medium; for thrusts, moments and displacements in the shell; and for the stresses and displacements throughout the medium. The method is applicable to conduits ranging from rigid to flexible which are embedded in any linearly elastic medium.

Hoeg (1968) derived the formulation for the more generalized case of $\sigma_h = K\sigma_v$, where σ_v , σ_h are vertical and lateral earth pressure and K is the coefficient of earth pressure at rest, respectively. Moore (2000) adopted Hoeg's solution for the analysis of buried circular pipes and culverts. However, to simplify the interpretation, the two-dimensional load system was divided into uniform (σ_m) and non-uniform components (σ_d) of pressures as shown in Figure 2.4. For a particular condition (i.e. for a certain K), the uniform (σ_m) and non-uniform components (σ_d) of pressures were expressed by Moore (2000) as:

$$\left. \begin{aligned} \sigma_m &= \frac{\sigma_v + \sigma_h}{2} \\ \sigma_d &= \frac{\sigma_v - \sigma_h}{2} \end{aligned} \right\} \quad (2.7)$$

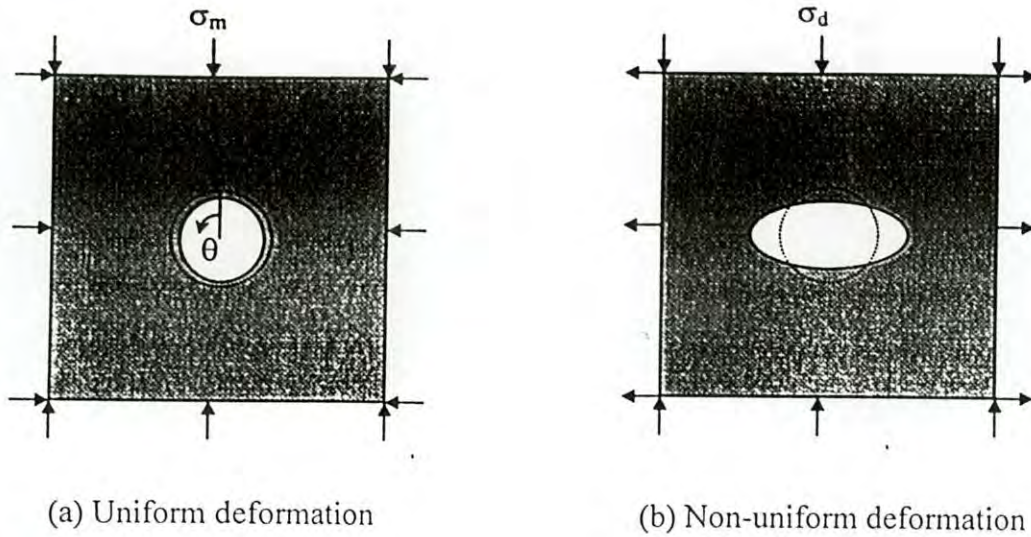


Figure 2.4: Uniform and non-uniform deformation of buried pipe (Moore, 2000)

Distributions of interface radial and shear stress on the external boundary of the pipe were then defined as:

$$\begin{aligned} \sigma &= \sigma_o + \sigma_2 \cos 2\theta \\ \tau &= \tau_2 \sin 2\theta \end{aligned} \tag{2.8a}(2.8b)$$

Where θ is measured from the vertical axis, and

$$\left. \begin{aligned} \sigma_o &= A_m \sigma_m \\ \sigma_2 &= A_{d\sigma} \sigma_d \\ \tau_2 &= A_{d\tau} \sigma_d \end{aligned} \right\} \tag{2.9a} \tag{2.9b} \tag{2.9c}$$

Factors A_m , $A_{d\sigma}$ and $A_{d\tau}$ are called arching factors. These provide interface stresses in terms of the mean and deviatoric field stresses.

$$A_m = \frac{2(1-\nu_s)}{1+C(1-2\nu_s)} \tag{2.10}$$

For a bonded interface

$$A_{d\sigma} = \frac{4(1-\nu_s)(4+3C(1-2\nu_s))-2F}{\Delta} \tag{2.11}$$

For a smooth surface

$$A_{d\sigma} = 12(1 - \nu_s)(2F + 5 - 6\nu_s) \quad (2.12)$$

For a bonded surface

$$A_{dr} = \frac{16(1 - \nu_s)(F + 1)}{\Delta} \quad (2.13)$$

For a smooth surface

$$A_{dr} = 0 \quad (2.14)$$

The denominator in Equation (2.11) and (2.13) is given by

$$\Delta = C(1 - 2\nu_s)(5 - 6\nu_s + 2F) + 2F(3 - 2\nu_s) + 4(3 - 4\nu_s) \quad (2.15)$$

The two stiffness parameters C and F are defined as:

$$C = \frac{EsD}{[2(1 + \nu_s)(1 - 2\nu_s)E_p A_p]} \quad (2.16)$$

$$F = \frac{E_s D^3}{[48(1 - \nu_s)E_p I_p]} \quad (2.17)$$

Where, C and F are used to define the compressibility and flexibility ratios of a pipe respectively. Table 2.1 provides a classification of pipe according to C and F values.

Table 2.1: Pipes Stiffness Classes (Moore, 2000)

Pipe class	C values	F values	Examples
Rigid Pipe Concrete	$0.1 > C$	$0.1 > F$	Cast Iron, Reinforce and clay
Semi-Rigid Pipe Iron CS	$0.1 > C$	$10 > F > 0.1$	Long span R/C, Ductile Rib Stiffened
Flexible Pipe	$0.1 > C$	$F > 10$	CS and Al.,PVC, GRP,PP, Plain PE
Compressible Pipe	$100 > C > 0.1$	$F > 10$	Profiled PE
Empty Pipe	$C > 100$	$F > 10$	

Thrust and moment on the pipe wall can be estimated from these interface pressure components σ_0 , σ_2 and τ_2 (Equation 2.9). For harmonic interface, stresses defined by Equation 2.8, thrusts at the crown, N_{cr} , and springline, N_{sp} , are given by:

$$N_{cr} = \sigma_o r - \left(\frac{\sigma_2}{3} - \frac{2\tau_2}{3} \right) r \quad (2.18)$$

$$N_{sp} = \sigma_o r - \left(\frac{\sigma_2}{3} - \frac{2\tau_2}{3} \right) r \quad (2.19)$$

The bending moments at the crown, M_{cr} , and at the springline, M_{sp} , are given by

$$M_{cr} = \left(\frac{\sigma_2}{3} + \frac{\tau_2}{6} \right) r^2 \quad (2.20)$$

$$M_{sp} = - \left(\frac{\sigma_2}{3} + \frac{\tau_2}{6} \right) r^2 \quad (2.21)$$

The arching factors are largely independent of soil modulus for rigid pipes and the magnitudes of the factors are greater than 1, meaning 'negative arching' where loads are attracted toward the pipe.

Moore (2000) proposed closed form equations for thrust and bending moment at the springline of buried rigid pipes, for C and F very small,

$$N_{sp} = \sigma_v r (1 - \nu_s) \left[1 + K + \frac{2(1-K)}{(3-4\nu_s)} \right] \quad \text{bonded interface} \quad (2.22)$$

$$N_{sp} = \sigma_v r (1 - \nu_s) \left[1 + K + \frac{2(1-K)}{(5-6\nu_s)} \right] \quad \text{smooth interface} \quad (2.23)$$

$$M_{sp} = -\sigma_v r^2 (1-K) \frac{(1-\nu_s)}{(3-4\nu_s)} \quad \text{bonded interface} \quad (2.24)$$

$$M_{sp} = -\sigma_v r^2 (1-K) \frac{2(1-\nu_s)}{(5-6\nu_s)} \quad \text{smooth interface} \quad (2.25)$$

2.5 NUMERICAL SOLUTION

The finite element method has been proven to be a powerful tool for tackling some of the problems that are difficult to solve in a closed form. For soil-structure interaction analysis, this method can represent important aspects such as nonlinear soil stress-strain behavior, non-homogeneous soil conditions, geometry variations, and construction effect. Computational output includes stresses and strains in the soil, thrust, moment and shear in the pipe wall, and pipe deflection. Several codes commonly used for soil-structure interaction analysis are SPIDA, SOILCON, CANDE etc.

2.5.1 SPIDA Code

Heger et al. (1985) developed a Soil-Pipe Interaction Analysis (SPIDA) program for analyzing buried concrete pipe. The program provides the stress distribution around pipe, moments and shear forces within pipe-wall, and area of required reinforcement. It supports the earth pressure distribution of Standard Installation Direct Design (SIDD). It uses a predefined finite element mesh of the soil-pipe system and is capable of incorporating construction sequence during analysis. The problem in SPIDA is idealized assuming a plane strain condition and symmetric about vertical centerline. Predefined material models based on hyperbolic elasticity can only be used in SPIDA.

2.5.2 SOILCON Code

The program SOILCON (SOIL CONduit analysis) models buried conduit installation behavior as well as the behavior under earth load. SOILCON was derived at UMass from NLSSIM which was developed by Duncan and his colleagues at the University of California, Berkeley. Some of the modifications are described by Haggag (1989).

The program calculates stresses, strains and displacements in soil elements, and internal forces, and displacements in structural elements. The structure is modeled

with straight beam-column elements. Horizontal and vertical motions, as well as rotation for each of the structural element nodes, are inherent in the model. The structural stress-strain behavior is assumed to be bilinear.

The soil model used is nonlinear and stress state dependent. It uses the Young's modulus and Bulk modulus in a hyperbolic formulation as described by Selig (1990). The author determined design parameters for a variety of soils and compaction levels from laboratory tests. These parameters were modified for flexible pipes by Haggag (1989) and then extended to other soil types and compaction levels by Selig (1990). The values are listed in Table 2.2.

Incremental construction is modeled using load steps which may represent placement of a layer of soil, placement of structure, or application of loads after the end of construction. To represent the nonlinear and stress-dependent stress-strain properties of the soil, each load increment is iterated twice. The first uses values of Young's modulus and bulk modulus based on the stresses at the beginning of the load step. The second uses Young's modulus and bulk modulus based on the average stresses during the load step. The incremental stresses, strains, and displacements in the soil elements, and the incremental internal forces, moments and displacements in the structural elements during each step are added to the values at the beginning of the step to get the final values for the current load step and the initial values for the next load step.

Placement of fill on top of the buried pipe is simulated by applying forces to represent the weight of the added layer. Preexisting soil may also be represented by SOILCON. The program reads initial stresses, strains, and displacements of the preexisting soil elements. The incremental values at the end of each load step calculated in the program are added to the initial values.

Table 2.2: Recommended Hyperbolic Parameters for Compacted Soils (Selig, 1990)

TETSED	SOIL TYPE		%		SOIL	γ_c	K_m	n_m	R_f	c_s	ϕ_{30}	$\Delta\phi_s$	B_i/P_a	ϵ_u	K_o		
			D698	D1557													
SOIL	USCS	AASHTO	T-99	T-180	NO.	(lb/ft ³)(lb/in. ³)	(psi) (deg) (deg)										
Gravelly Sand (SW)	SW, SP, GW, GP	A1, A3	100	95	27	148	0.0856	1300	0.90	0.65	0	54	15	272.0	0.007	1.5	
			95	90	21	141	0.0816	950	0.60	0.70	0	48	8	187.0	0.014	1.3	
				90	85	1	134	0.0775	640	0.43	0.75	0	42	4	102.0	0.036	1.1
				85	80	22	126	0.0729	450	0.35	0.80	0	38	2	31.8	0.057	0.9
				80	75	2	119	0.0689	320	0.35	0.83	0	36	1	15.3	0.078	0.8
			61	59	3	91	0.0527	54	0.85	0.90	0	29	0	4.3	0.163	0.5	
Sandy Silt (ML)	GM, SM, ML; Also	A2, A4	100	95	28	134	0.0775	800	0.54	1.02	5.5	36	0	197.5	0.021	1.5	
			95	90	23	127	0.0735	440	0.40	0.95	4	34	0	120.8	0.043	1.2	
				90	85	4	120	0.0694	200	0.26	0.89	3.5	32	0	46.0	0.071	0.9
				85	80	24	114	0.0660	110	0.25	0.85	3	30	0	23.8	0.100	0.8
				80	75	5	107	0.0619	75	0.25	0.80	2.5	28	0	12.8	0.143	0.7
			49	46	6	66	0.0382	16	0.95	0.55	0	23	0	3.3	0.305	0.5	
Silty Clay (CL)	CL, MH, GC, SC	A5, A6	100	90	29	125	0.0723	170	0.37	1.07	11	12	0	81.3	0.064	1.0	
			95	85	25	119	0.0689	120	0.45	1.00	9	15	4	53.0	0.092	0.8	
				90	80	7	112	0.0648	75	0.54	0.94	7	17	7	25.5	0.121	0.6
				85	75	26	106	0.0613	50	0.60	0.90	6	18	8	13.0	0.149	0.5
				80	70	8	100	0.0579	35	0.66	0.87	5	19	8.5	8.8	0.178	0.4
			45	40	9	56	0.0324	16	0.95	0.75	0	23	11	1.8	0.391	0.3	
CH	A7		100	90	7	112	0.0648	75	0.54	0.94	7	17	7	25.5	0.121	0.8	
			95	85	26	106	0.0613	50	0.60	0.90	6	18	8	13.0	0.149	0.6	
			90	80	8	100	0.0579	35	0.66	0.87	5	19	8.5	8.8	0.178	0.5	
			45	40	9	56	0.0324	16	0.95	0.75	0	23	11	1.8	0.391	0.3	

2.5.3 CANDE Code

CANDE (Culvert Analysis and Design) was first introduced in 1976 for the structural analysis and design of buried culverts (Katona et al., 1976). The code was modified twice (Katona et al., 1981; Musser, 1989).

As with SOILCON, CANDE is based on a two-dimensional geometry called plane-strain. Plane-strain implies that there is no deformation in the longitudinal direction and that every cross section deforms in the same manner.

CANDE has two execution modes; analysis and design. Analysis means that a particular soil-pipe system is completely defined in terms of geometry, material properties, and loading conditions. The problem is then solved and output consists of structural responses (displacements, stresses, strains) and soil responses, as well as an evaluation of culvert performance in terms of safety factors. Design requires the same input definition except that the culvert wall section properties are not specified.

Instead desired factors of safety are input. CANDE finds the wall properties that satisfy the given problem by a trial and error procedure.

CANDE can design and analyze pipe installations for any one of four pipe types: corrugated aluminum, corrugated steel, reinforced concrete, and plastic pipe. Only analysis can be performed on a fifth type, called BASIC, which allows for the description of non-standard pipe materials or built-up pipe properties.

Three solution levels are available in CANDE. Level 1 uses the exact elasticity solution as described by Burns and Richard (1964). It is restricted to circular pipes deeply buried in a homogeneous soil. Levels 2 and 3 use the finite element methodology. In level 2 the finite element mesh is automatically generated. Level 3 requires data input to define the mesh. This provides the user with a modeling flexibility in case the predefined meshes of level 2 are not applicable.

CANDE can model slippage at the soil-structure interface as well as structural joint slippage. As in SOILCON, incremental construction is modeled using load steps to represent placement of a structure or placement of a soil layer.

The pipe structure is modeled by a sequence of connected straight beam-column elements with nonlinear stress-strain behavior. The soil can be modeled using one of several choices of constitutive models including the hyperbolic model used in SOILCON.

2.6 OTHER FINITE ELEMENT MODELS FOR BURIED PIPE ANALYSIS

Researchers are also using several other finite element programs for soil-pipe interaction analysis. Taleb and Moore (1999) and Wong et al. (2002) used a general purpose finite element program AFENA (A Finite Element Numerical Algorithm) for analysis buried rigid structures. Noor and Dhar (2003) used another general purpose finite element program ANSYS. Other FE programs used for analysis of buried pipe-soil interaction include DIANA, ADINA, ABAQUS etc.

2.7 SUMMARY

Design of buried rigid pipe generally relies on empirical methods specified in the design codes. Different analytical tools such as Continuum Theory solution, Finite Element analysis, etc were also developed for analysis of buried pipe under earth load. In those analyses pipe-soil system was idealized as plane-strain problem and a 2D analysis was performed. The surface live load was considered as uniformly distributed load acting at the top level (crown level) of the pipe. Then the live load is treated in a similar manner to the earth load. However, researchers have realized the implication of three-dimensional effects of surface live load. Three-dimensional analysis is therefore warranted to effectively investigate the effects of surface live load on pipe response.

CHAPTER 3

FINITE ELEMENT MODEL FOR SOIL-PIPE INTERACTION ANALYSIS

3.1 GENERAL

Digital computers appeared first in the early 1950's but their real significance to both theory and practice did not become widely apparent immediately. Certain individuals did foresee this impact, however, and undertook the codification of the well-established framework analysis procedures in a format suited to the computer, the matrix format. Two noteworthy developments were the publications authored by Argyris and Kelsey (1960) and Turner et al. (1956). These publications wedded the concepts of framework analysis and continuum analysis and cast the resulting procedures in a matrix format. They represent the predominant influence on the development of the finite element method in the subsequent decades.

The technology of finite element analysis has advanced through a number of indistinct phases in the period since the mid-1950's. A detailed review of this progress is given by Zienkiewicz (1994). Motivated by the specific formulation of elements for plane stress, researchers established element relationships for solids, plates in bending, thin shells, and other structural forms. Once these had been established for the purpose of linear, static, elastic analysis, attention turned to special phenomena such as dynamic response, buckling, and material and geometric nonlinearities. It was necessary to extend not only the element formulations but also the general framework of analysis. These developments were followed by a period of rather intensive development of "general-purpose" computer programs, intended to place the capabilities of the method in the hands of the practitioner. The ready availability of such programs at a modest cost of acquisition accounts for the abundance of practical applications of the finite element method.

The finite element method provides a convenient alternative to overcome the simplified pipe response approximations associated with analytical and semi-empirical solutions. Furthermore, the finite element method can be used to account for a whole range of nonlinear and time dependent material (soil and pipe) response. This analysis might be considered for use in the design of certain high cost structures. Alternatively, the finite element analysis can be used to conduct parametric studies and develop simplified design equations.

Finite element analysis has been performed in this research in order to investigate the behavior of rigid pipes considering both two-dimensional and three-dimensional phenomena. The idealized two-dimensional and three-dimensional FE models have been verified by comparing the results from the continuum mechanics theory solution. The continuum mechanics theory was used to develop solutions for thrusts, moments and deflections for buried cylinder by Burns and Richard (1964) and Hoeg (1968). Thus the behavior of rigid pipes under deep burial has been considered in the development of FE model to meet the assumptions applied in continuum solution. A general purpose finite element software ANSYS has been used in the FE analysis.

3.2 TWO-DIMENSIONAL FINITE ELEMENT MODEL

In the two-dimensional FE analysis, the soil was modeled using the two-dimensional 6-Noded Triangular Solid Element (PLANE2 in ANSYS). The element can be used as a plane element (plane stress or plane strain) or as an axisymmetric element. The element is capable of simulating plasticity, creep, swelling, stress stiffening, large deflection, and large strain. The pipe was modeled using the two-dimensional elastic beam-column element (BEAM3 in ANSYS) or the continuum element (PLANE2). BEAM3 is a uniaxial element with tension, compression, and bending capabilities. Half of the geometry was modeled to take the advantages of symmetry. Figure 3.1 shows the finite element mesh developed for idealization of a soil-pipe system.

3.2.1 Geometry Formulation

Figure 3.1 shows a 2D section of the geometry used in this analysis. Surrounding soil has been divided into two different zones, representing the backfill soil and native

soil. Backfill soil is limited to a smaller area, mainly the trench portion. Backfill soil modulus can vary depending upon the degree of compaction during placement. Native soil represents field condition which can be simulated by a unique value of soil modulus for a particular case. $TCOVER$, $BCOVER$, DS in Fig. 3.1 correspond to soil cover above pipe crown, below invert point and side width respectively. It is therefore can be assumed that the thrust and moment of the pipe wall at crown, invert, springline are highly affected with $TCOVER$, $BCOVER$, DS respectively. The depth D_0 below the invert, called bedding thickness, dimensionally equal to the pipe diameter, was assumed to be the backfill soil. SIDD recommends a minimum bedding thickness of $1/24^{th}$ the pipe outer diameter for type I installation, the best of four installation types defined in SIDD. However, a greater bedding thickness is chosen in this analysis to obtain a better bedding support. The effects of boundaries were studied extensively for the finite element simulation.

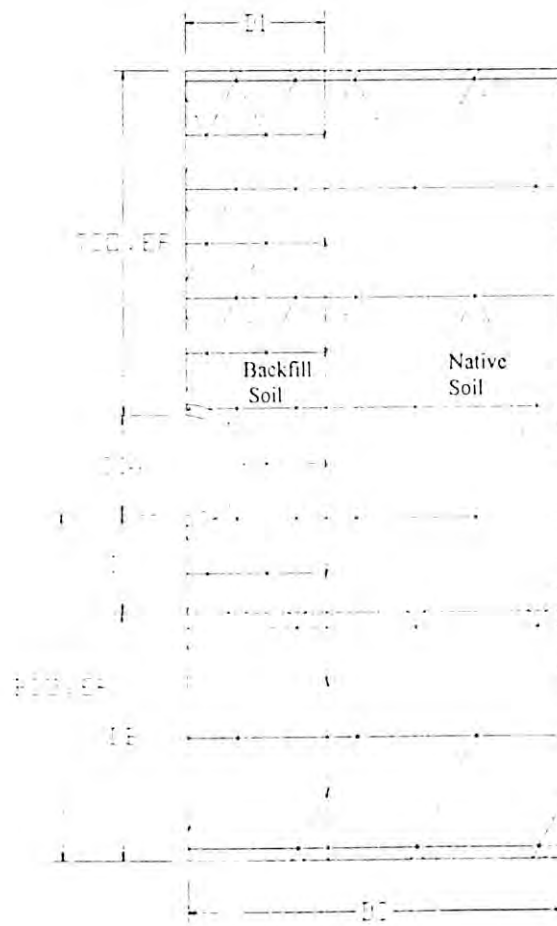


Figure 3.1: Different Soil Zones in Finite Element Mesh

3.2.2 Materials Used in FE Analyses

In order to select the geometry for finite element mesh, a study was undertaken to determine the distance of boundaries for the finite element mesh such that the pipe behavior is not affected by the boundaries. The study was conducted for a typical value of sectional parameter of concrete pipe with wall thickness, $t = 100$ mm and diameter, $D = 800$ mm (i.e., $A = 100$ mm²/mm, $I = 83333.33$ mm⁴/mm). Uniform pressure (P) is considered as surface load in this chapter.

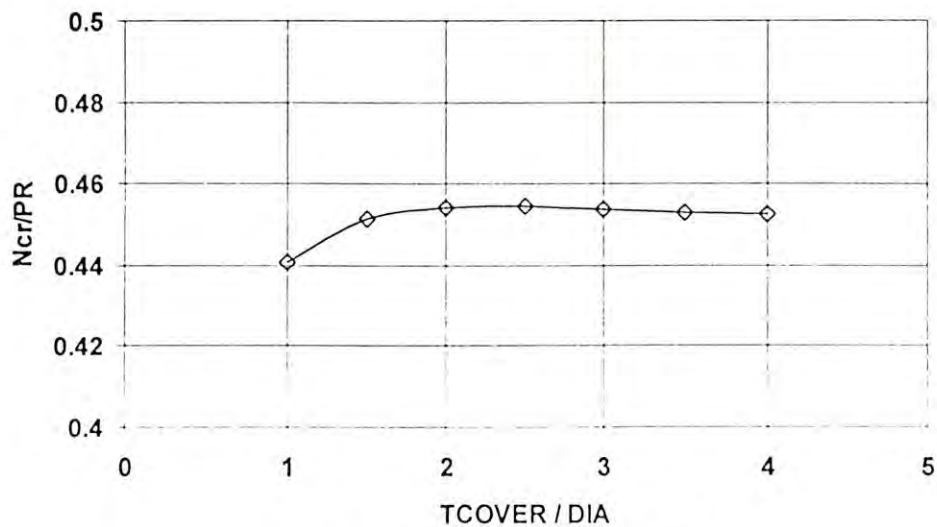
Linear elastic model was used for the concrete pipe in the finite element analysis, since the pipe response will be compared with the continuum theory solution, which is based on linear approximation. Modulus of elasticity of the pipe material was chosen as the typical values for concrete (i.e. 1500 to 30000 Mpa) and the Poisson's ratio was used as 0.2.

Both elastic and perfectly plastic model were used for the soil in the analysis. Soil parameters (Modulus of elasticity, Poisson's ratio) of the soil depend on the type of soil and the degree of compaction. Granular material is generally recommended as the (sand or gravel) backfill material for pipe. Assuming well-graded or poorly graded sand as the backfill material modulus of elasticity may vary from 5 MPa at the loosest condition to 30 MPa at the densest condition for typical installation according to McGrath (1998). The range of soil modulus (5 Mpa - 30 Mpa) has been used in this investigation. Poisson's ratio of the soil was used to be 0.2

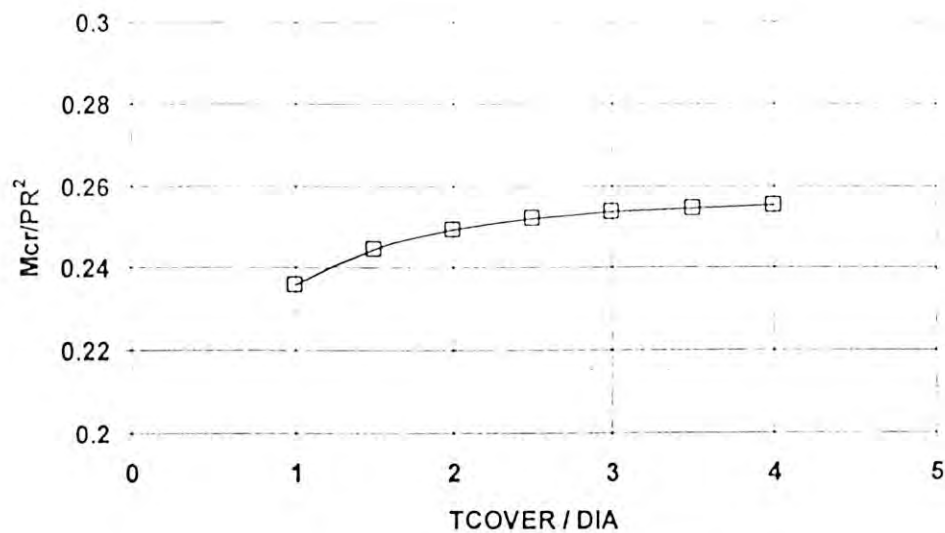
3.2.3 The Study of Boundary Effect

An extensive analysis has been done with different cover and side width to obtain the dimensions so that boundary effects on the results of FE analysis can be minimized. For determining the optimum value of $TCOVER$, $BCOVER$, and DS ; the pipe wall thrust and moment has been considered at the crown, invert and springline respectively, assuming quantities at these location will be affected by the corresponding dimensions. Figure 3.2 shows $TCOVER$ versus pipe wall moment and thrust at the crown of the pipe. For consistency, moment and thrust are always described by M and N respectively where subscripts 'cr', 'sp', 'inv' represents

locations around the pipe circumference (crown, springline and invert respectively). The thrust and moment were expressed in a non-dimensional form (N/PR and M/PR^2 respectively). Figure 3.2 reveals the relationships for typical range of sectional parameters with the typical range of the modulus of elasticity of pipe material and it has been formulated by taking surface load 1 Newton per mm length in plain strain condition. Figure 3.2 shows that crown thrust and moment to some extent increases with the increase of $TCOVER$, albeit by a small amount. For $TCOVER$ greater than 3 times pipe diameter, the effect on crown moment is minimized.



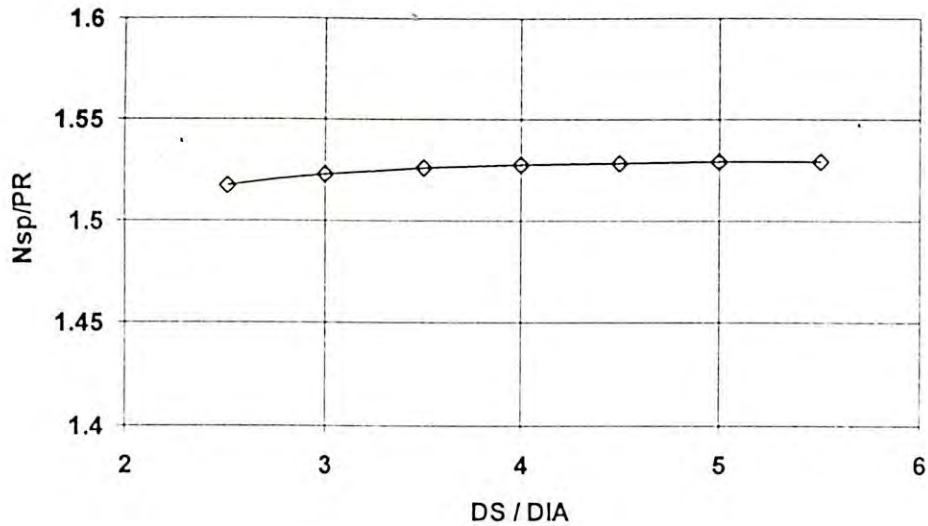
(a) Thrust at Crown with $TCOVER$



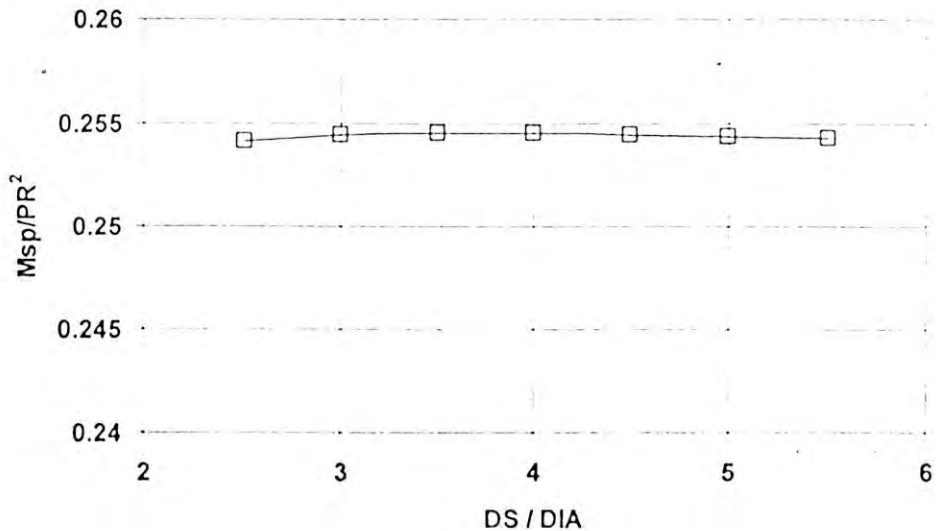
(b) Moment at Crown with $TCOVER$

Figure 3.2: Effects at Crown due to uniform Surface Load

Figure 3.3 shows DS versus pipe wall moment and thrust relationship at springline and Figure 3.4 shows DB versus moment and thrust relationship at invert. It revealed that the thrust and the moment were not affected significantly when the boundaries are placed at a distance of 3 times the pipe diameter on each side. Boundaries at a distance of 3 times pipe diameter were used in the finite element analysis.

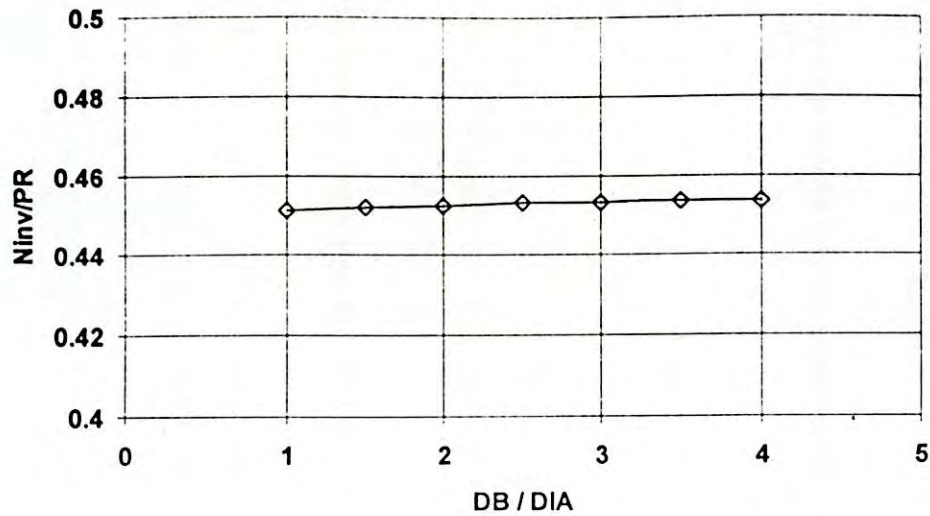


(a) Thrust at Springline with DS

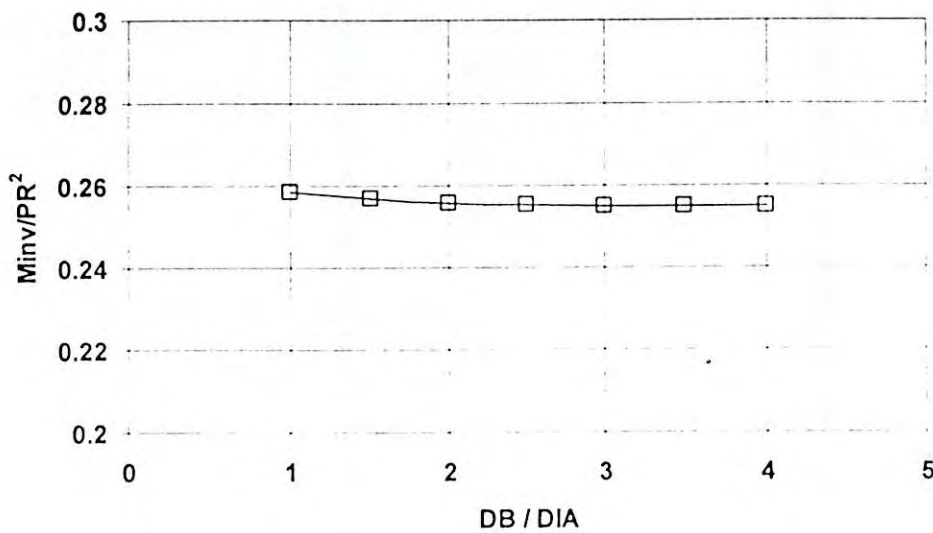


(b) Moment at Springline with DS

Figure 3.3: Effects at Springline due to uniform Surface Load



(a) Thrust at Invert with DB



(b) Moment at Invert with *DB*

Figure 3.4: Effects at Invert due to uniform Surface Load

3.2.4 Effect of Mesh Refinement

A similar investigation was performed to determine optimum mesh density in the finite element mesh. In ANSYS, mesh densities are represented by the command

“SMRTSIZE”. This command specifies meshing parameters for automatic (smart) element sizing and its value controls the fineness of the mesh. It can have an integer value from 1 (fine mesh) to 10 (coarse mesh). Figure 3.5 shows stress distribution in soil above the pipe crown with depth below the ground surface for different values of SMRTSIZE. It appears that the SMRTSIZE values used (2 to 5) do not have significant effect on the calculated quantities. Figure 3.6 shows that the pipe crown moment against SMRTSIZE. The figure indicates no significant changes of moments for the typical ranges of sectional parameters and materials chosen in this study. The SMRTSIZE value of 3 appeared to work reasonably and therefore, considered for the analysis performed in this study. Figure 3.7 shows the finite element mesh used. Smooth rigid boundaries were used on the line of symmetry and on to the right. Rough rigid boundary was used at the bottom of the mesh.

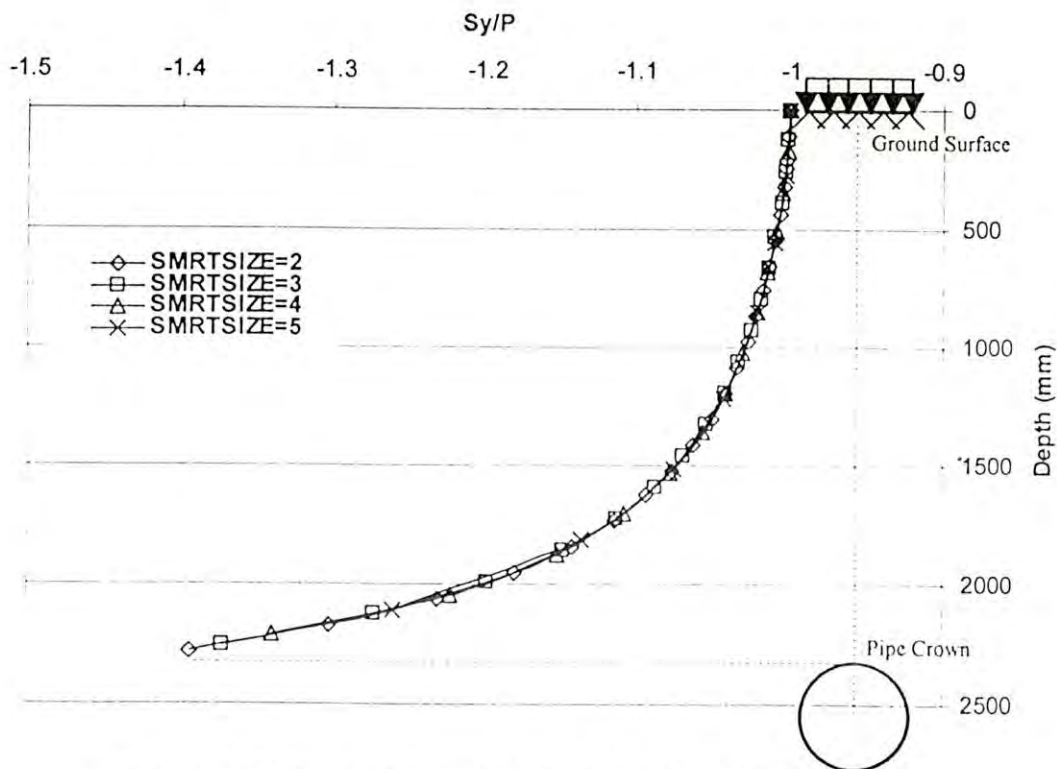


Figure 3.5: Vertical Stresses with Mesh Density (2D Model)

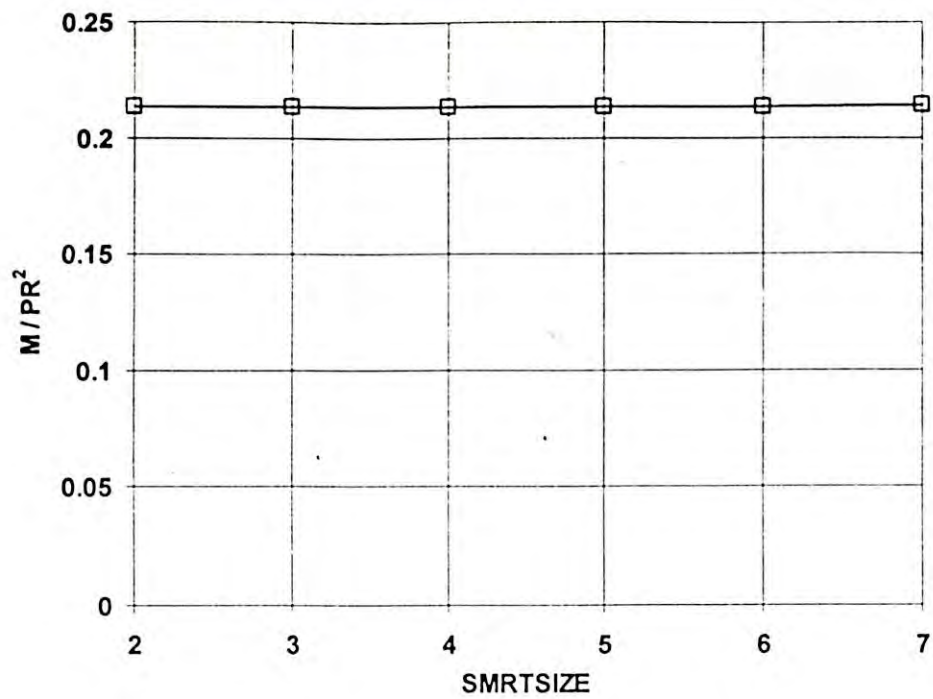


Figure 3.6: Crown Moment with Mesh Density

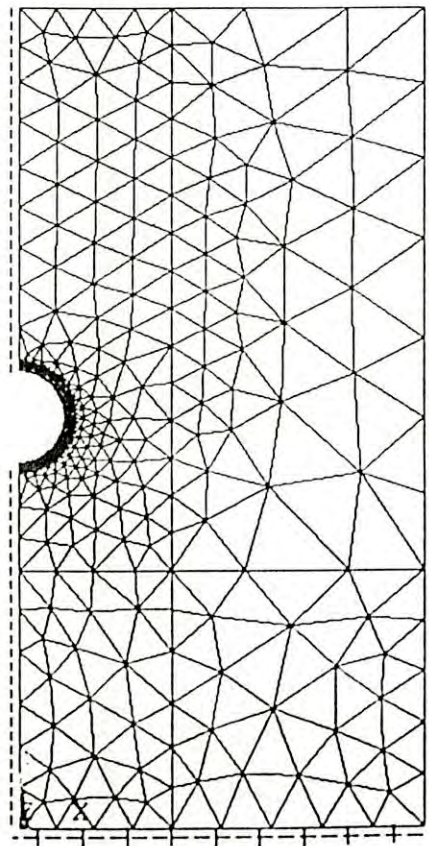


Figure 3.7: Finite Element Mesh (2D)

3.2.5 Effect of Soil-Pipe Interaction

Figure 3.5, discussed earlier, shows that the soil stress increases with depth under a uniformly distributed surface load. However, a constant stress would be expected with the depth in a homogeneous soil under uniform surface load. The stress increase observed in Figure 3.5 is due to the interaction between the pipe and soil during distribution of load. The rigid pipe with greater stiffness relative to the soil appeared to attract load toward the pipe causing greater load reaching to the pipe crown. The mechanism is called 'Arching'. Contours of soil and pipe stress are shown in Appendix A. Figure A-1 and A-2 reveal the distribution stress between the pipe and soil due to the interaction. Soil-pipe interaction for the ground stress around pipe under concentrated surface load has been discussed further in Chapter 4 (Art. 4.3.4).

3.2.6 Evaluation Using Close-form Solution

The finite element mesh developed for analysis of pipe-soil interaction has been evaluated comparing the results of analysis with those from the Continuum Theory solution (Burns and Richard, 1964). An extensive analysis has been performed to compare the results of different models for deeply buried pipes. Figure 3.8 shows springline thrust, N_{sp} versus surface load relationship under a uniformly distributed load applied on top of the pipe. Load was applied on top of the finite element mesh during the finite element analysis. Solution from finite element analysis, considering both elastic and elasto-plastic material model, and Continuum theory is included in Fig. 3.8. In linear elasto-plastic analysis, Drucker-Prager model has been used with the consideration of soil having same value for friction angle and dilatancy angle (associated flow rule). The figure reveals that the FE analysis calculates the same springline thrust as given by the Continuum Theory solution. Figure 3.9 shows springline bending moment, M_{sp} calculated using different methods. The Continuum Theory solution also appeared same as the springline moment found by the FEM. The coefficient of lateral earth pressure, K_0 in the continuum solution was estimated as 0.25 using $\frac{\nu_s}{1-\nu_s}$ relation to ensure a similar value as in the finite element analysis.

The earth pressure co-efficient was not required in the finite element analysis.

Figure 3.9 also reveals that the effect of soil plasticity on the pipe response was not significant for the buried rigid pipe considered here. This is due to the fact that the zone of soil plasticity was not significant since deformation of the rigid pipe was insignificant. Also, the pipe usually takes the greater portion of the load relative to the soil.

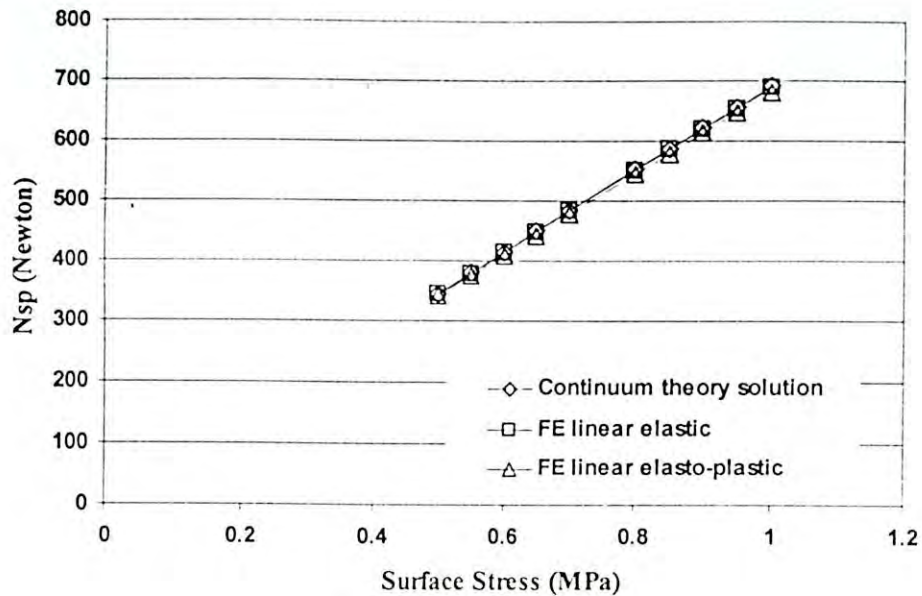


Figure 3.8: Thrust at Springline with Surface Load

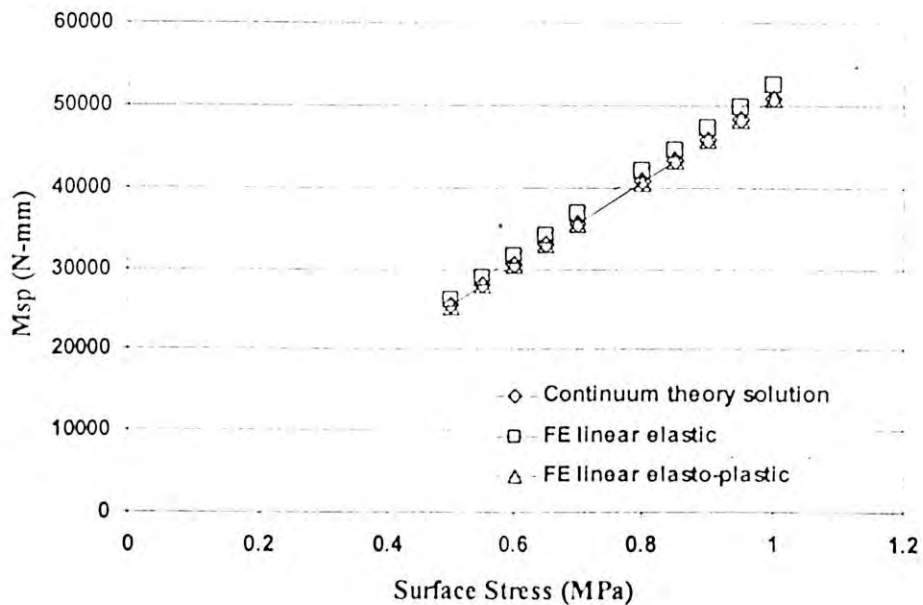


Figure 3.9: Moment at Springline with Surface Load

3.3 THREE-DIMENSIONAL FINITE ELEMENT MODEL

Three-dimensional finite element analysis was performed in this research for analysis soil-pipe interaction under three-dimensional load (surface live load). The soil and pipe were modeled using the 3D structural solid element (SOLID45 in ANSYS) for the three-dimensional analysis. The element is defined by eight nodes having three degrees of freedom at each node: translations in the nodal x, y, and z directions. The element has plasticity, creep, swelling, stress stiffening, large deflection, and large strain capabilities.

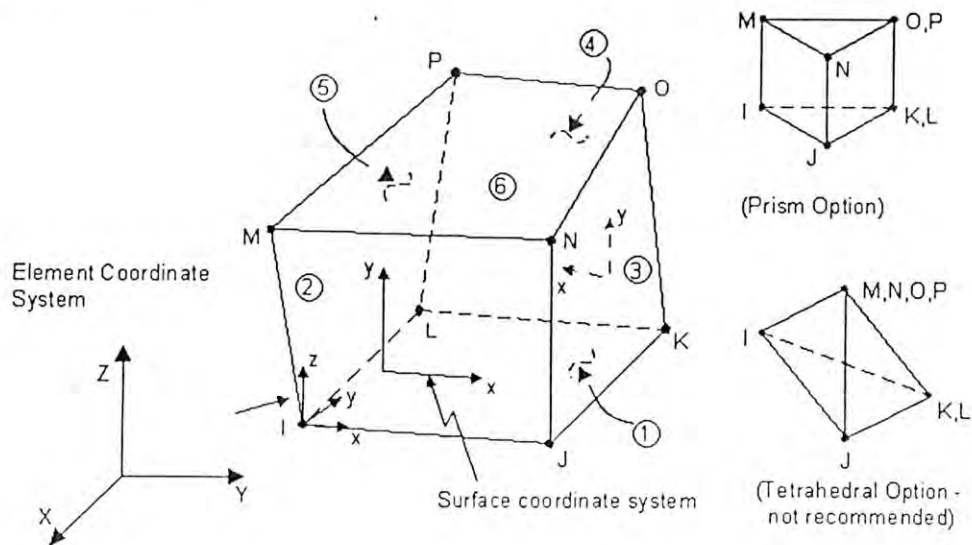


Figure 3.10: 3-D Structural Solid Element (SOLID45 in ANSYS)

The geometry, node locations, and the coordinate system for this element are shown in Figure 3.10. The element is defined by eight nodes and the orthotropic material properties. Orthotropic material directions correspond to the element coordinate directions. Element loads are described in "Node and Element Loads". Pressures may be input as surface loads on the element faces as shown by the circled numbers on 'SOLID45'. Positive pressures act into the element.

3.3.1 Geometry Formulation

The 3D model geometry has been formulated by extruding 2D section of the geometry used. In this case, the full 2D section was developed by using 4-noded plastic small strain shell (SHELL143 in ANSYS) in the order first. The shell element

plastic small strain shell (SHELL143 in ANSYS) in the order first. The shell element was then replaced by SOLID45 element. Surrounding soil has been divided into two different zones, representing the backfill soil and native soil as before. The final 3D mesh has been developed by considering the 2D finite element mesh discussed earlier. The same materials as in 2D analysis were also used in the 3D model. Figure 3.11 shows the geometry of 3D finite element model used in the study.

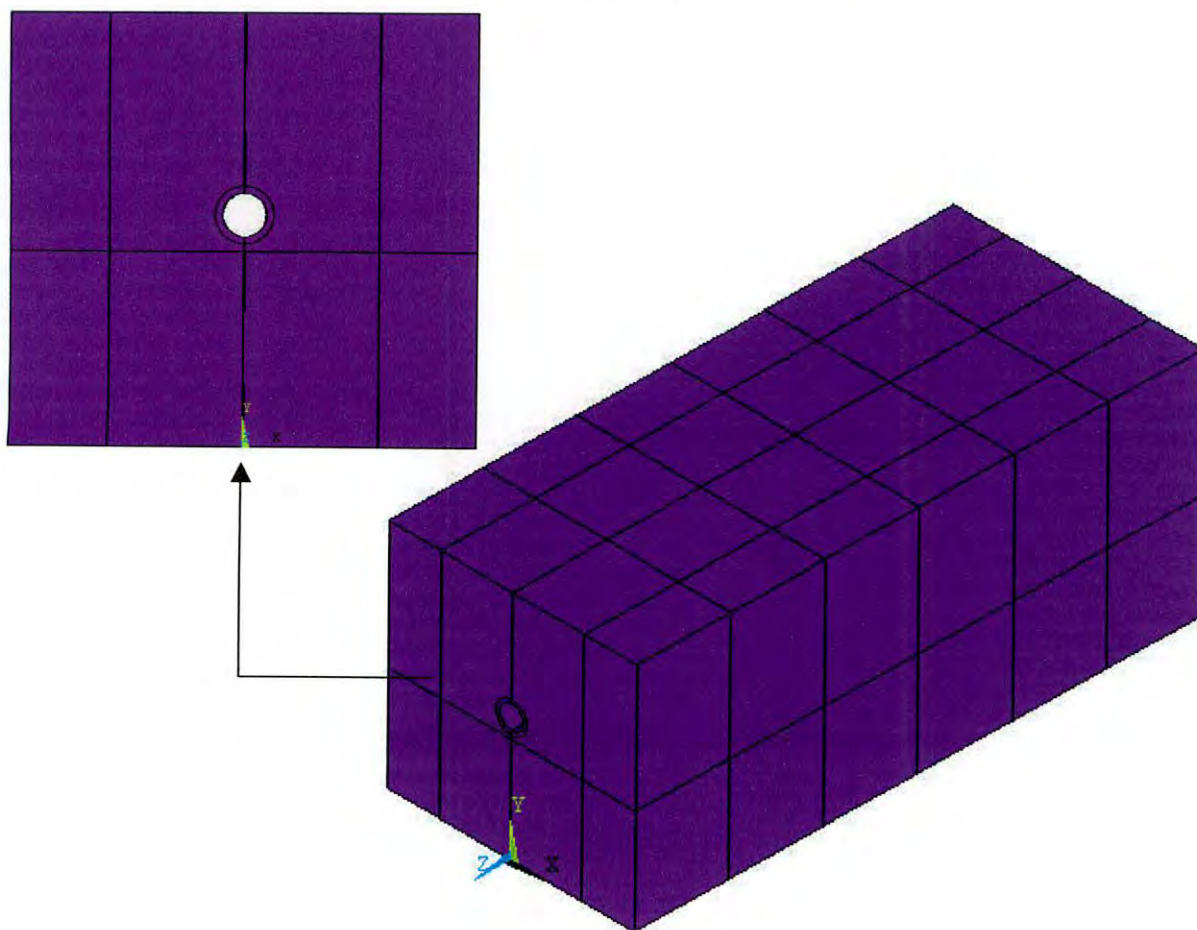


Figure 3.11: Finite Element Model Geometry (3D)

3.3.2 Tuning of Three-dimensional Mesh

An extensive analysis was performed to develop an optimum 3D mesh such that the results of analyses are not affected by the element size and the boundaries of the mesh. Though the idealization has been done by 2D model results and continuum theory solution, the final tuning has been done by changing SMRTSIZE value. Like in 2D model, it is also found in 3D model that the SMRTSIZE value considered (2 to 5) do not affect significantly the stresses in the soil, as shown in Fig. 3.12. However,

SMRTSIZE value 5 was taken into consideration in this study as the fine mesh make the calculation more tedious.

A study was also performed to examine the effect of plane-strain idealization of pipe-soil interaction involving two materials with different stiffness and Poisson's ratio. Analysis was performed using 2D and 3D finite element methods and the results of the analysis were compared.

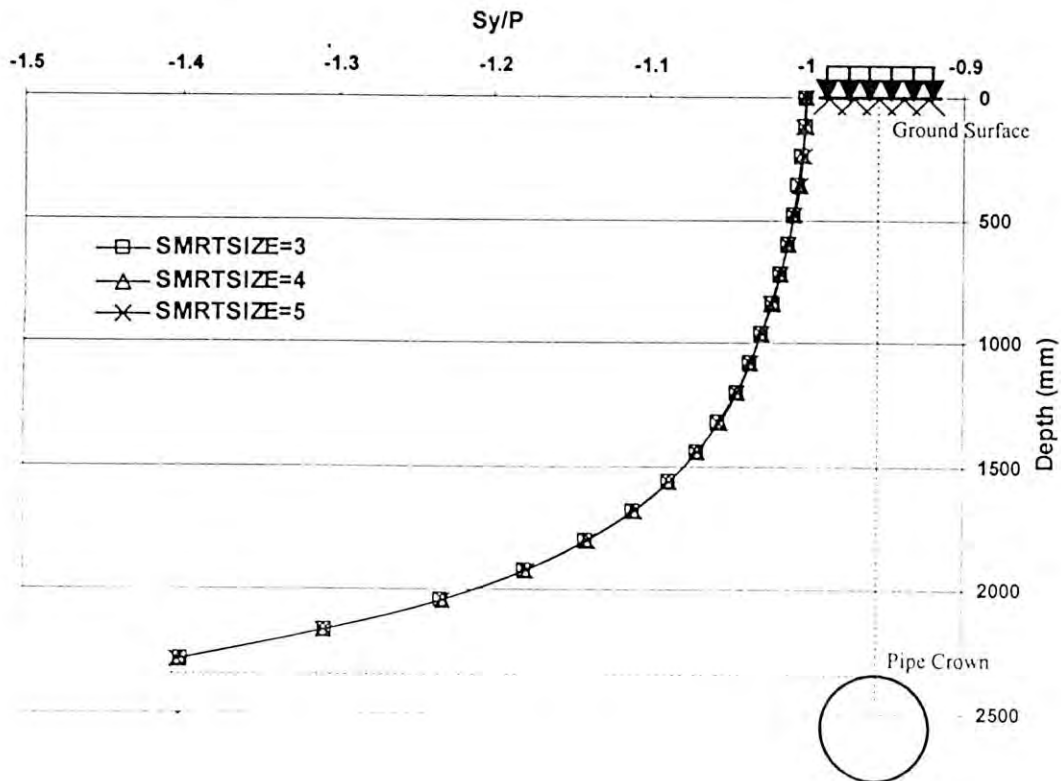


Figure 3.12: Vertical Stresses with Mesh Density (3D Model)

3.4 PARAMETRIC STUDY

A parametric study has been conducted here to identify the effects of different pipe and soil parameters on the results of analysis. Material parameters generally used for elastic materials are modulus of elasticity, E and Poisson's ratio, ν . Poisson's ratio generally does not vary significantly for concrete pipe and soil material. Therefore the effects of modulus of elasticity of pipe with respect to that of soil are investigated. Figure 3.13 to 3.16 reveals the effect of pipe/soil stiffness of the pipe response.

Figure 3.13 and 3.15 shows the circumferential stresses at the crown and springline of the pipe outer surface respectively, for different pipe to soil modulus. Circumferential stress at crown, S_x , and at springline, S_y , were normalized with applied pressure, P . The figures shows that when both pipe and soil has the same modulus of elasticity, the 3D and 2D finite element analysis calculate the almost same stress at the crown and springline. However, as the pipe modulus was increased, the 3D analysis underestimated both the crown and springline stresses. The study indicates that variation of modulus of the materials in the interaction has an effect on the two-dimensional idealization of a three-dimensional problem. For the ratio of pipe modulus, E_p , to soil modulus, E_s , up to 50, the effect is not significant. However, for greater ratio the differences can be high. Figure 3.14 and 3.16 reveals the percentage of stress deviation at crown and springline of the pipe respectively in both 2D and 3D models with respect to E_p/E_s . For a concrete pipe with $E_p=20000$ MPa in a standard soil (with $E_s=20$ MPa), the stresses deviation at crown is about 4 percent while it is about 6.5 percent at springline.

Thus, it is revealed that while 2D plane-strain idealization may be reasonable for pipes with low modulus (i.e., thermoplastic pipes). However, 3D analysis is desirable for concrete pipe and pipes with stiffer materials. Nonetheless, the error associated with 2D idealization is not significant (4 to 6%) from practical point of view.

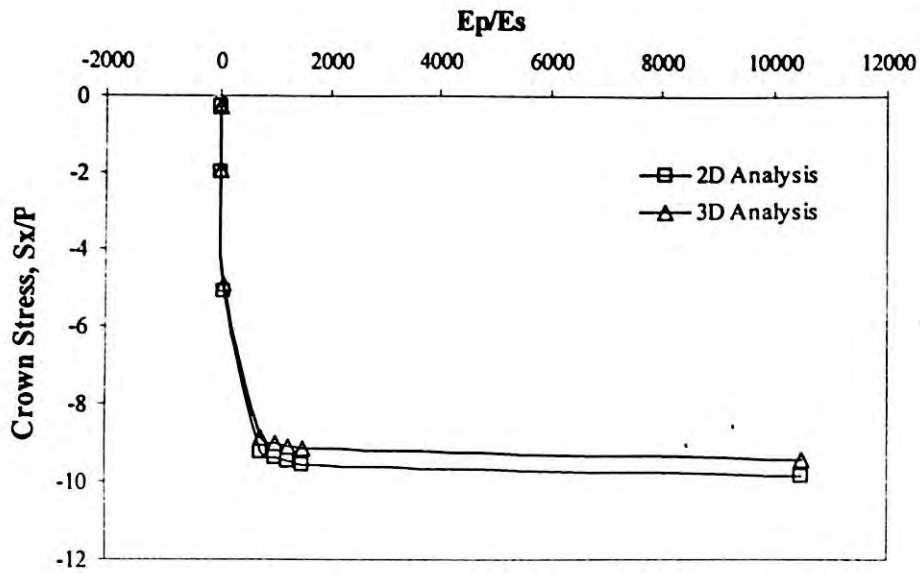


Figure 3.13: Crown Stresses in Different Pipe-Soil Modulus

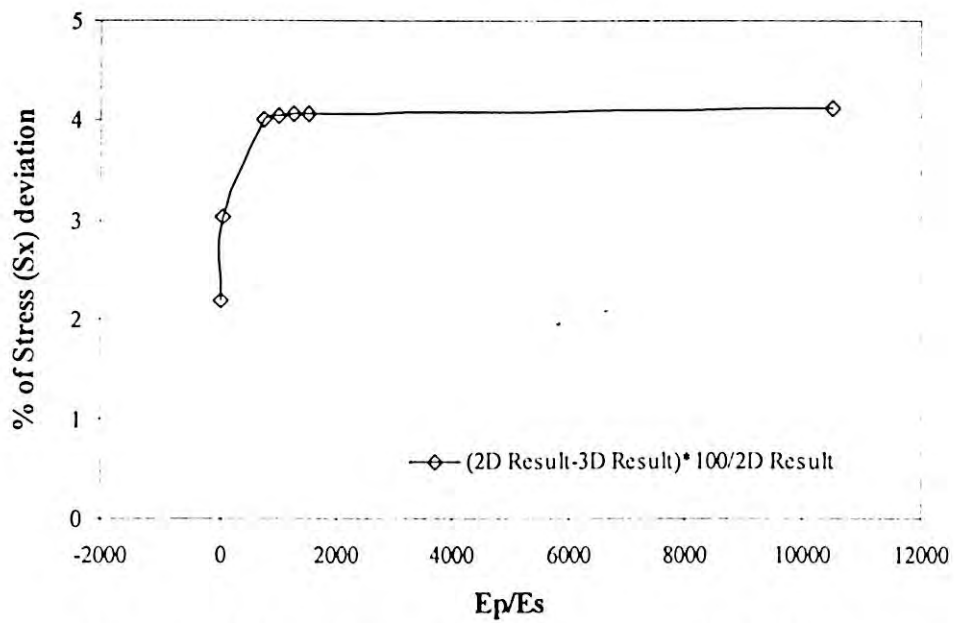


Figure 3.14: Variation of Crown Stresses in 2D & 3D Model

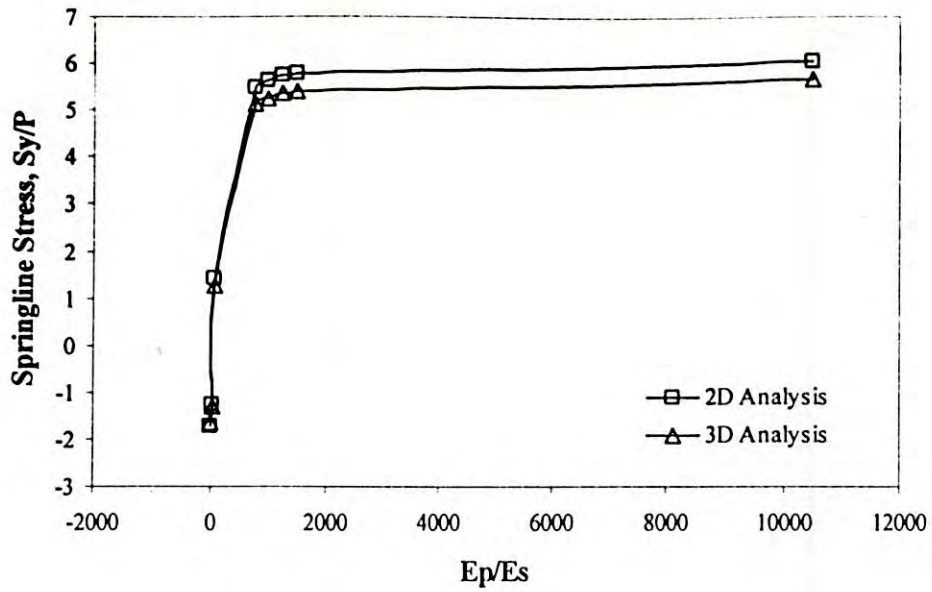


Figure 3.15: Springline Stresses in Different Pipe-Soil Modulus

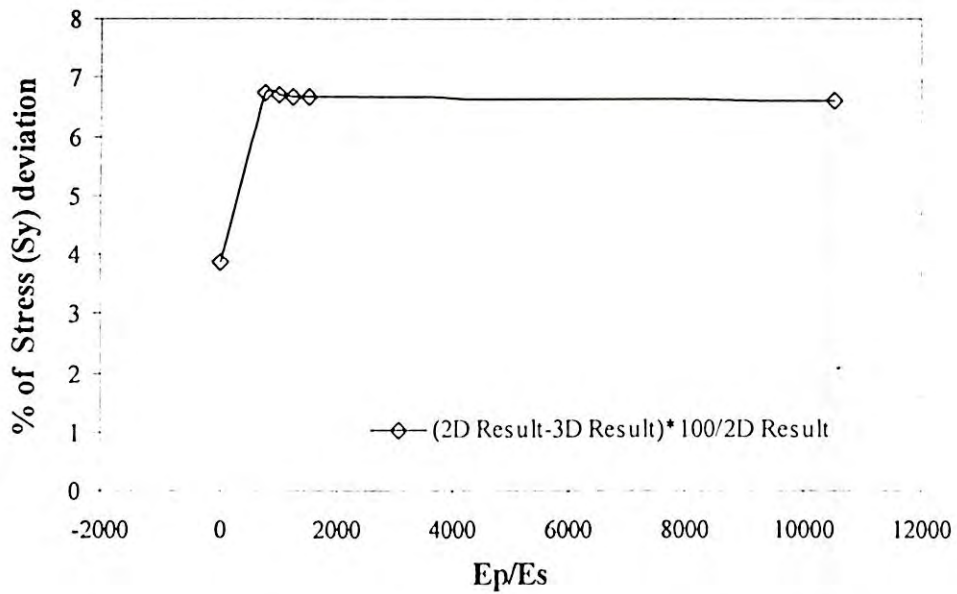


Figure 3.16: Variation of Springline Stresses in 2D & 3D Model

3.5 SUMMARY

This chapter focuses the development of a two-dimensional and three-dimensional finite element mesh. For this a sensitivity analysis was carried out to eliminate error associated with the density of mesh as well as extent of the boundary taken into consideration. Results of the continuum theory solution were used to evaluate finite element model. The study revealed that the thrust and the moment of a pipe are not affected significantly when the boundaries are placed at a distance of 3 times the pipe diameter on each side. SMRTSIZE value of 3 appeared reasonable for mesh generation in both 2D and 3D analysis. Effect of pipe-soil interaction was found to govern the distribution of stress around the pipe and in the soil due to surface load. The rigid pipe with greater stiffness attracted load from the soil, resulting in a greater stress at the crown level of pipe, due to development of arching. Effect of soil plasticity on the pipe response was found to be insignificant for buried rigid pipe.

The parametric study conducted shows that the ratio of the pipe to soil modulus has an influence on the results from 2D plane-strain idealization and 3D idealization. Plane-strain idealization appeared very good for pipes with low material modulus, while for pipe with higher modulus, results from 2D analysis deviates from 3D analysis by 4 to 6% for the cases considered in this study.

CHAPTER 4

SOIL STRESSES DUE TO SURFACE LOAD

4.1 GENERAL

In traditional design of rigid pipe, earth load on top of the pipe is calculated using the Marston-Spangler theory (Spangler and Handy, 1973) with no consideration of surface load. However, recent codes (ASCE 1993, CSA 2000, AASHTO 2002), developed based on finite element analysis consider the live load to be distributed uniformly at crown level of the pipe. The uniformly distributed load is added to the earth load to calculate the earth pressure around the pipe based on SIDD. The Standard Installation Direct Design (SIDD) method provides four different earth pressure distributions around the pipe for four standard installation types. The pressure distribution is used to calculate bending moments and stresses on the pipe during design.

The assumption of uniformly distributed live load at crown level may not be true, particularly for pipes under shallow burial. Under shallow burial condition, the effects of live load would be a three-dimensional phenomenon. A complete three-dimensional analysis is therefore necessary to understand the phenomena reasonably.

This chapter presents three-dimensional finite element analyses of a buried concrete pipe under surface live loads. Stresses above the pipe and the surrounding soil are calculated using finite element analysis. The stresses are then compared with corresponding values proposed by the different design codes (ASCE 1993, CSA 2000 & AASHTO 2002) for evaluation of the codes.

4.2 ACCOUNT FOR LIVE LOAD IN THE DESIGN CODES

4.2.1 ASCE 15-93 Code

ASCE 15-93 adopted a direct design method known as Standard Installation Direct Design (SIDD) for buried rigid pipes. The design method is based on an earth pressure distribution around a pipe developed using soil-pipe interaction analysis. During the early 1980's, Heger et al. (1985) developed earth pressure distribution around concrete pipes based on a rigorous finite element analysis of soil-pipe interaction using a FE software named SPIDA (Soil-Pipe Interaction Design and Analysis). The distribution of earth pressure is commonly known as 'Heger Earth Pressure'. Four standard variations of the Heger's earth pressure distribution were developed to represent a range of installation conditions. Table 4.1 describes the four installation types considered in the SIDD. Figure 4.1 shows the related terminologies for those four standard installations. Type I specifies the highest quality of backfill materials and soil compaction effort in the embedment zone below the pipe's springline, while Type IV installation requires no imported bedding material at the foundation or the haunches and limited field control. The Type IV installation utilizes the inherent strength of the pipe with little assistance from the surrounding soil. SIDD classifies backfill soil into three categories, namely non-cohesive soil (e.g., sand), sandy silt and silty clay to clay.

Table 4.1: Standard Installation of concrete pipes and backfill Requirements (ASCE, 1993).

Installation type	Bedding Thickness	Soil type and level of compaction (%Standard Proctor)	
		Haunch and outer bedding	Lower side
Type I	$D_o/24$ minimum, not less than 3 in. (75 mm). If rock foundation, use $D_o/12$ minimum, not less than 6 in. (150 mm)	SW (95%)	SW (90%), ML (95%), or CL (100%)

Type I I	$D_o/24$ minimum, not less than 3 in. (75 mm). If rock foundation, use $D_o/12$ minimum, not less than 6 in. (150 mm)	SW (90%) or ML (95%)	SW (85%), ML (90%), or CL (95%)
Type I I I	$D_o/24$ minimum, not less than 3 in. (75 mm). If rock foundation, use $D_o/12$ minimum, not less than 6 in. (150 mm)	SW (85%), ML (90%), or CL (95%)	SW (85%), ML (90%), or CL (95%)
Type I V	No bedding required, except if rock foundation, $D_o/12$ minimum, not less than 6 in. (150 mm)	No compaction required, except if CL, use 85% CL	No compaction required, except if CL, use 85% CL

The SIDD method accounts for the interaction between the pipe and soil envelope in determining loads and distribution of earth pressure on a buried pipe. Figure 4.2 shows the earth pressure distribution for four different standard installations considered in SIDD. The loads and pressure distributions are used to calculate moment, thrust and shear in the pipe wall, and required pipe reinforcement.

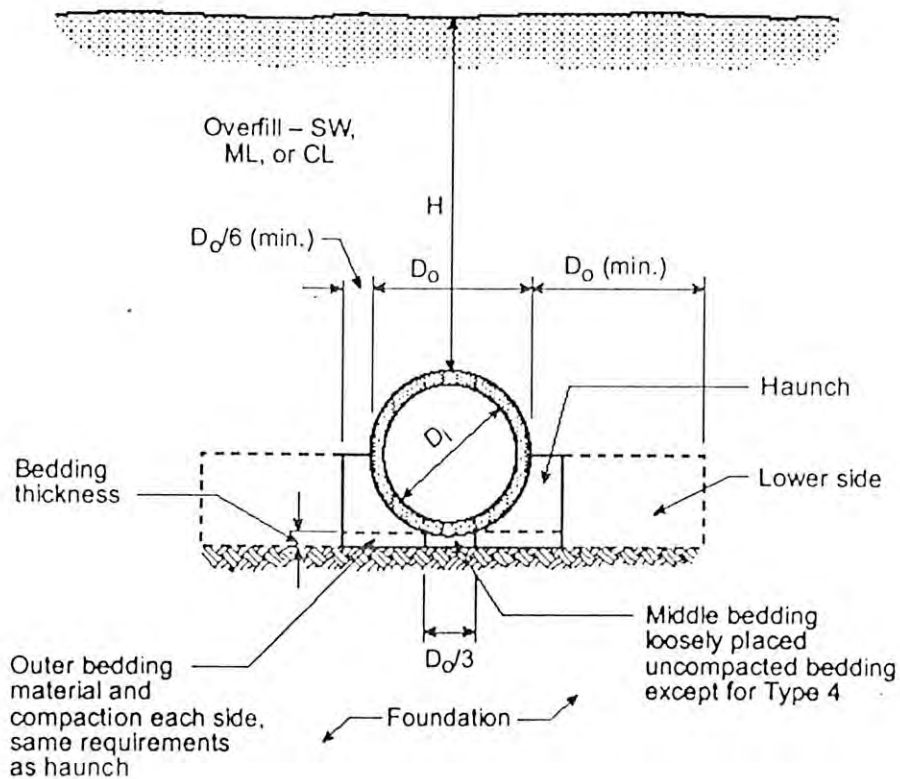
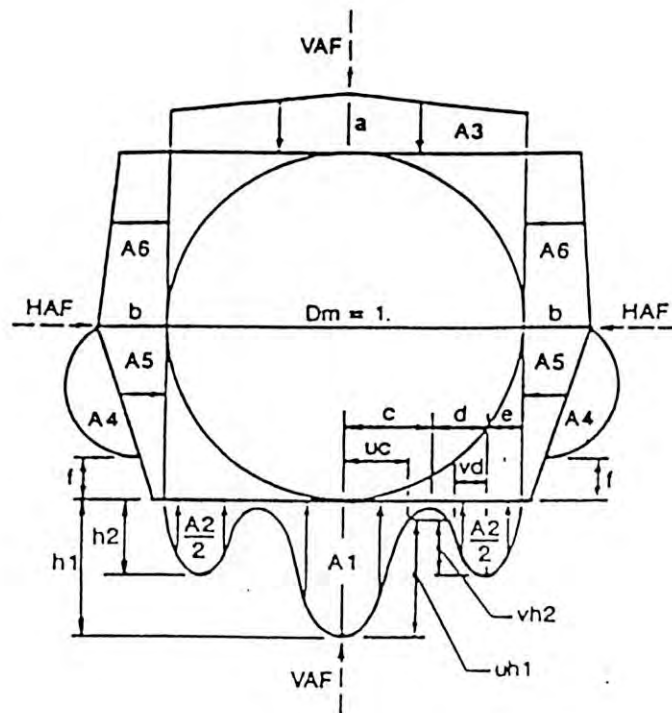


Figure 4.1: Standard Embankment Installations (ASCE, 1993)



Type	VAF	HAF	A1	A2	A3	A4	A5	A6	A	b	c	E	f	U	v
I	1.35	0.45	0.62	0.73	1.35	0.19	0.06	0.18	1.40	0.40	0.18	0.06	0.05	0.80	0.80
II	1.40	0.4	0.85	0.55	1.40	0.15	0.06	0.17	1.45	0.40	0.19	0.10	0.05	0.82	0.70
III	1.40	0.37	1.05	0.35	1.40	0.10	0.10	0.17	1.45	0.36	0.20	0.12	0.05	0.85	0.60
IV	1.45	0.30	1.45	0.00	1.45	0.00	0.11	0.19	1.45	0.30	0.25	0.00		0.90	

$$d = 0.5 - c - e, h_1 = \frac{1.5(A1)}{c(1+u)}, h_2 = \frac{1.5(A2)}{d(1+v) + 2e}$$

Figure 4.2: Arching Coefficients and Heger Earth Pressure Distribution (Heger et al. 1985)

The surface live load in the ASCE code is assumed to be distributed uniformly over top of the pipe. Figure 4.3 shows the effective area of load distribution over a buried pipe. Overlapping pressures at the top of the buried pipe from adjacent surface wheels are uniformly distributed over the combined effective uniform pressure area for each individual load as shown in Figures 4.4 and 4.5.

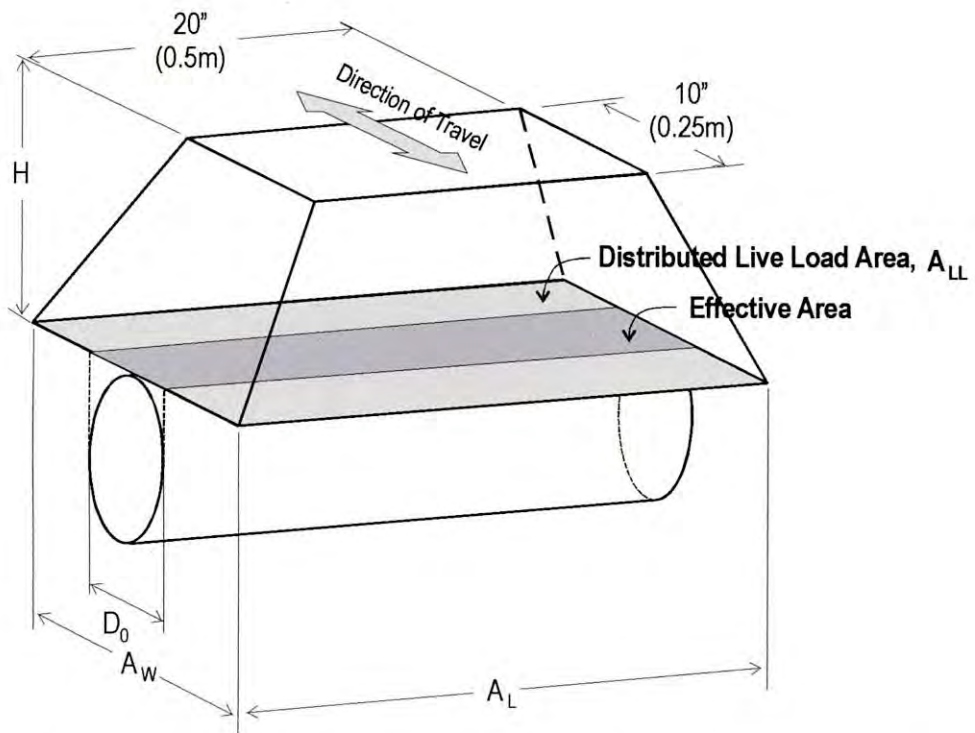


Figure 4.3: Effective Area of the Live Load (After ASCE, 1993)

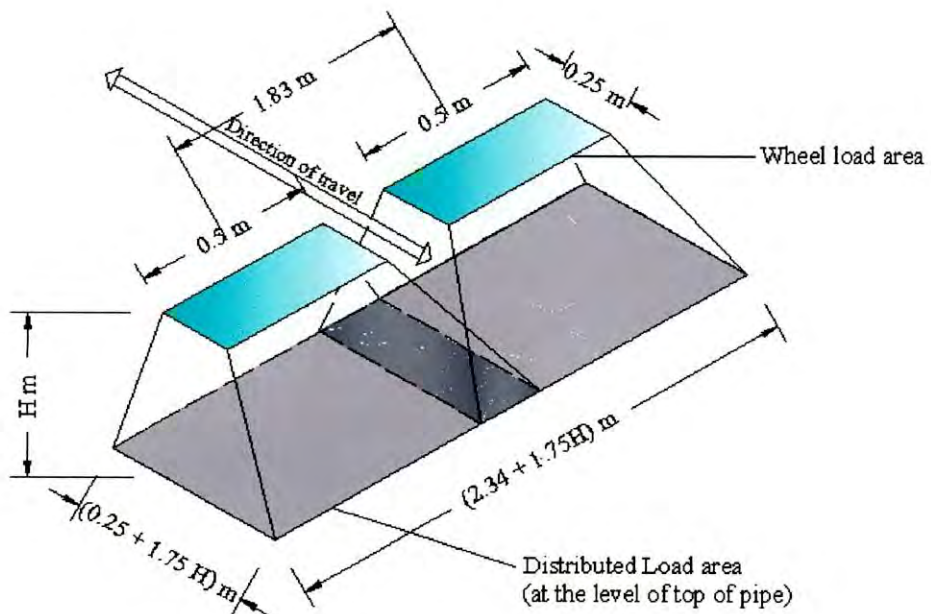


Figure 4.4: Distributed Load Area Two HS 20 Trucks Passing

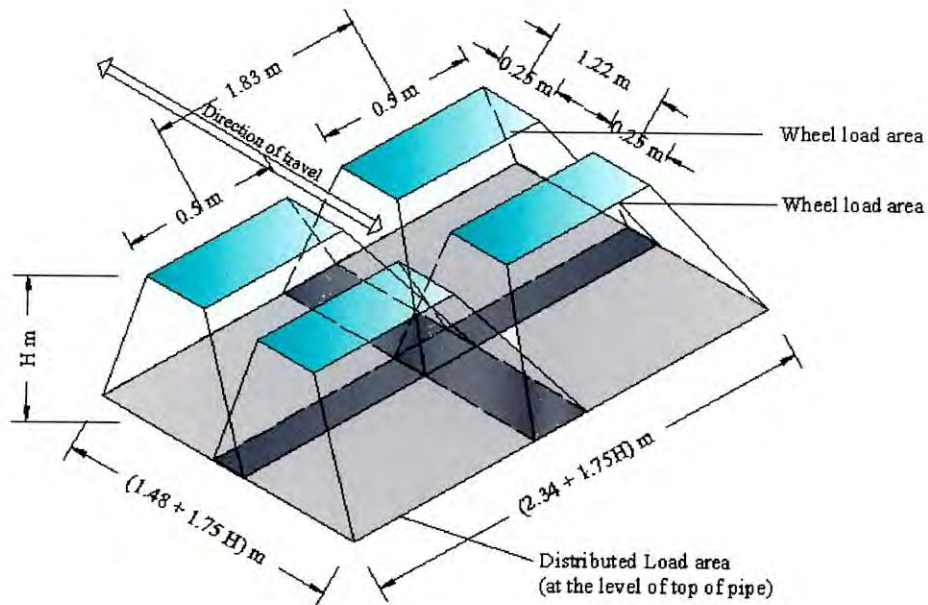


Figure 4.5: Distributed Load Area Alternative Loads in Passing Mode

The load and pressure distribution at the top of the pipe produced by the surface live load and the pressure distribution applied to a buried pipe are determined from that portion of the effective combined uniform pressure area that extends over the outside diameter of the pipe. Thus, the equivalent load on top of the pipes is estimated in ASCE (1993) as:

$$P_p = \frac{P_w D_o L}{A_e} \quad (4.1)$$

Where

D_o = Outer pipe diameter

L = Dimension of the effective area along the length of the pipe

P_w = Wheel load

A_e = Effective area on top of the pipe

The effective length, L_e , of the buried pipe that resists the applied live load calculated above is the length that is subject to the effective combined uniform pressure area plus an additional length equal to 1.75 times $\frac{3}{4}$ of the pipe outside diameter, split equally between each side of the pressure area as shown in Figure 4.6. The total pressure per unit length of the pipe is obtained as:

$$P_L = \frac{P_p}{L + 1.75 \times 0.75 D_o} \quad (\text{N/m}) \quad (2)$$

Where

P_L = Live load per unit length of the pipe

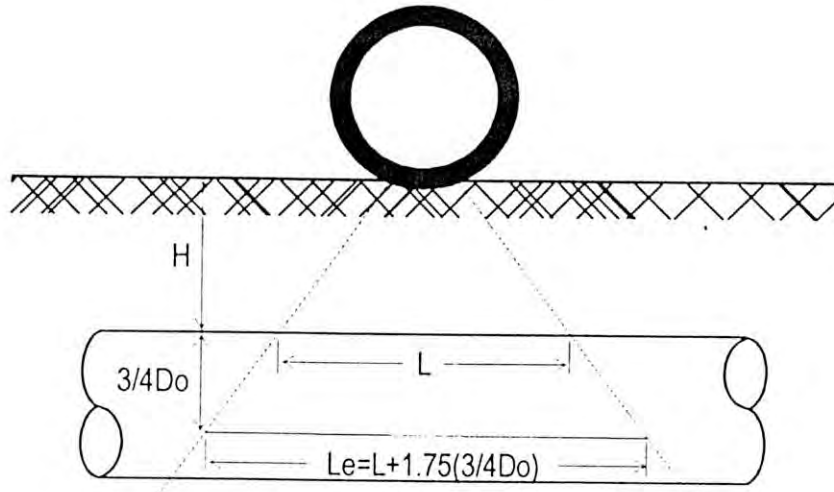


Figure 4.6: Effective Supporting Length (after ASCE, 1993)

The total load per unit length of pipe is the applied live load divided by the effective length of pipe, L_e . Critical loading configurations are shown in Table 4.2.

Table 4.2: Critical Live Loads and Spread Dimensions at the top of the Pipe (ASCE, 1993)

H (m)	P_w (kg)	A_w (m)	A_{LL} (m)
$H < 0.76$	7,250	$0.25 + 1.75H$	$0.50 + 1.75H$
$0.76 < H < 1.25$	14,500	$0.25 + 1.75H$	$2.34 + 1.75H$
$H > 1.25$	21,800	$1.48 + 1.75H$	$1.48 + 1.75H$

The supporting pressures under the pipe are assumed to have the same distribution as those for earth load for each standard installation type.

4.2.2 Canadian Highway Bridge Design Code

The surface live load in the CHBDC (Canadian Highway Bridge Design Code) is approximated using a uniform pressure on top of the pipe distributed over a rectangle. The area of the rectangle depends on the depth of fill over the structure. If the depth is 0.60 m or more, sides of the rectangle will be the footprint of the wheel of the CLS Truck plus 1.75 times the depth of fill. When area of the distributed loads from two or more wheels overlaps, total loads of those wheels are distributed over the smallest area that includes their individual areas. Extent of the area can not be greater than the total width of the structure supporting the fill. No distribution beyond the footprint is considered for depth of fill less than 0.60 m. The reacting earth pressure at the bottom of the concrete pipe due to surface live loads is determined using the same non-dimensional pressure distribution, developed for earth loads (Heger et al. 1985). Figure 4.7 shows the Heger pressure distribution used in CSA (2000). To obtain the actual bottom pressures for an installation type, the force ratios $F1$ and $F2$ is to be multiplied by the total live load acting on the pipe divided by the vertical arching factor. Lateral earth pressure is neglected. Table 4.3 shows the force factors used in this code for earth loads. Earth pressure factors and length factors for earth pressures are shown in Table 4.4 and 4.5.

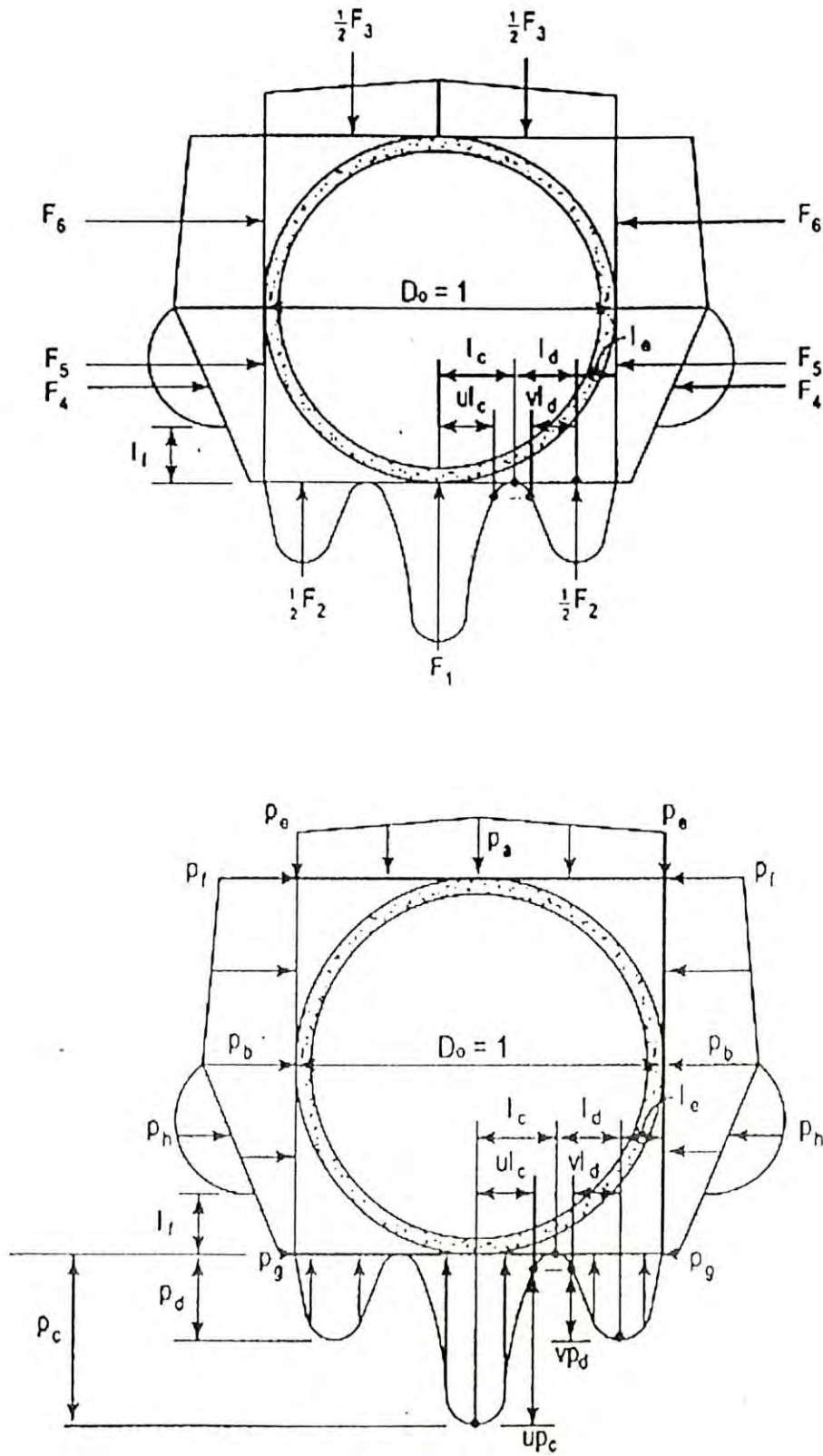


Figure 4.7: Earth Pressure Distribution for Standard Installations of Circular Concrete Pipes (Heger et al. 1985)

Table 4.3: Force Factors for Earth Loads (Heger et al. 1985)

Installation Type	F ₁	F ₂	F ₃	F ₄	F ₅	F ₆
C1	0.62	0.73	1.35	0.19	0.08	0.18
C2	0.85	0.55	1.40	0.15	0.08	0.17
C3	1.05	0.35	1.40	0.10	0.10	0.17
C4	1.45	0.00	1.45	0.00	0.11	0.19

Table 4.4: Earth Pressure Factors (Heger et al. 1985)

Installation Type	P _a	P _b	P _b	P _d
C1	1.40	0.40	2.87	1.85
C2	1.45	0.40	3.51	1.48
C3	1.45	0.36	4.26	0.99
C4	1.45	0.30	4.58	0.00

Table 4.5: Length Factors for Earth Pressures (Heger et al. 1985)

Installation Type	l _c	l _e	l _f	u	v
C1	0.18	0.08	0.05	0.80	0.80
C2	0.19	0.10	0.05	0.82	0.70
C3	0.20	0.12	0.05	0.85	0.60
C4	0.25	0.00	-	0.90	-

4.2.3 AASHTO Design Code

The AASHTO (2002) LRFD design loads are the HS 20 with a 32,000 pound (14,515 kg) axle load in the Normal Truck configuration, and a 25,000 pound (11,340 kg) axle load in the Alternate Load Configuration (Figure 4.8). In addition, the AASHTO LRFD requires the application of a 640 pound (290 kg) per linear foot Lane Load applied across a 10 foot (3 meter) wide lane at all depths of earth cover over the top of the pipe, up to a depth of 8 feet (2.44 meter). This Lane Load converts to an additional

live load of 64 pounds (29 m) per square foot, applied to the top of the pipe for any depth of burial less than 8 feet (2.44 kg). The average pressure intensity caused by a wheel load is calculated by Equation 4.2. The Lane Load intensity is added to the wheel load pressure intensity in Equation 4.3.

$$w = \frac{P_w (1 + IM)}{A_{LL}} \quad (4.2)$$

Where,

P_w = Total applied surface wheel loads, kN

A_{LL} = Distributed live load area, m^2

IM = Impact factor

$$W_T = (w + L_L)LS_L \quad (4.3)$$

Where,

W_T = Total Live Load

w = Wheel Load average pressure intensity

L_L = Lane Loading

L = Length of ALL Parallel to Longitudinal Axis of Pipe

SL = Outside Horizontal Span of Pipe or Width of ALL Transverse to Longitudinal Axis of Pipe, Whichever is less.

The HS 20, 32,000 pound (14,515 kg) and the Alternate Truck 25,000 pound (11,340 kg) design axle are carried on dual wheels (Figure 4.9). The contact area of the dual wheels with the ground in AASHTO, LRFD is assumed to be a rectangle (Figure 4.9), with dimensions of width is equal to 0.5 meter while length is 0.25 meter.

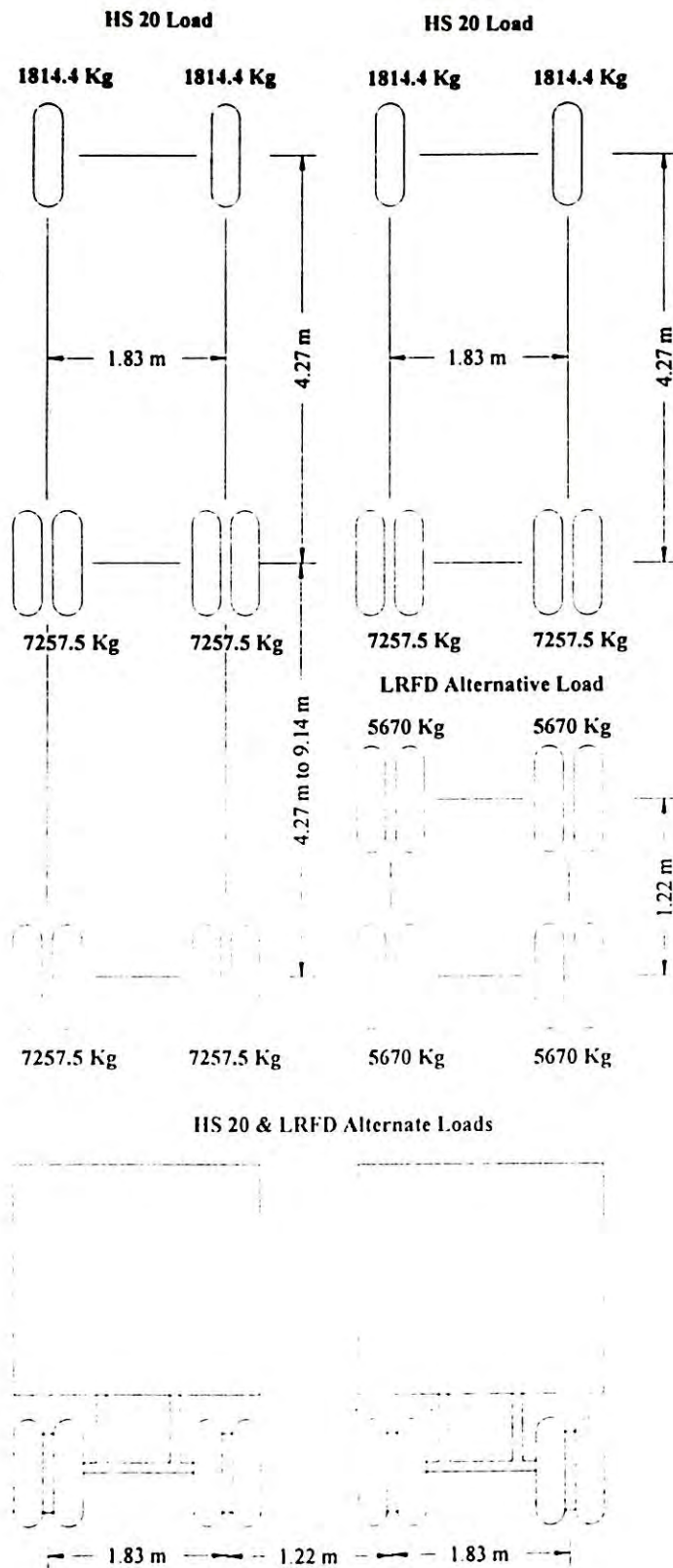


Figure 4.8: AASHTO (2002) Wheel Loads and Wheel Spacing

7257.5 Kg HS 20 Load
5670 Kg LRFD Alternative Load

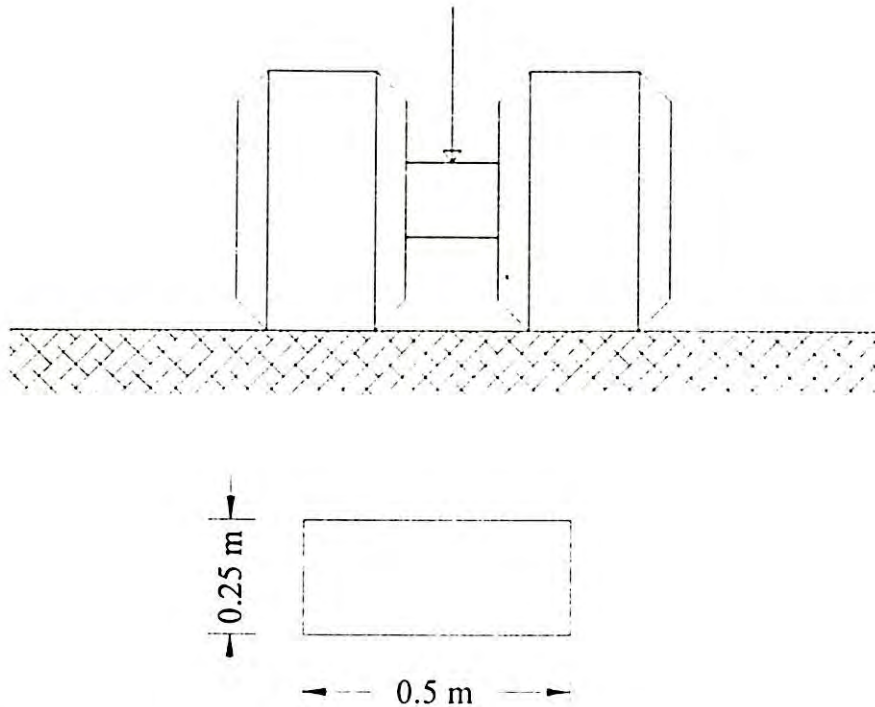


Figure 4.9: AASHTO (2002) Wheel Load Surface Contact Area (Foot Print)

The AASHTO LRFD Standard applies a dynamic load allowance to account for the truck load being non-static. The dynamic load allowance, IM , is determined by Equation 4.3.

$$IM = \frac{33(1.0 - 0.125H)}{100} \quad (4.3)$$

Where,

H = Height of Earth Cover Over the Top of the Pipe, ft.

4.3 FINITE ELEMENT ANALYSIS

Effect of surface live load on soil stress at pipe crown has been investigated using finite element analyses. Detailed analyses of the pipe-soil system have been carried out using three-dimensional finite element computer software ANSYS. A linear elastic analysis is performed with three-dimensional modeling of the pipe-soil system. The study has been performed for four different depths of soil cover above the pipe. The soil covers considered are 0.5, 1, 2.2 and 3 times the outer pipe diameter. Outer diameter of the pipe has been taken as 800 mm and the wall thickness as 100 mm.

The typical finite element mesh used during numerical analysis by the ANSYS has been shown in Chapter 3 (Figure 3.7). In addition, Chapter 3 contains the mesh-sensitivity analysis that was carried out to eliminate numerical error associated with the density of mesh as well as extent of the boundary taken in the analysis. It was revealed that if the boundary is placed at a distance of 3 times the diameter, the effect of boundary on the simulated pipe behavior is minimized.

Wheel load is modeled as concentrated load acting on the ground surface. A unit single wheel load (1 N) is considered. Since a linear elastic analysis is performed, the response obtained from this analysis can be multiplied by the magnitude of any wheel load to obtain the actual response. The load acting directly on top of the pipe represents the most severe condition and therefore considered in this investigation of live load effects. It is worth mentioning here that this thesis focuses on determination of the complete effect of a truckload on the pipe-soil response. The analysis of the effect of truck load and the interpretation of a full-scale test observation of soil stresses around pipes under surface load is discussed in Chapter 5. Effect of the surface live load on the pipes with different burial depth has been investigated through varying the depth from 0.5 to 3 times pipe diameter. Figure 4.10 shows a schematic view of the cross-section of the pipe-soil system along with the concentrated live load used in the analysis. At shallow burial, behavior of the pipe under surface load carries a complex phenomenon. A complete three-dimensional analysis was therefore performed to capture the three-dimensional effects.

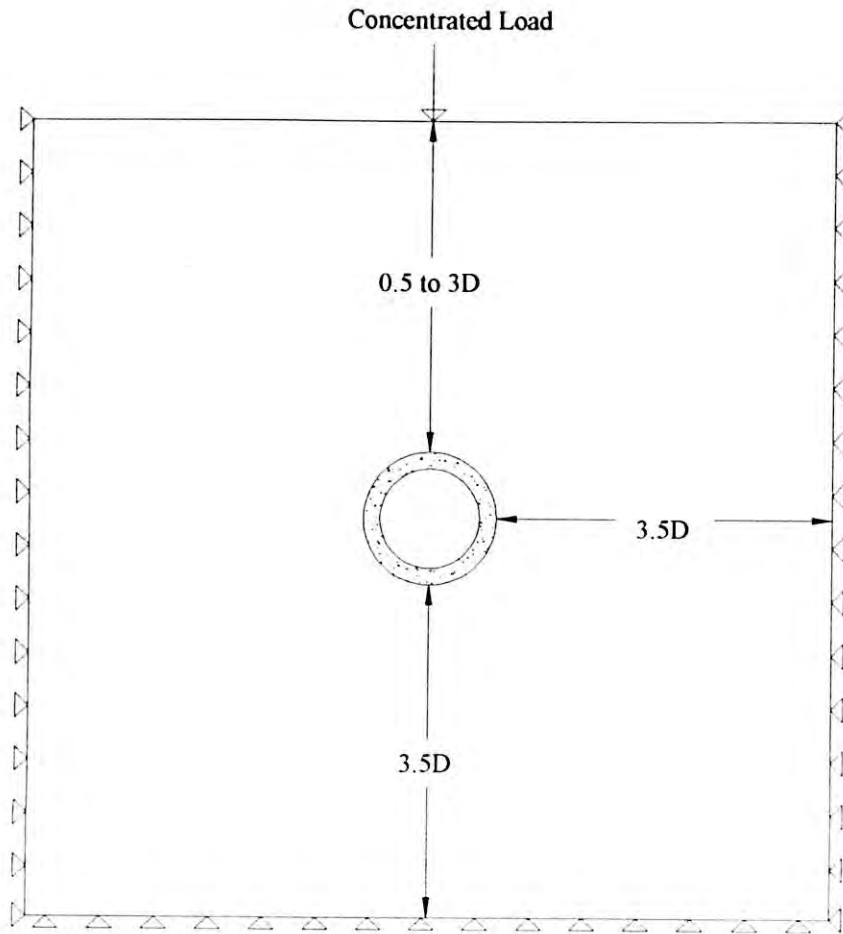
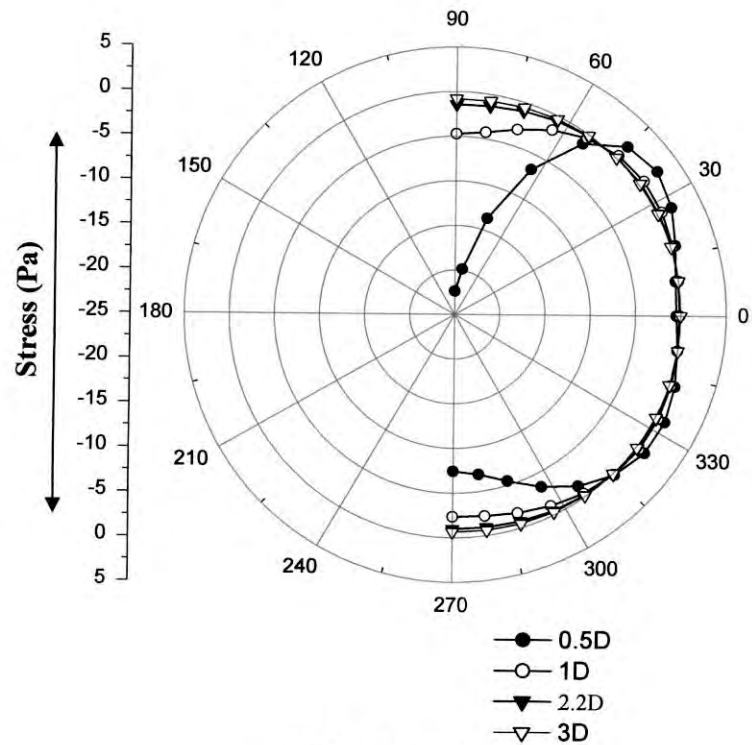


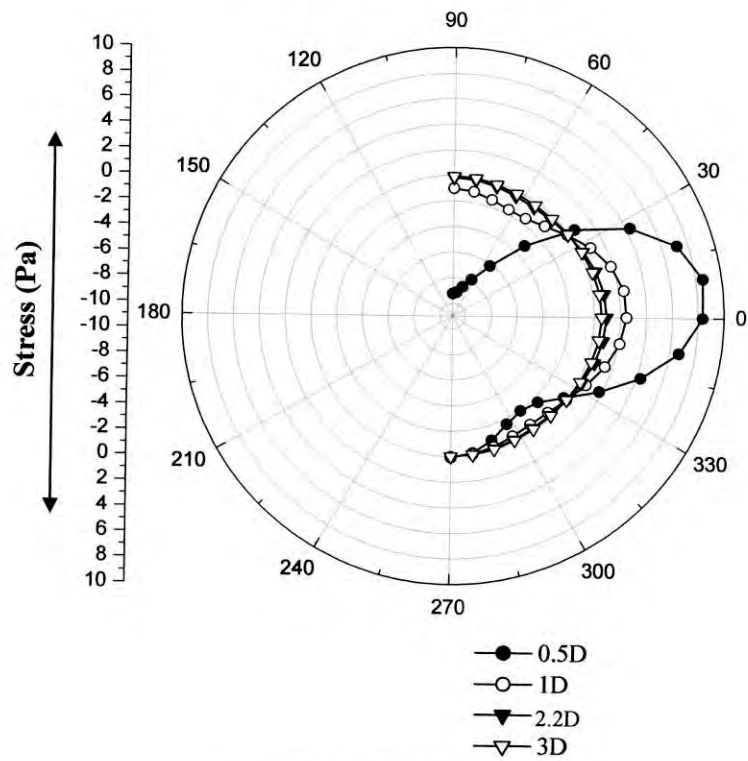
Figure 4.10: Schematic View of Pipe Cross-section with Surrounding Soil

4.3.1 Pipe Stresses from FE Analysis

Figure 4.11 shows stresses on exterior pipe wall due to a concentrated load above pipe crown, as obtained from the finite element analysis. The stresses shown in the figure are calculated using $E_p=20,000$ MPa and $E_s=20$ MPa as assumed in chapter 3. Compression negative sign convention is used for all stresses in this study. Horizontal and vertical stresses on exterior pipe wall for four different burial depths of the pipe are plotted in Figure 4.11(a) and 4.11(b) respectively.



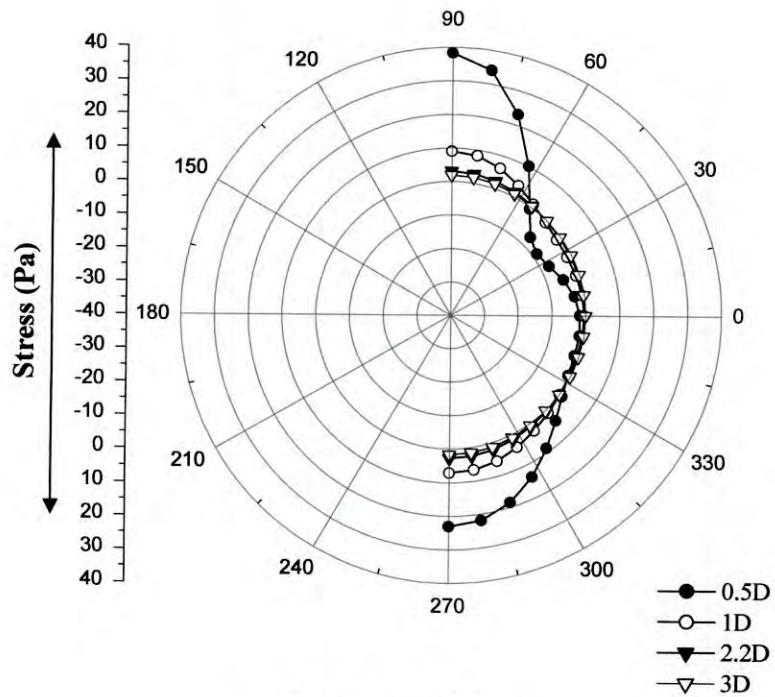
(a) Horizontal Stress



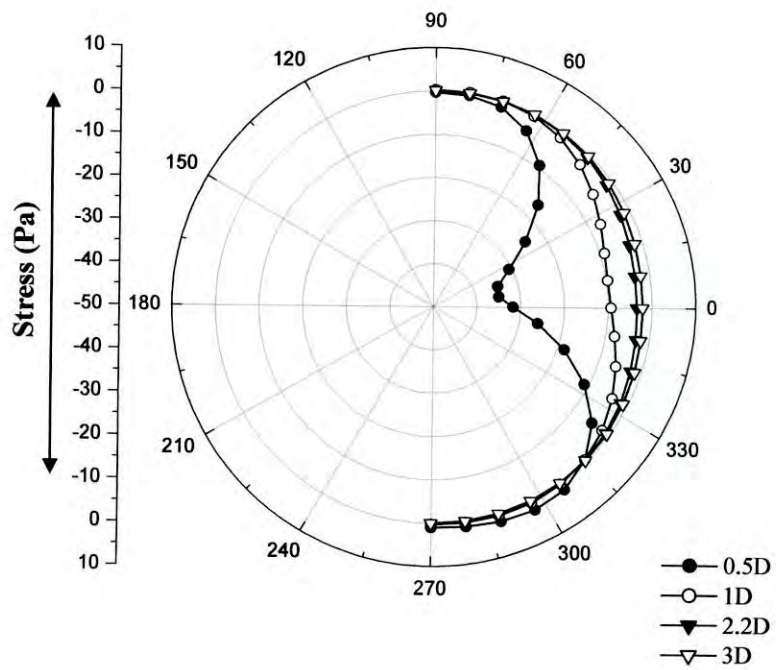
(b) Vertical Stress

Figure 4.11: Stress Distribution on Exterior Surface of Pipe ($E_p/E_s = 1000$)

Figure 4.11 depicts that if the depth of soil cover decreases, greater magnitude of stress due to concentrated surface load reaches to the pipe. Figure 4.11 (a) shows that horizontal stress is -22.5 Pa at the crown and -7.5 Pa at the invert for a pipe buried at a depth of 0.5 times the pipe diameter, while the stresses are around -1 Pa for the same pipe buried at a depth of 3 times pipe diameter. Negative magnitude of stress indicates that the stresses are compressive in the exterior wall at crown and invert, as expected. However the horizontal stress at the springline did not increase due to surface load. The horizontal wall stresses at the crown and invert represent the circumferential stress at the pipe wall that develop due to bending moment and thrust at the wall, while the horizontal stress at the springline represent the radial stress. The stresses in the radial direction on pipe-wall are not caused by the wall thrust and bending moment. This is the reason why the horizontal stress at the springline was not increased in Figure 4.11 (a). The circumferential wall-stress governs the design of the pipe. Similarly, Figure 4.11 (b) shows that vertical stress is 8.5 Pa at the springline for a pipe buried at a depth of 0.5 times the pipe diameter, and the stresses are almost zero for a burial depth of 3 times pipe diameter. Positive magnitude of stress indicates that the stresses are tensile in the exterior wall at springline. Again, the vertical wall stresses at the springline represent the circumferential stress at the pipe wall that develops due to bending moment and thrust of the wall and the vertical stress at the crown and invert represent the radial stress. The radial stress at the crown is increased for shallow buried pipe. However, the stress is not affected by the burial depth at the invert.



(a) Horizontal Stress



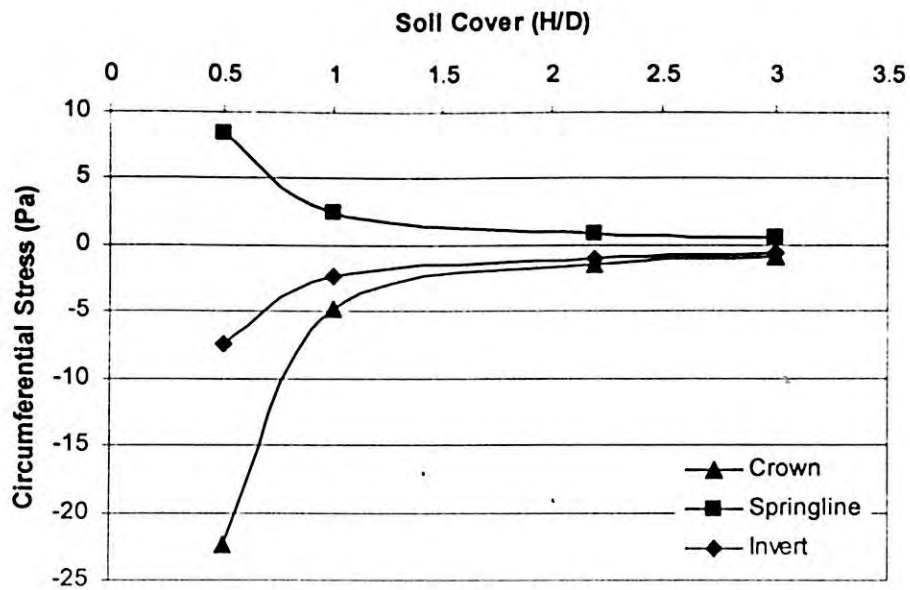
(b) Vertical Stress

Figure 4.12: Stress Distribution on Interior Surface of Pipe ($E_p/E_s=1000$)

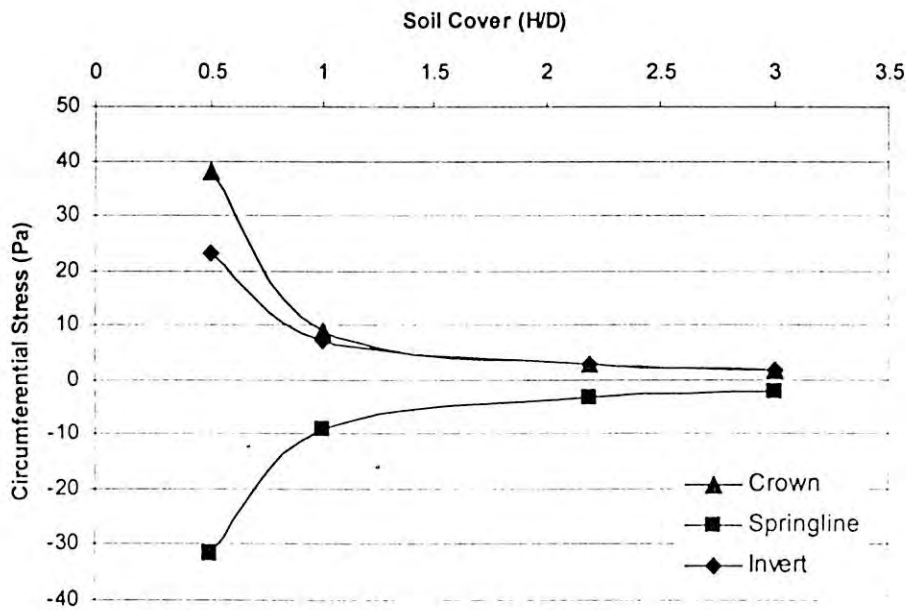
Stresses on the interior surface of the pipe wall are plotted in Figure 4.12. The figure shows greater circumferential tension on interior wall at crown and invert if the depth of soil cover decreases with greater effect at crown. The horizontal stress (circumferential stress) is 38 Pa at the crown and 23 Pa at the invert for a pipe buried at a depth of 0.5 times the pipe diameter. The circumferential stresses are around 1 Pa for the pipe with a burial depth of 3 times pipe diameter. High tension on interior wall and high compression on exterior wall at the crown and invert characterizes significant bending of the pipe wall at those locations. Figure 4.12 (b) shows vertical stress is -32 Pa at the springline (circumferential stress) for a pipe buried at a depth of 0.5 times the pipe diameter, while the stresses are less than -2 Pa for the same pipe buried at a depth of 3 times pipe diameter. The observation of stresses at the crown, springline, and invert reveals that the crown is most significantly affected by live load followed by springline and invert respectively for shallow buried pipe.

4.3.2 Effect of Soil Cover on Pipe Stress

Variation of circumferential stress at the pipe's most typical points such as crown, springline, and invert as a function of the depth of soil cover above pipe is plotted distinctively in Figure 4.13. It is evident from Figure 4.13 that for pipes buried at depths greater than 3 times the diameter, stress increase on pipe circumference due to surface load is insignificant as discussed earlier. But at burial depth 0.5 times the diameter, significant amount of tensile stresses may develop at the springline and compressive strength may develop at the crown and invert on pipe's exterior surface (Figure 4.13a) and vice-versa on pipe's interior surface (Figure 4.13b). Stresses under shallow burial condition (0.5 times the diameter) were found to be 7 to 23 times the stress under deep burial condition (3 times the diameter) on exterior surface and 22 to 39 times on the interior surface. The magnitude of compressive/tensile stress at the crown is the greatest of all the stresses developed around the pipe circumference. It was revealed through the analysis as discussed earlier that x-component of stress governs at crown and invert whereas y-component of stress governs at springline on the pipe circumference, indicating the circumferential stress as the critical stress.



(a) Exterior Surface



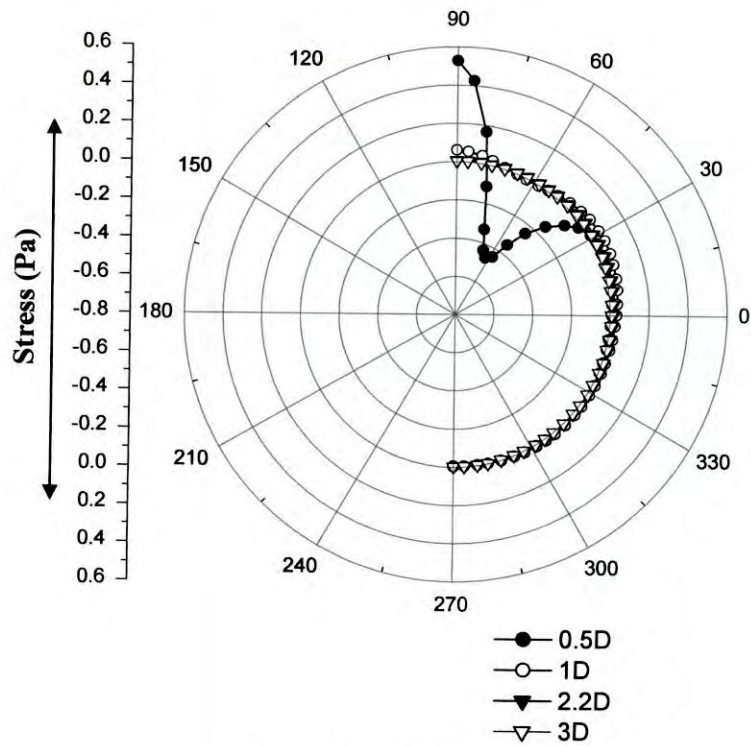
(b) Interior Surface

Figure 4.13: Variation of Stresses with Cover Depth

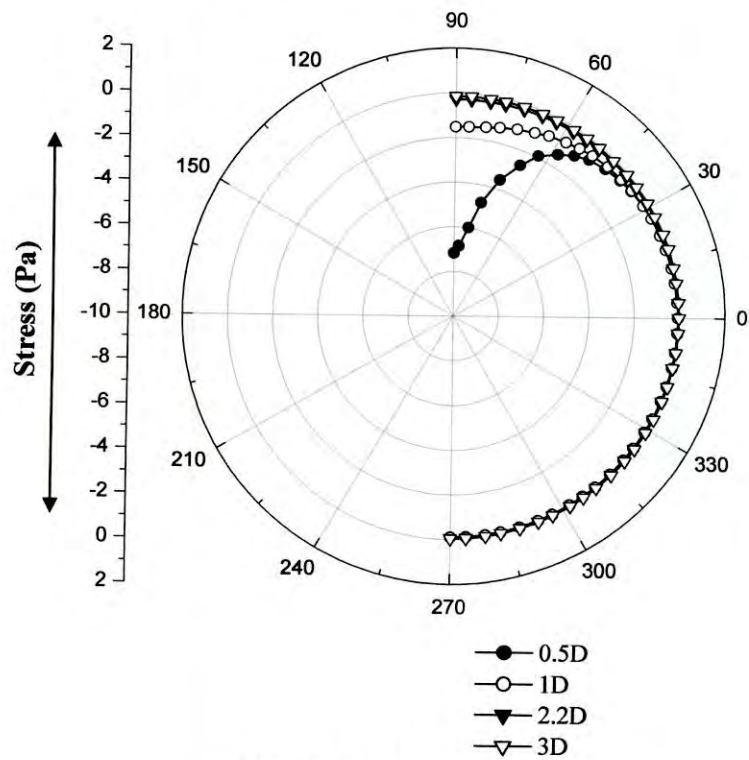
4.3.3 Ground Stresses from FE Analysis

Figure 4.14 reveals the horizontal and vertical stresses on soil element at a radial distance 100 mm from the pipe outer circumference. Interpolation was used to calculate the stresses if the nodal points were not available at the desired location in FE mesh. Figure 4.14 (a) shows that horizontal stress is 0.523 Pa at 100 mm above the crown, -0.006 Pa at 100 mm below the invert and 0.007 Pa at 100 mm away from the springline for a pipe buried at a depth of 0.5 times the pipe diameter. The stresses become insignificant (almost zero) for the same pipe buried at a depth of 3 times pipe diameter. On the other hand, Figure 4.14(b) shows that the vertical stresses are -7.19 Pa at 100 mm above the crown, -0.12 Pa at 100 mm below the invert and -0.07 Pa at 100 mm away from springline for a pipe buried at a depth of 0.5 times the pipe diameter. The horizontal stresses at crown level indicate a soil tension (positive stress) for pipe buried at a depth of 0.5 times the pipe diameter in Figure 4.14(a). To investigate the issue further, crown stress is plotted against the buried depth in Figure 4.15. Figure 4.15 shows that the horizontal crown stress can be highly tensile for burial depth of 0.5 times pipe diameter which decay down rapidly with the increase of burial depth. An elasto-plastic analysis would be required to capture the effect of soil tension on pipe-soil interaction. Figure 4.14(b) shows the vertical stress increase is very insignificant for the pipe buried at a depth greater than 3 times pipe diameter. The ratio of vertical to horizontal stress at crown, invert and springline are 13.7, 17.7 and 6.70 respectively for pipes buried at a depth of 0.5 times the pipe diameter.

It is also revealed from this investigation that the effect of the concentrated surface load is the maximum at the crown followed by springline and the invert. This is expected since the crown level is closer to the ground surface, while the springline and the invert are at greater depths respectively. Stress increase due to surface load at the invert is $\frac{1}{8}$ th of the stress increase at the crown for the pipe considered. The effect at the springline was $\frac{1}{2}$ to $\frac{1}{3}$ rd of that at the crown.



(a) Horizontal Stress



(b) Vertical Stress

Figure 4.14: Stress Distribution on Soil ($E_p/E_s=1000$)

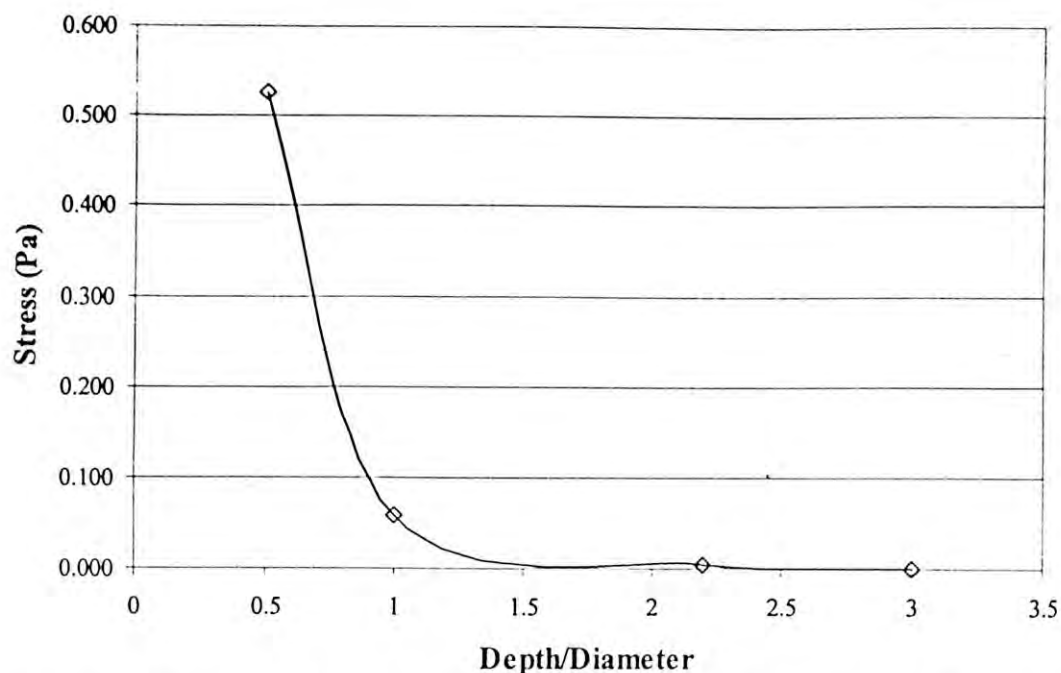


Figure 4.15: Horizontal Stress Distribution on Soil at Crown Level ($E_p/E_s=1000$)

4.3.4 Effect of Soil-Pipe Interaction

To investigate the effect of pipe-soil interaction on distribution of concentrated surface load in the soil, an investigation has been performed to calculate the soil stress in a soil with a hole without pipe and in a soil with a pipe in the hole. The calculated soil stress is compared with those calculated using the Boussinesq solution. It is here to note that Boussinesq solution provides stresses in a uniform soil without consideration of any hole or pipe. Thus comparison of soil stresses with those calculated using Boussinesq solution reveals the effect of the presence of a hole and the pipe on the stress distribution.

Figure 4.16 shows the vertical stress distribution on soil at pipe springline level obtained using FE analysis and Boussinesq solution. The comparison of stresses in the figure shows that the stress in the vicinity of the pipe is greater for the solution with a hole without any pipe in it. The Boussinesq solution provides in-between stress. The vertical soil stress is the smallest at the pipe vicinity if a hole with a rigid pipe in it is considered. Since the pipe having greater stiffness attracts the loads, the vertical stress on the soil adjacent to the pipe is significantly lower in this case than that is given by Boussinesq solution. At a distance significantly away from the pipe wall, each of

solutions gives similar soil stresses. Thus the presence of a hole or pipe in the soil causes a redistribution of the stress due to surface load in the vicinity of pipe, which is not considered during pipe design.

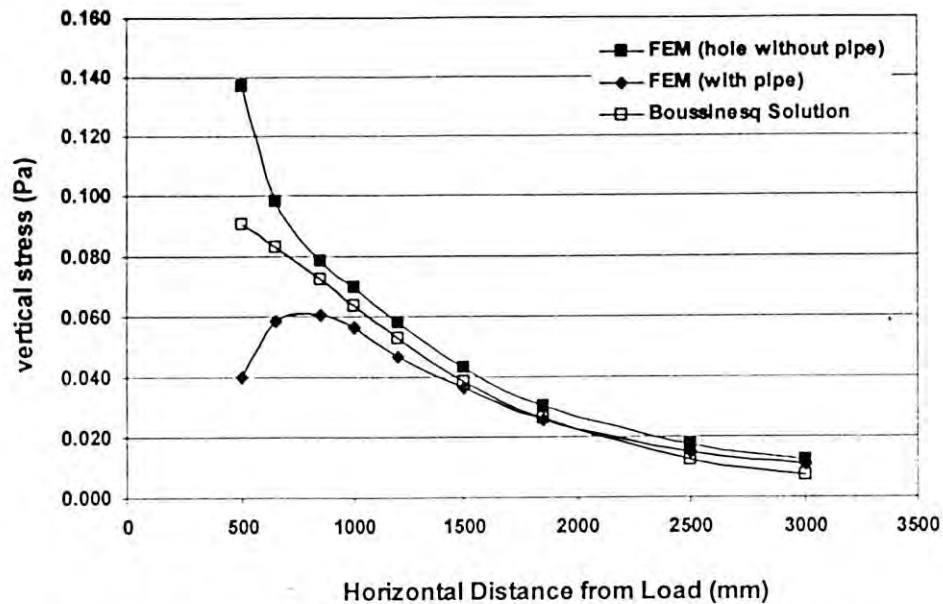


Figure 4.16: Vertical Stresses on Soil at Pipe Springline Level

4.3.5 Effect of Cover Depth on Ground Stress

Figure 4.17 shows vertical soil stresses along the line of the concentrated load above pipe's crown for four different burial depth of the pipe. The depths are measured from the pipes crown and normalized using the depth of soil cover in each case. Thus, the zero depth corresponds to a point on the crown of the pipe and a depth of 1 represents a point on the ground surface. The stress from the Boussinesq solution is included in the figure to represent the soil stress in uniform ground (without any pipe or opening).

Asymptotic vertical stress at depth =1, in Figure 4.17, means infinite stress at the ground surface right below the concentrated load. The stress decreases with the increase of depth below the ground surface, as expected. Figure 4.17 also depicts that if burial depth of the pipe is less, a greater magnitude of stress reaches to the pipe. Vertical stress calculated using the continuum theory (Boussinesq, 1885) is included in Figure 4.17 for two different depths of pipe burial (i.e., 0.5D and 3D). It is to be noted here that the burial depth is only used to normalize the depth below the ground surface in Boussinesq (1985) solution.

Figure 4.17 shows that the Boussinesq solution underestimate the stress at the pipe crown for shallow burial condition (Burial depth = $0.5D$). However, for burial depth of 3 times the pipe diameter, the solution matches with those calculated using the finite element analysis. This indicates that the presence of pipe does not influence the soil stress when buried at the depth of 3 times the pipe diameter. The Boussinesq solution does not consider the presence of pipe or opening, while the finite element analysis presented in Figure 4.17 consider an opening in the soil. Thus, for a burial depth greater than 3 times the diameter, the finite element model represents a homogenous semi-infinite continuum, based on which the Boussinesq solution was developed. For a burial depth of 0.5 times the diameter, the crown stress calculated from finite element analysis is much greater than that calculated using the Boussinesq theory. This is not surprising because the pipe with greater stiffness attracts loads from the surrounding soil which is not considered in the Boussinesq solution. The finite element stress matches with the continuum solution for the pipe near the ground surface, indicating minimization of the influence at greater distance from the pipe.

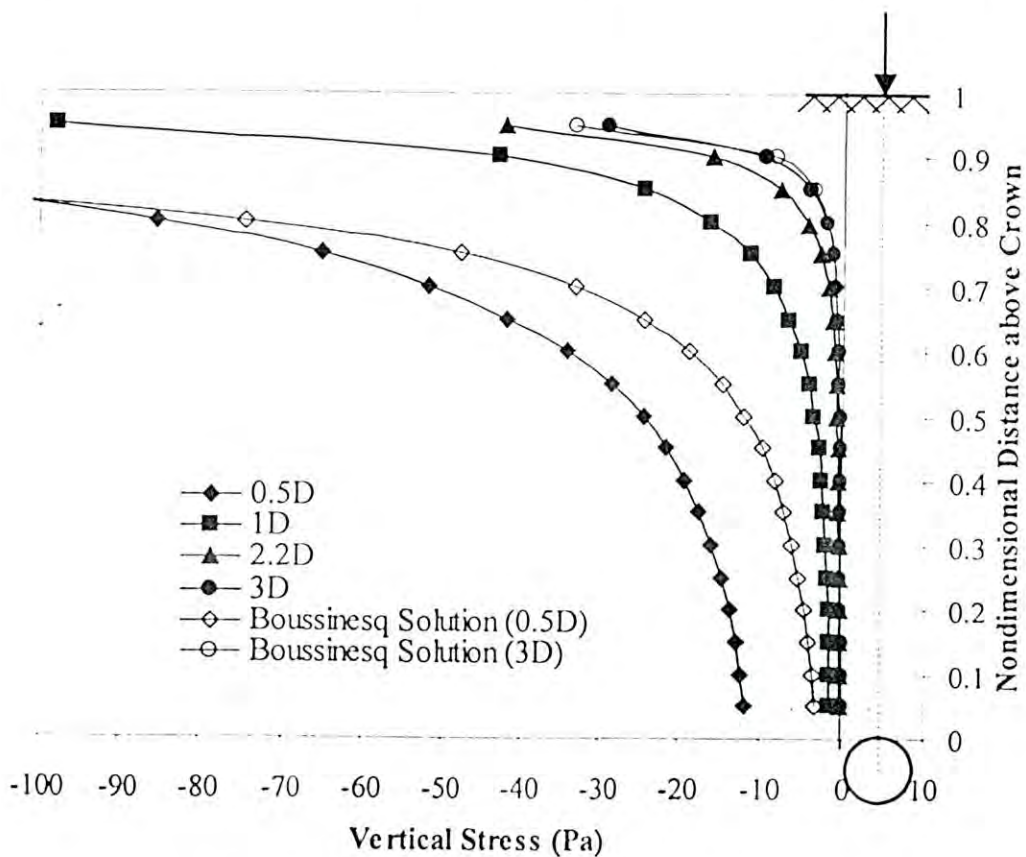


Figure 4.17: Variation of vertical soil stress with depth

4.4 COMPARISON OF SOIL STRESS WITH DESIGN MODELS

Soil stresses estimated using the ASCE 1993 and AASHTO 2002 design practice are compared with those calculated using the FE and the continuum theory in Figure 4.18. The pipe with 0.5 times the diameter of soil cover is considered in this comparison. The pipe at this depth appeared to affect the pipe stresses due to surface load (Figure 4.17). Figure 4.18 shows that ASCE and AASHTO standard provide greater stress than the Boussinesq solution. However, the standards provide unconservative stress relative to the finite element solution in region near to crown. It is also observed here that AASHTO gives conservative stress between the two standards. The finite element stress is the maximum stress at the crown level of the pipe. However, a sharp rise of stress is observed near to ground where the standards provide conservative stress relative to the finite element and continuum theory solution.

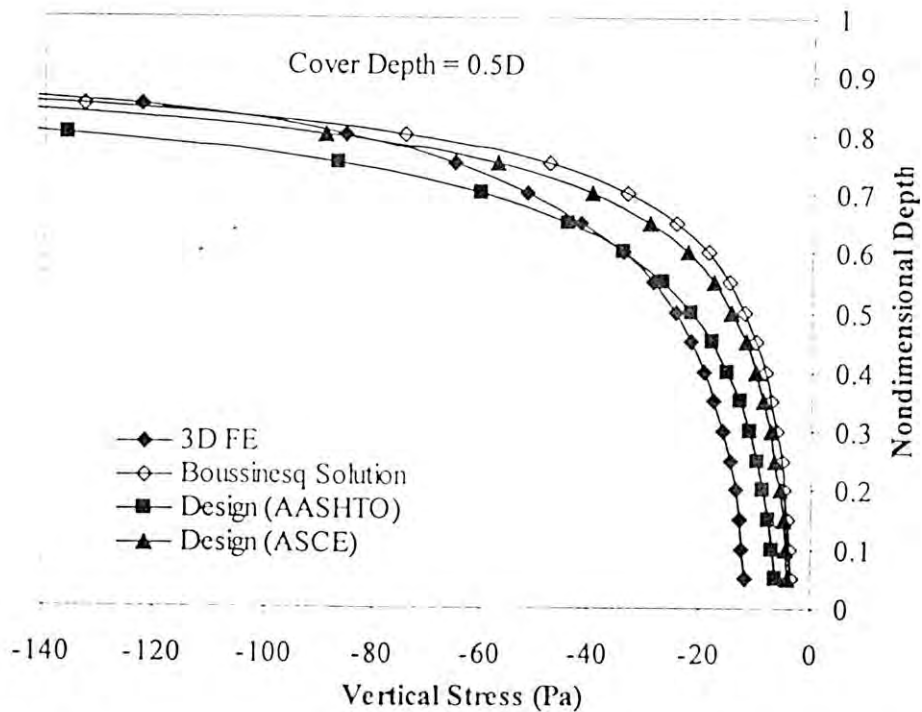
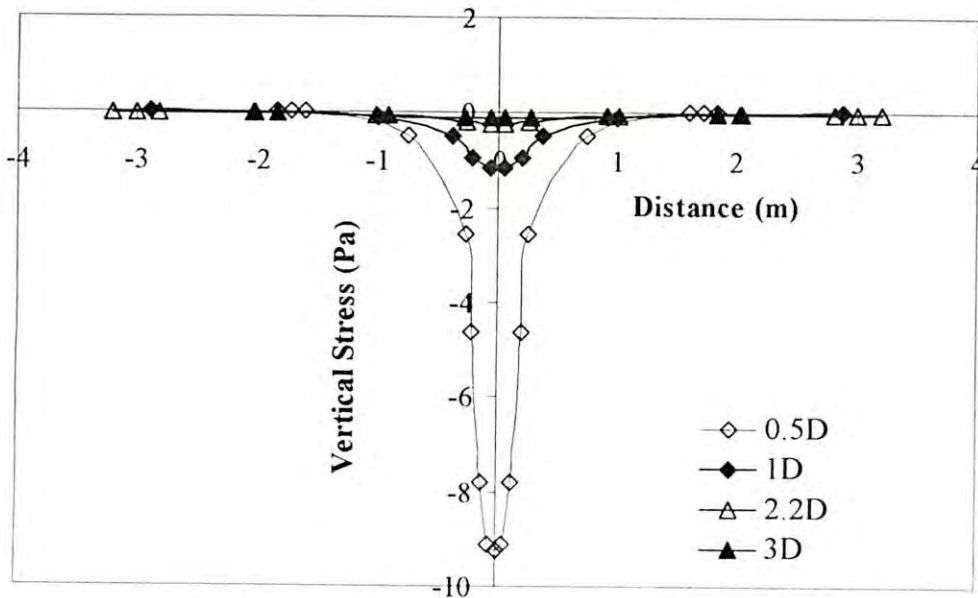


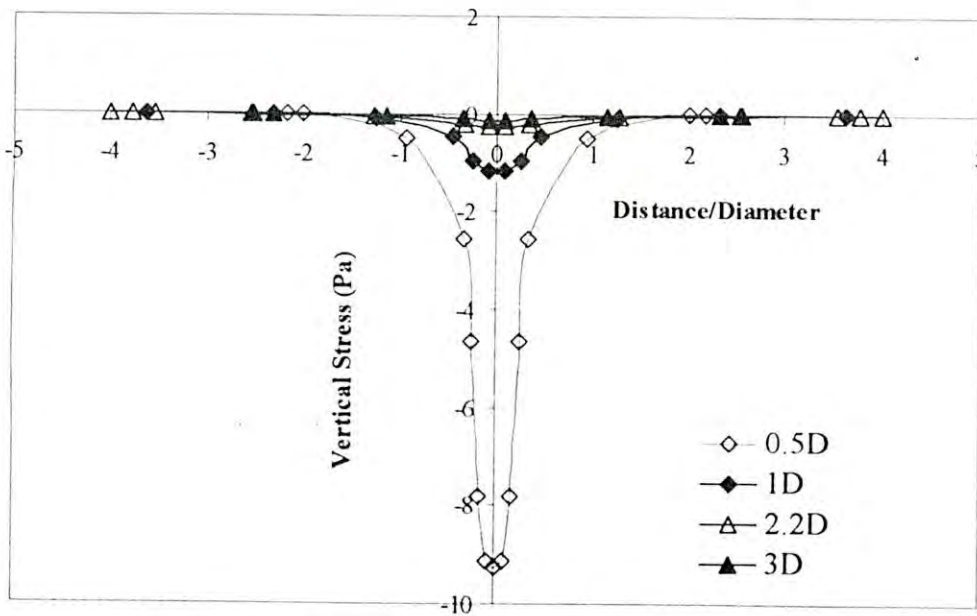
Figure 4.18: Comparison of Finite Element Stresses with Design Standards

4.5 LATERAL DISTRIBUTION OF THE GROUND STRESS

Horizontal distribution of the stresses at crown level is investigated to understand the mechanism of load spreading of concentrated surface load. It will also provide information about how far the stress reaching to the pipe from any wheel/axle load be affected by the stresses from the other wheels/axles of the same truck. Obviously, the effect will be less as the stress drops quickly away from the load.



(a) Vertical Stress versus Horizontal Distance

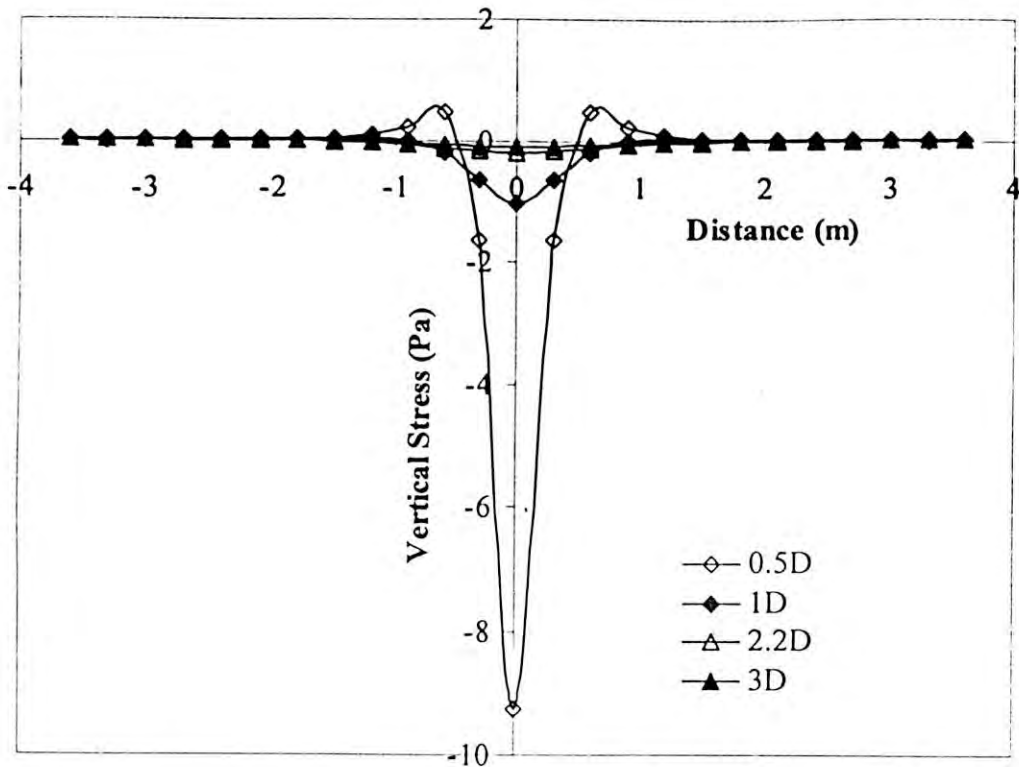


(b) Vertical Stress versus Non-dimensional Distance

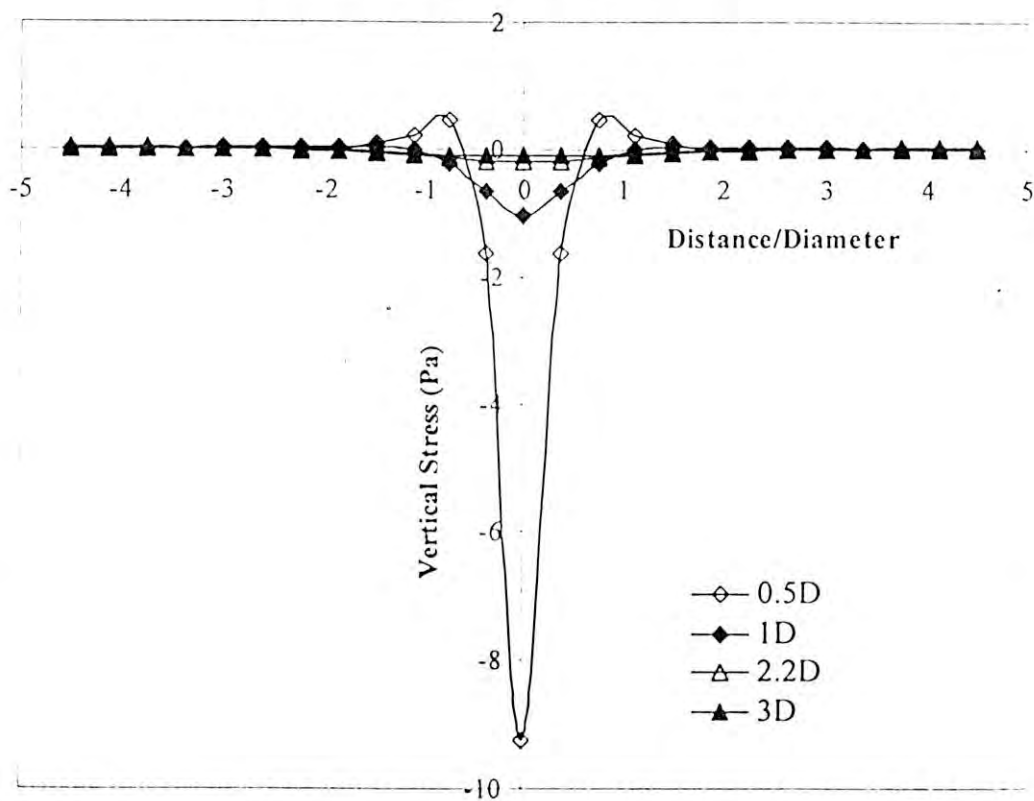
Figure 4.19: Distribution of Vertical Stress in Transverse Direction

Figure 4.19 shows lateral distribution of the vertical stress at the crown level in transverse direction across the pipe. The stresses for the four burial depths are plotted in the figure. In each case, stress is the maximum at crown (below the load) and it decreases away from the pipe. The crown stress is very high for the pipe at $0.5D$ depth, due to the arching effect for the shallow buried pipe.

Figure 4.19 also depicts that the effect of live load is minimized at a distance 1.5 m away from the load, even in the case of shallow burial. Considering the distance between the axles for any truck (i.e. HS20) as greater than 1.5 m (2 times the diameter), it is reasonable to assume that the stress resulting from any axle load will not be affected by the stresses from the other axles. The effect of full-scale truckload on buried pipe will be discussed further in Chapter 5 in this thesis.



(a) Vertical Stress versus Horizontal Distance

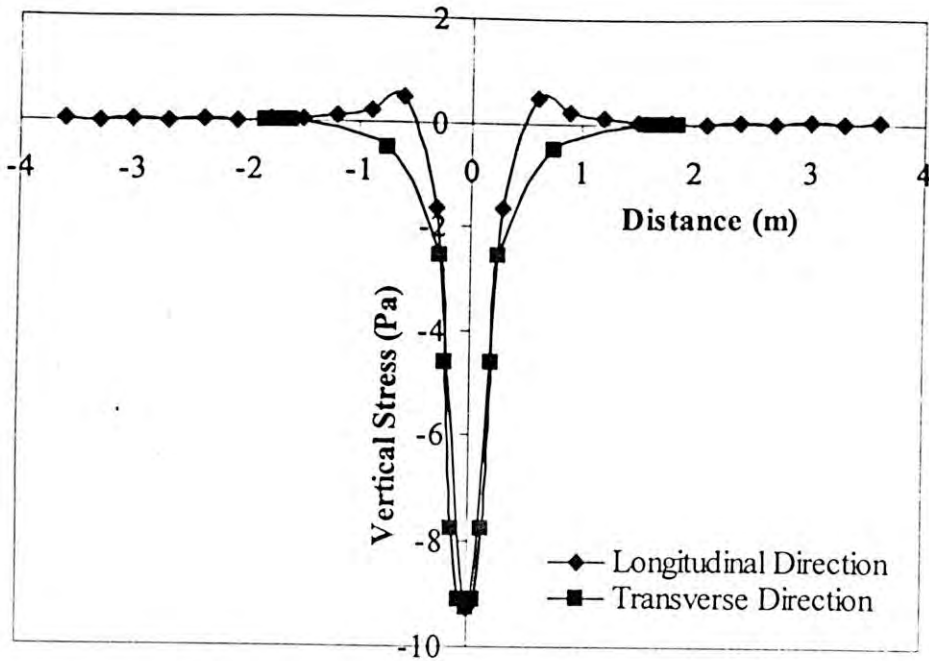


(b) Vertical Stress versus Non-dimensional Distance

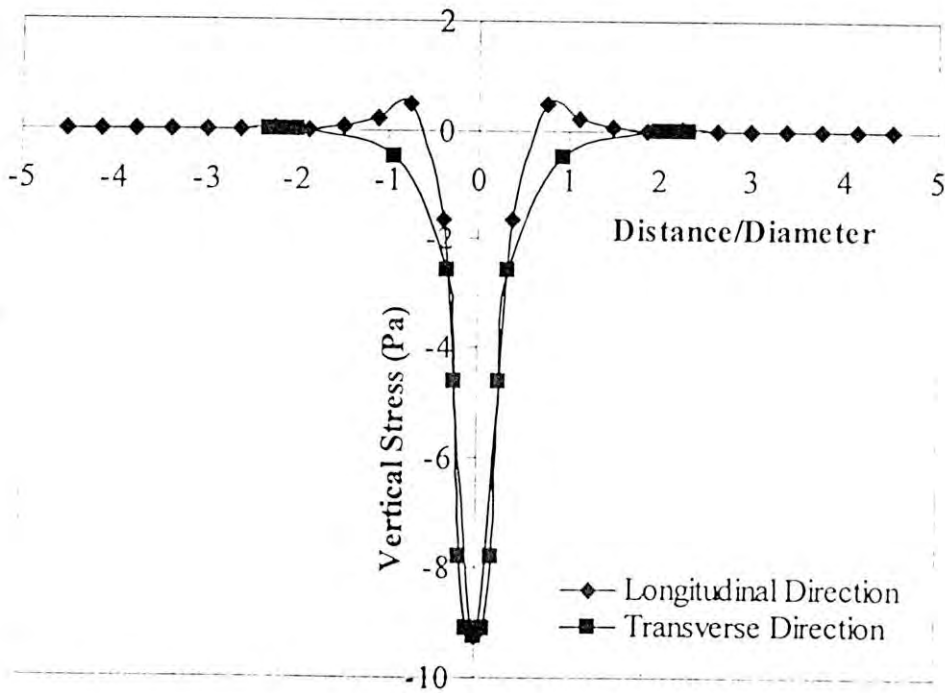
Figure 4.20: Distribution of Vertical Stress in Longitudinal Direction

Figure 4.20 shows lateral distribution of the vertical stress at crown in longitudinal direction of the pipe. As before, the stresses for the four burial depths are plotted in the figure. In each case, stress is also the maximum at the point below the load and it decreases away from load. The crown stress is very high for the pipe at 0.5D depth, due to the three-dimensional effects at the shallow burial. The effect of live load is minimized at a distance 1.5 m (2 times the diameter) away from the load along the pipe, even in the case of shallow burial (Burial depth = 0.5D). The distance of the load transfer is greater in longitudinal direction than in lateral direction. Thus it is reasonable to assume that the stress resulting from any wheel load will not be affected by the stresses from the other wheels considering the distance between the wheels an axle for any truck as greater than 1.5 m (2 times the diameter). However, the severity of the stress may always depend on the magnitude of the surface load with respect to the earth load.

Distribution of the stresses in both transverse and longitudinal directions of the pipe is compared in Figure 4.21 for pipe burial at a depth of 0.5 times the diameter. The figure shows similar distribution of stresses in two directions, except some tension develop in the longitudinal direction at a distance away from the load along the pipe. Elasto-plastic analysis may be required to evaluate the soil tension, if the influence of this tension is significant.



(a) Vertical Stress versus Horizontal Distance



(b) Vertical Stress versus Non-dimensional Distance

Figure 4.21: Stresses along Longitudinal and Transverse Direction
(Burial depth = 0.5D)

4.6 SUMMARY

Current codes of rigid pipe design incorporating live load are studied in this chapter. Three-dimensional finite element analysis is performed to study the effect of surface live load on the behavior of pipe-soil interaction. Based on the study, the following conclusions can be drawn:

- Concentrated surface load may cause significant stress on pipe wall for shallow buried pipe, which is the greatest at crown followed by springline and invert respectively (Figure 4.11 to 4.15).
- For pipes buried at depths greater than 3 times the diameter, influence of pipe on the mechanism of wheel/axle load transfer is insignificant (Figure 4.17). Therefore, pipe-soil interaction analysis may not be required to calculate the pipe stress. Classical theory (Boussinesq, 1885) can be used to calculate the soil stresses at pipe crown. However, if the burial depth is less than 3 times the diameter, pipe-soil interaction analysis should be performed to obtain the stresses.
- ASCE and AASHTO design standard provides a reasonable estimate of the effects of live load where AASHTO shows more conservative results (Figure 4.18). But at shallow burial condition, the standards provide 30 to 50 percent unconservative estimate of the stress at crown with respect to finite element results.
- The pattern of stress distributions in longitudinal and transverse direction of the pipe is very similar. However, for shallow burial condition, maximum of 5 to 6 percent tensile stress with respect to the highest compressive stress was developed along the longitudinal direction (Figure 4.20 and 4.21).
- The effects of the surface load of a single wheel become insignificant at 1.5 m (2 times the diameter) away from the load (Figure 4.19 and 4.20). Thus, the stresses resulting from any wheel/axle will not be affected by the nearby wheel/axle if these are located further than 1.5 m (2 times the diameter).

CHAPTER 5

ANALYSIS AND INTERPRETATION OF FULL-SCALE TEST

5.1 GENERAL

Computer modeling is an important and economical tool for investigating the behavior of buried structures. The process of calibrating computer models with limited field test data and then using the models to investigate the behavior of structures with a much wider range of variables has proven an effective process for both research and design.

Buried pipes under live load are generally analyzed based on an assumption that the load is distributed uniformly over the area above the pipe crown (Taleb et al. 2000, Jayawikrama et al. 2002, Dhar et al. 2004). Although the assumption of uniformly distributed live load may be reasonable for deeply buried pipe; the idealization may not work for pipes under shallow burial. At shallow burial, behavior of the pipe under live load would be a three-dimensional phenomenon. A complete three-dimensional analysis is therefore required to interpret the full-scale test observation reasonably.

A live load testing program was undertaken by Ontario Concrete Pipe Association (OCPA), Canada to collect data on soil stresses around a full-scale pre-cast concrete pipe test bed under vehicle loads across Ontario, Canada (Allouche et al. 2004). Allouche et al (2004) compared the measured stresses with those obtained using SIDD design method. Test results will be analyzed in this study using finite element method to interpret the observed behavior in full-scale tests for a better understanding of the soil-pipe interaction.

5.2 LIVE LOAD TEST (PROGRAM AT UWO, CANADA)

5.2.1 Introduction

Allouche et al. (2004) undertook a live load testing program in a full-scale concrete pipe test bed located at Barrie, Ontario, Canada. The test bed was installed in conformance to the Standard Installation Direct Design (SIDD) Type IV installation specifications, along with three other test beds located at Cambridge, Guelph and Whitby in Ontario, Canada. The test beds were prepared with a goal to collect long-term data of soil stresses around full-scale concrete pipe installations. Details of the test bed configurations and soil data are available elsewhere (Allouche and Wong, 2002). A live load testing program was undertaken in the summer of 2002 at the test bed at Ontario using full-scale trucks. The site is located near a weighing station where it was possible to take the gross weight of the trucks passing over the test bed. The test bed was instrumented with 12 earth pressure cells located at the vicinity of the pipe's invert, haunch, springline and crown.

5.2.2 Test Bed Configuration

The test pipe at the Barrie, Ontario site is located underneath an approach ramp to a truck weigh scale at a Gravel Pit site. Figure 5.1 shows a plan view of the approach ramp. A longitudinal view of the test bed is shown in Figure 5.2. The test bed consists of five 2.4 m long pipe segments of 600 mm inner diameter and 800 mm outer diameter concrete pipes. Three central pipe segments, labelled 2, 3 and 4, were instrumented to collect the desired data. Segment 3 located beneath the centerline of the approach ramp was the most heavily instrumented segment and was referred to as the 'Test Section' and the other two segments were termed as control segments (Allouche et al. 2004). Twelve earth pressure cells were installed around the test and control pipe segments during installation. A Data Acquisition System (DAS) connected to the pressure cells recorded the earth pressures around the test bed. The DAS was programmed during the live load tests to record the readings of the pressure cells in 15-second intervals in order to capture the response of the soil envelope to the truck loads. Figure 5.3 shows the trench geometry for the test bed. The trench was

backfilled using uncompacted native soil in accordance with SIDD Type IV specifications.

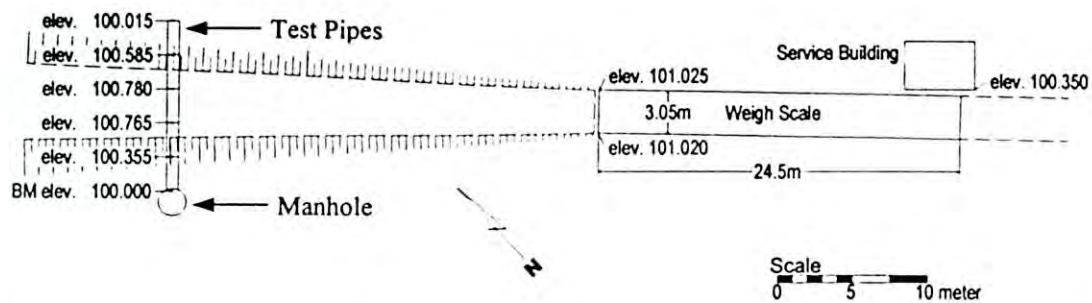


Figure 5.1: Plan View of the Pipe Bed at the Barrie Test Site (Wong, 2002)

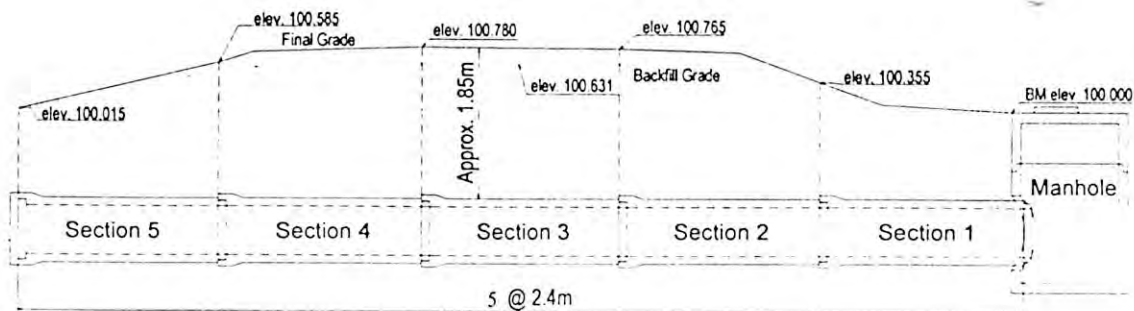


Figure 5.2: Longitudinal Profile of the Approaching Ramp along with Test Pipes (Wong, 2002)

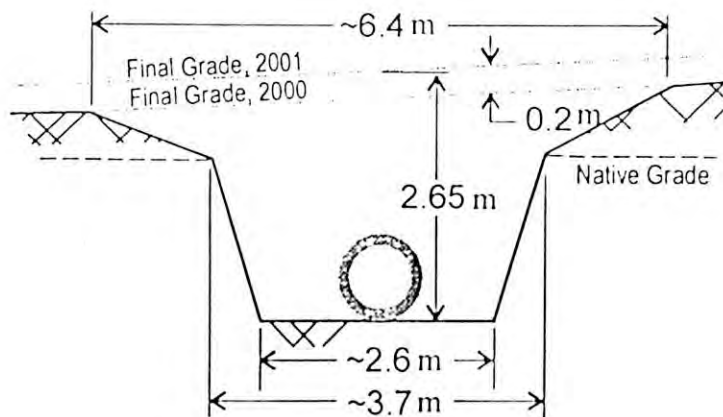
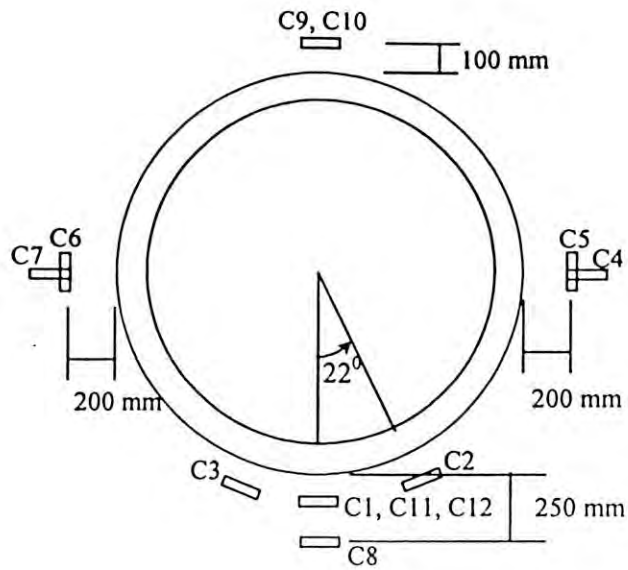


Figure 5.3: Trench Geometry (After Wong, 2002)

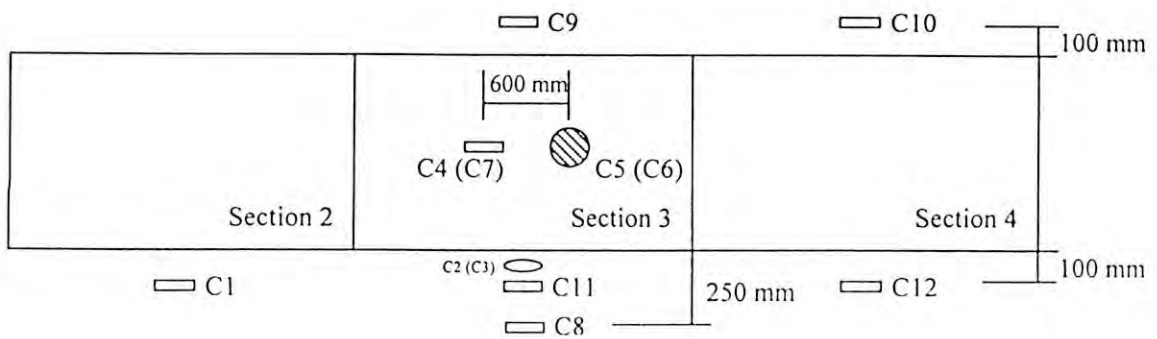
Twelve Geokon earth pressure cells were installed around the test pipe sections. A schematic diagram of the configuration of earth pressure cells is given in Figure 5.4. Three cells, designated as Cells 1, 11 and 12 were installed 100 mm beneath the invert of pipe sections 2, 3 and 4 of the installation, respectively. One (Cell 8) was installed 250 mm beneath pipe section 3, two other cells (Cells 9 and 10) were installed 100 mm above the crown of the test sections 3 and 4, respectively. Test section 3 had four earth pressure cells installed at the springline, 200 mm away from the exterior wall of the pipe, two (Cells 4 and 7) with horizontal orientation on either side of test section 3 and two other cells (Cells 5 and 6) with vertical orientation on either side of the springline of the same section. The horizontal and vertical cells were offset longitudinally at a distance of 600 mm from each other. Additionally, two cells were installed at the haunch of the pipe at a 22 degrees offset from the vertical centerline. The designations and locations of the various earth pressure cells are revealed in Table 5.1.

Table 5.1: Crown Cell Location and Designation at the Barrie Site (Wong, 2002)

Cell	Stress Rating (kPa)	Location	Orientation	Section
1	340	100 mm below invert	Horizontal	2
2	340	Offset 22° from vertical between invert and springline	Oblique	2
3	340	Offset 22° from vertical between invert and springline	Oblique	2
4	340	At Springline	Horizontal	3
5	170	At springline	Vertical	3
6	170	At springline	Vertical	3
7	340	At springline	Horizontal	3
8	340	250 mm below invert	Horizontal	3
9	340	100 mm above crown	Horizontal	3
10	340	100 mm above crown	Horizontal	4
11	680	100 mm bellow invert	Horizontal	3
12	680	100 mm bellow invert	Horizontal	4



(a) Cross-Sectional View



(b) Longitudinal View

Figure 5.4: Location of Earth Pressure Cells

5.2.3 Test Procedure

In the live load test program, soil stresses were measured around the pipe due to wheel/axle loads from loaded trucks as they approach the weigh scale station. Each truck was requested to stop as each of its axles was directly above the test bed. The minimum stoppage time for each axle was 30 sec to ensure that at least two readings were taken for each axle. The approach ramp was marked to identify the pipe's horizontal position. Two 10,000 kg-portable scales were placed under the footprint of

the wheel to measure the single dual wheel load when the truck stops with a particular axle on the line of measurement. The distance between two axles was also measured during passes of the truck. Finally, the truck proceeded to the weigh scale where the gross weight of the vehicle was obtained.

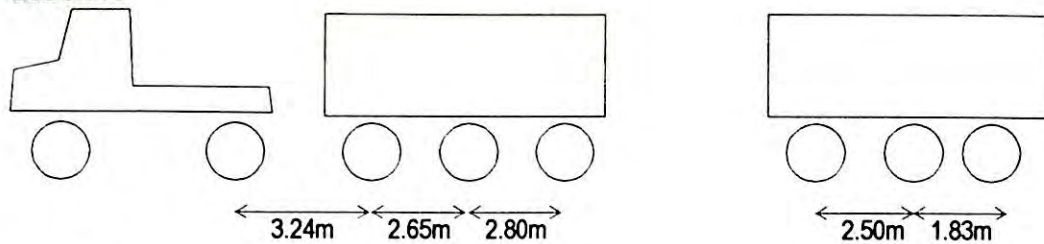
5.2.4 General Vehicle Information

Six different vehicles were used in the live load study (Allouche et al. 2003). The information of each vehicle is summarized in Table 5.2. The detailed axle configuration for each vehicle is shown in Figure 5.5. For vehicle A (a Crobra truck), the trailer was separated from the track, thus it could be considered as two individual vehicles. Vehicles B and C had the same axle configuration with wheelbase of 18.50m. Vehicle D is a Dodge Caravan (Mini Van) with a gross weight of 1940 kg and wheelbase of 3.05 m. Vehicles E and F have a similar axle configuration with a wheelbase of 15.65 m and 15.35 m, respectively. Shaded wheels in Figure 5.5 indicate weight data not available for those axles. One or two axle load data were not available for truck B, C and E, while distance between front two axles was not available for Truck A (Allouche et al. 2003). However, all the axle information was available for truck F in the live load test. Analysis of live load for Truck F and partial analysis for Truck A were therefore emphasized in this thesis.

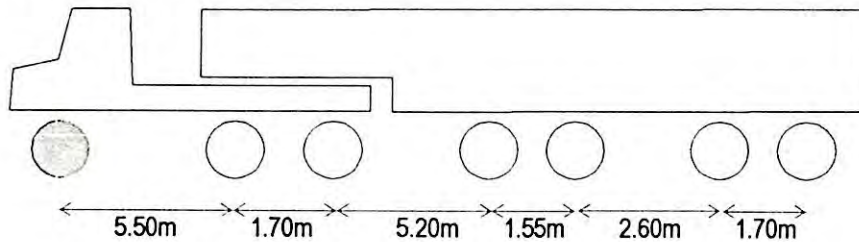
Table 5.2: General Information of the Tested Vehicles (Wong, 2002)

Vehicle	Model	Gross Weight (kg)	Wheel Base (m) Truck [incl. Trailer]	Axles
A	Cobra	60360	NA	1+4+3
B	Peterbilt	59600	7.2 [18.5]	1+3+4
C	CAP 475	59600	7.2 [18.5]	1+2+(2)+2
D	Dodge Caravan	1940	3.05	1+1
E	N/A	52310	6.4 [15.65]	1+2+(2)+2
F	N/A	51760	6.55 [15.35]	1+2+2

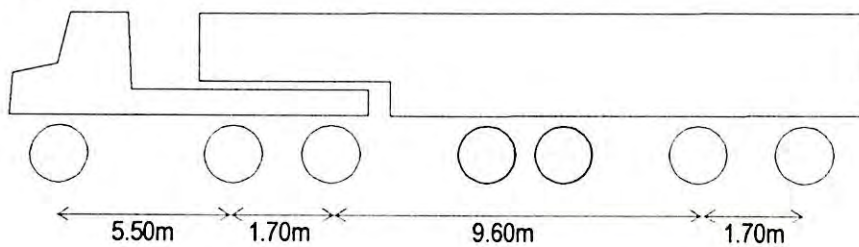
Truck A



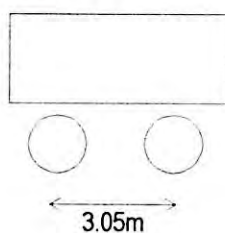
Truck B



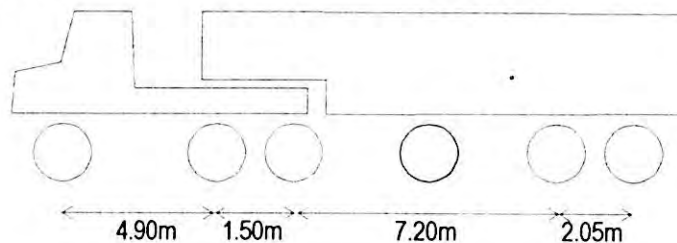
Truck C



Truck D



Truck E



Truck F

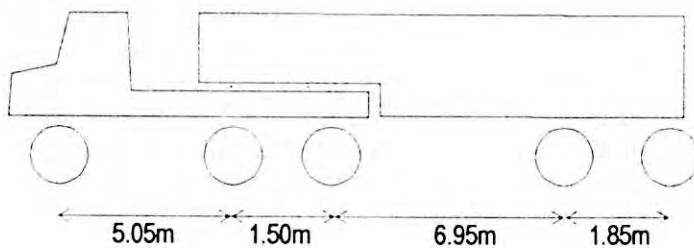


Figure 5.5: Axle Configuration for Vehicles A to F (Wong, 2002)

5.3 PRESSURE CELL RESPONSE

5.3.1 Crown Cells

Figure 5.6 shows the crown cell readings (Cells 9 and 10) during passage of vehicles Truck A and F. The DAS was programmed to read the stresses at 20 and 15-second intervals for truck A and F respectively. The tested vehicles were asked to stop over the test bed for approximately 30 to 40 sec with each axle on top of the test bed, in order to capture the response corresponding to the static loads applied with the axles of the vehicle. Pressure Cells 9 and 10 in Figure 5.6 shows similar readings with a deviation of about 5 kPa (<10% of the measured stresses) from each other. The average of the readings by the two cells was used as the stress intensity value in the soil above the crown of the pipe.

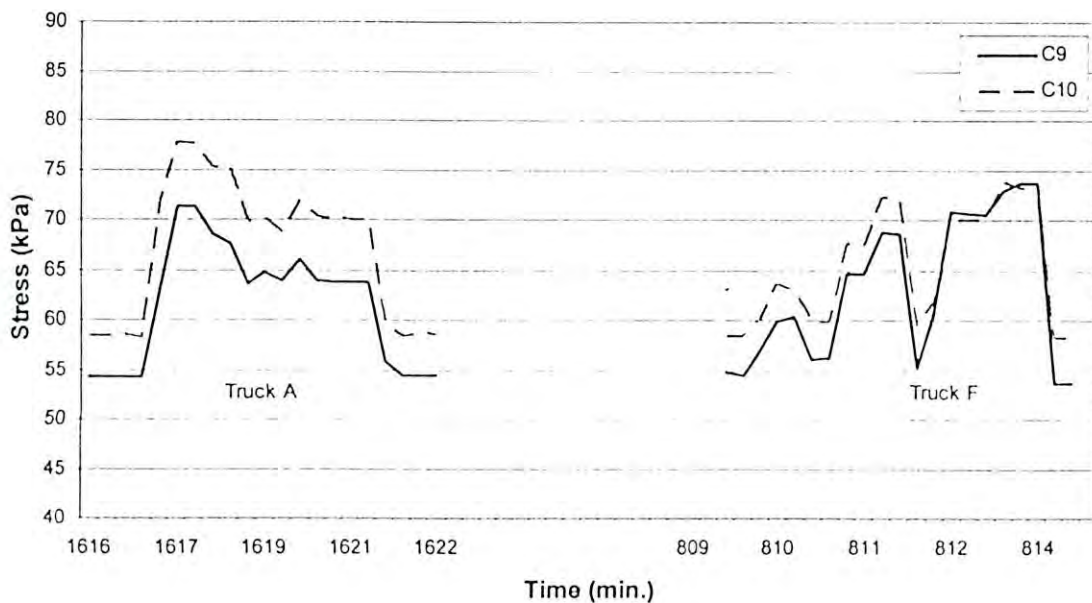


Figure 5.6: Crown Cell Response at the Barrie Site due to Truck A and F (After Wong, 2002)

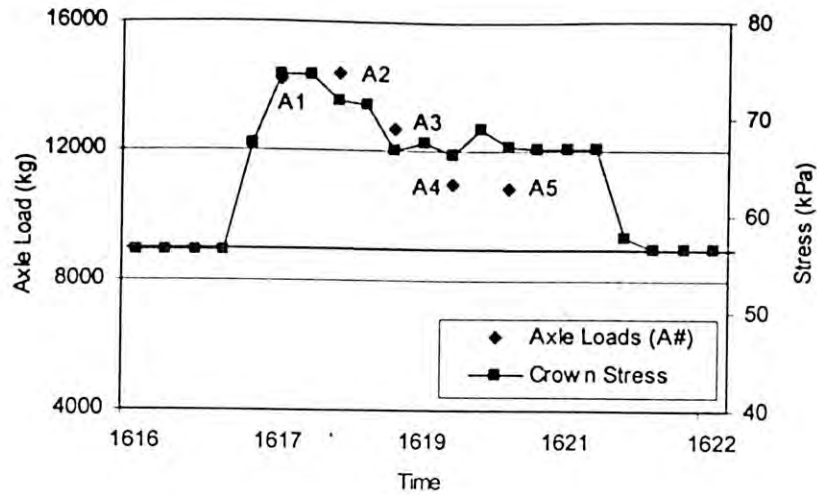


Figure 5.7: Average Crown Stresses due to Truck A (After Wong, 2002)

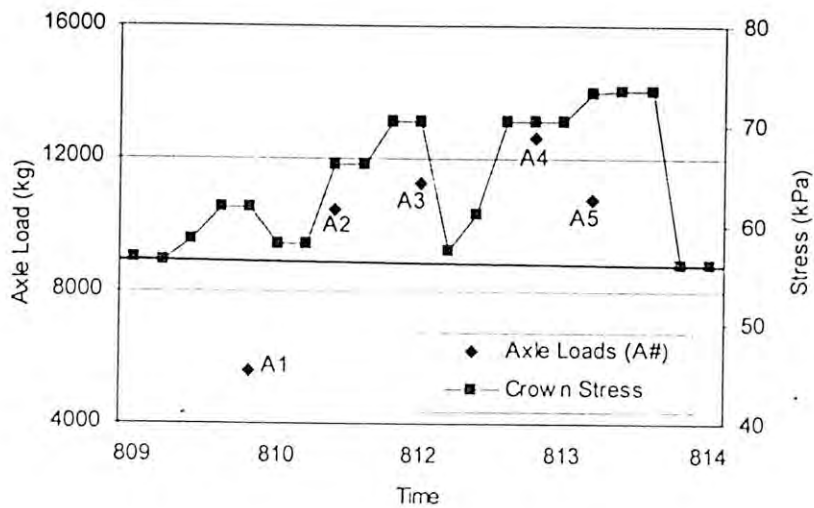


Figure 5.8: Average Crown Stresses due to Truck F (After Wong, 2002)

Figure 5.7 shows the average of stresses measured at crown Cells 9 and 10 for different axle loads above the pipe crown due to the presence of first part of Truck A. The distance found, on basis of data availability, between adjacent axles for that part of Truck A ranges from 2.65 m to 3.24 m. Figure 5.7 shows that the crown stress increased from 56.4 kPa to 74.5 kPa upon the displacement of the first axle above the test section. The crown stress recorded 71.8 kPa when the 2nd axle was placed above it. The smaller distance between adjacent axles did not decrease significantly the

stress on the pipe crown due to inclusion of greater combined effect. A gradual decreasing crown stress recorded due to gradual decrease in axle load of Truck A from front to rear. However, the Cells 9 and 10 registered an average stress at crown by 67.6 kPa, 69.0 kPa, 67.2 kPa due to placing 3rd, 4th, 5th axle respectively above it. Crown stress reached the maximum (74.5 kPa) with the first axle reaching the test section. It is important to note that the second axle was the heaviest one for this truck whose weight is 14400 kg while first axle is 14208 kg.

Figure 5.8 shows the average crown stresses for different axle loads above the pipe crown due to Truck F. The distance between adjacent axles for Truck F ranges from 1.5 m to 6.95 m. Figure 5.8 shows that the crown stress increased from 56.4 kPa to 61.7 kPa upon the displacement of the first axle above the test section, but decreased to 58.0 kPa when the axle moved away. The crown stress increased again and reached 66.1 kPa when the 2nd axle was placed above it. However, the stress did not decrease when the 2nd axle moved away from the test section due to the combined effect of the 2nd and 3rd axles. These axles are placed 1.5 m apart. Thus, the influence of a nearby axle on the soil stress was shown to be significant for the 2nd and 3rd axles of this truck. The crown stress then increased to 70.5 kPa when 3rd axle reached the test section. The crown stress returned to static load level upon the departure of the 3rd axle, indicating no influence of wheel loads. The distance between third and fourth axles was 6.95 m. Crown stress increased again due to the influence of the fourth axle and reached the maximum (73.4 kPa) with the fifth axle reaching the test section. It is worth noting that the fourth axle was the heaviest one for this truck (12605 kg). However, the maximum crown stress was reached with the passage of the fifth axle (10752 kg). This was attributed again to the combined effect of the loads from adjacent axles.

Table 5.3: Crown Stresses due to Axle Loads (Truck A & F) (After Wong, 2002)

	Axle	Wheel Load (kg)	Wheels per Axle	Axle Load (kg)	Avg. Crown stress (kPa)	Stress increase (kPa)	Stress increase (%)
Truck A	1	3552	4	14208	74.5	17.9	31.6
	2	3600	4	14400	71.4	14.8	26.1
	3	3168	4	12672	67.6	11.0	19.4
	4	2752	4	11008	69.0	12.4	21.9
	5	2720	4	10880	67.2	10.7	18.9
Truck F	1	2800	2	5600	61.7	5.1	9.0
	2	2616	4	10464	66.1	9.5	16.8
	3	2822	4	11290	70.4	13.8	24.4
	4	3151	4	12605	70.4	13.9	24.6
	5	2688	4	10752	73.7	17.2	30.4

Table 5.3 shows the axle loads for Truck A and F and its corresponding crown stress and stress increase values. The maximum changes of the soil stress due to the presence of Truck A and F are 17.9 kPa and 17.2 kPa respectively. This corresponds to the increase of 31.6% and 30.4% of the geostatic stresses respectively. The maximum stress occurred when the first axle was placed over the test section for Truck A, whereas for Truck F the maximum stress occurred when the last axle was placed over the test section.

5.3.2 Springline and Oblique Cells

Figure 5.9 shows the response of the springline cells (Cells 4, 5, 6 and 7) due to presence of Truck A and F. Cells 4 and 7 measured the vertical stresses while Cells 5 and 6 measured the horizontal stresses at the springline, respectively. Readings of the oblique cells are plotted in Figure 5.10. Average readings of the horizontal cells, vertical cells at springline and oblique earth pressure cells are summarized in Table 5.4. Truck loads were non-symmetric about the test section. Therefore readings in the

springline and oblique cells were not identical on both sides of the pipe test section. Nevertheless, the average of the cell readings was considered in the test observations.

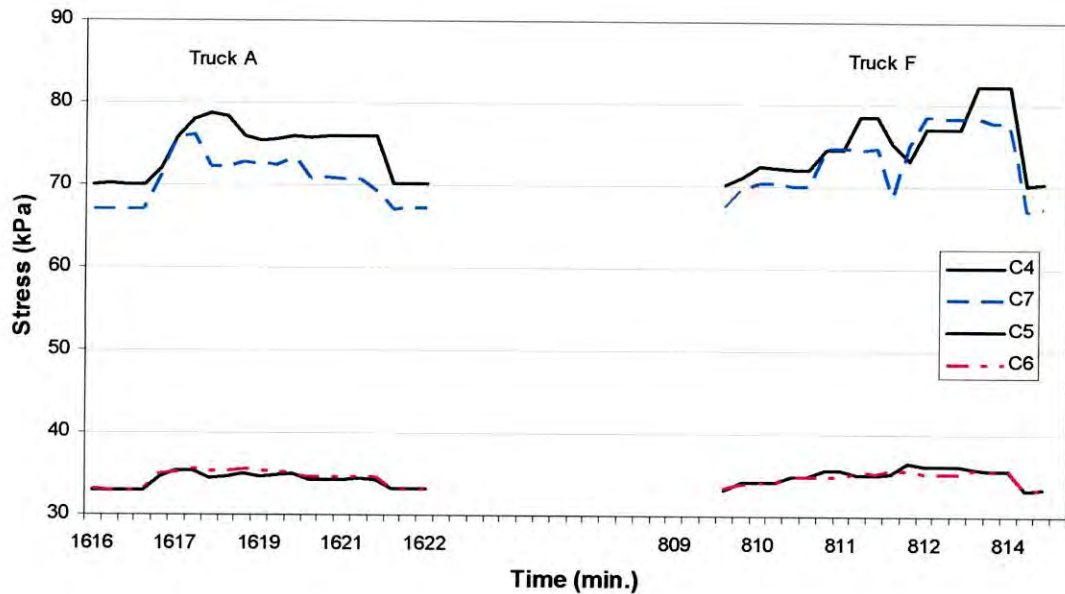


Figure 5.9: Springline Cell Response at the Barrie Site due to Truck A and F (After Wong, 2002)

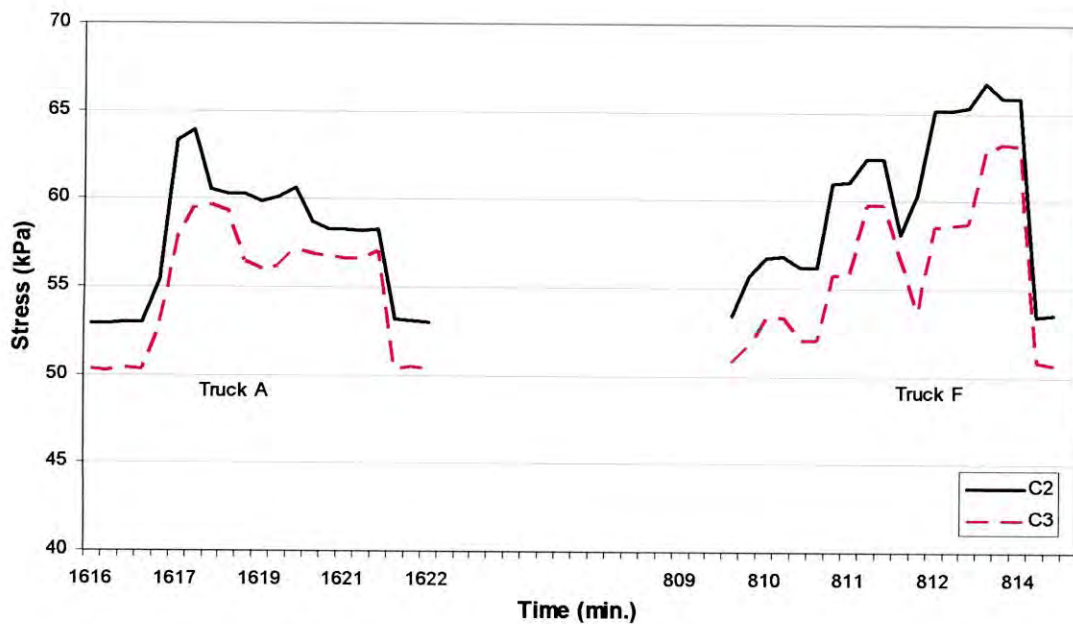


Figure 5.10: Oblique Cell Response at the Barrie Site due to Truck A and F (After Wong, 2002)

Table 5.4: Springline and Oblique Stresses due to Axle Loads (Truck A&F)
(After Wong, 2002)

	Axle	Springline (Vertical)			Springline (Horizontal)			Oblique		
		Total	Increase		Total	Increase		Total	Increase	
			kPa	%		kPa	%		kPa	%
Truck A	1	76.9	8.3	12.1	35.2	2.1	6.3	61.7	10.0	19.3
	2	75.5	6.9	10.1	34.8	1.7	5.1	59.6	7.9	15.3
	3	74.1	5.5	8.0	34.8	1.7	5.1	57.9	6.2	12.0
	4	74.5	5.9	8.6	35.2	2.1	6.3	59.0	7.2	13.9
	5	73.4	4.8	7.0	34.5	1.4	4.2	57.6	5.9	11.4
Truck F	1	71.4	2.8	4.1	34.1	1.0	3.0	55.1	3.3	6.4
	2	77.9	9.3	13.6	35.2	2.1	6.3	58.5	6.8	13.2
	3	76.6	8.0	11.7	35.1	2.0	6.0	61.1	9.3	18.0
	4	77.7	9.1	13.3	35.7	2.6	7.9	61.9	10.2	19.7
	5	80.0	11.4	16.6	35.6	2.5	7.6	64.5	12.8	24.8

5.4 COMMENTS ON FULL-SCALE TEST RESULTS

It is seen in the previous sections that crown stress is affected more significantly than springline stress of the pipe due to the live loads. A similar observation was noticed from finite element analysis presented in Chapter 4. The vertical stress increase at the springline ranged from 55% to 65% of the stress increase at the crown of the pipe during the live load test. The ratio of the horizontal to vertical stress increase at the springline ranges between 0.2 and 0.3. This indicates that the relative increase of horizontal stress due to live load at the springline is less than that for the vertical stress.

The increase of haunch stress (oblique cell readings) due to the presence of live load is greater than the stress increase at the springline of the pipe. This is since the additional live load carried by the concrete pipe is transferred to the bedding partially

through the haunches. The increases in haunch stresses during this live load test were 65% to 75% of the increase of crown stresses.

In the present study, measured stresses have been evaluated with the results of Finite Element analyses. A particular attention was paid on the increase of pipe crown stress due to truck load. The increase of stress at the crown was the maximum during the live load test.

5.5 3-D FINITE ELEMENT MODELING OF FULL SCALE TESTS

Detailed numerical analyses of the pipe-soil system have been carried out using three-dimensional finite element computer software ANSYS. A linear elastic analysis is performed with three-dimensional modeling of the pipe-soil system. Figure 5.11 shows the finite element mesh used for 3-D analysis of the full scale test.

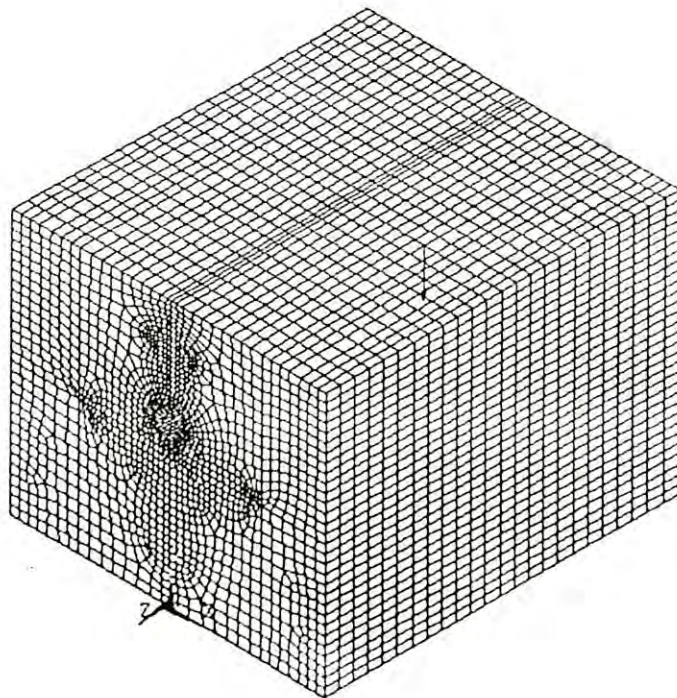


Figure 5.11: Finite Element Mesh

5.5.1 Mesh

The in-plane geometry of the finite-element mesh used for three-dimensional analysis was the same as used for the 2-D analysis (Chapter 3) but the trench geometry was chosen in accordance with Figure 5.3. For simplification, the surface of the trench was considered horizontal and the section rectangular. The provision, for handling backfill and native soil distinctly, has also been taken into consideration in the model. In finite element method, mesh density in the area adjacent to pipe highly affects the results. For that, the provision for using two types of soils simultaneously has made the model easy to run with two different desirable densities even though the model was studied by a unique type of soil. The mesh of the inner core of soils was considered fine and the outer was coarse. However, the model was then extruded in 300-mm increments to maintain an adequate aspect ratio on the size of the elements. The total length of the 3-D model was 7.2 m, representing the length of the three central pipe segments, labeled sections 2, 3 and 4 (Figure 5.4b). The soil and the pipe are modeled using 3-dimensional (3-D) brick elements. The boundary conditions for the 3-D model are similar to those of the 2-D analysis presented in Chapter 3. However, an additional work was performed for the optimum 3-D mesh same as Chapter 4.

5.5.2 Material Models

Modulus of elasticity of the pipe material was chosen as the typical value for concrete (15000, 20000 MPa) and the poisson's ratio was used as 0.2. Soil parameters (Modulus of elasticity, poisson's ratio) of the soil depend on the type of soil and the degree of compaction. Granular material is generally recommended as the (sand or gravel) backfill material for pipe. Assuming well-graded or poorly graded sand as the backfill material modulus of elasticity may vary from 5 MPa at the loosest condition to 30 MPa at the densest condition for typical installation, according to McGrath (1998). In the full scale test, well graded gravelly sand with little fines was used. Thus the soil modulus (20, 30 MPa) has been used in this investigation. Poisson's ratio of the soil was used 0.2.

5.5.3 Influence Line for Vertical Soil Stress at Pipe Crown

To represent the stress induced near the pipe by a moving vehicle, analyses were performed with different locations of a concentrated surface load. A unit surface load with variation of the location was used to develop influence line of desired stresses due to the surface load as shown in Figure 5.12. The load was moved from a distance of 2 to 3 m up to the pipe crown. The load was moved along both longitudinal and transverse direction of the pipe.

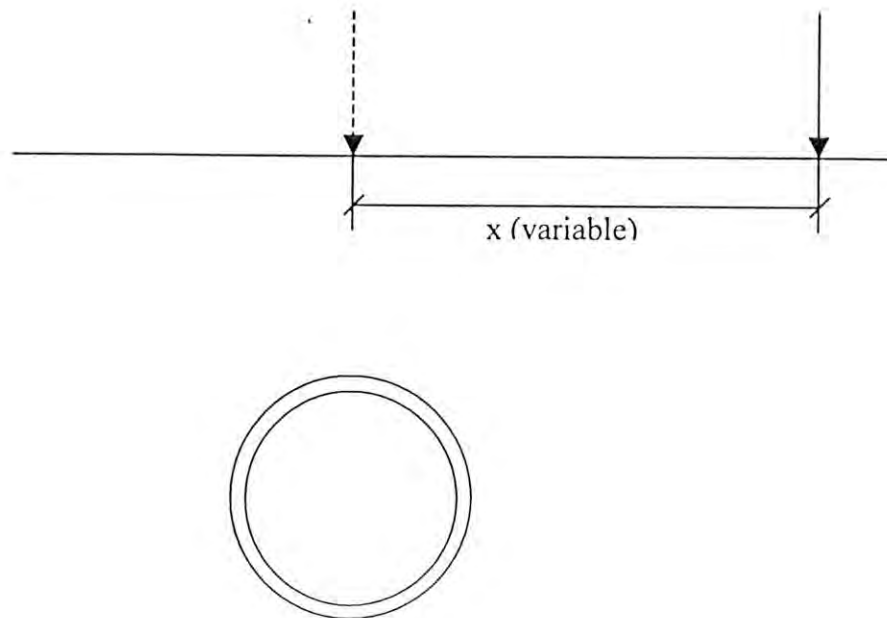


Figure 5.12: Location of Unit Surface Load for FE Analysis

Figure 5.13 shows vertical stresses at 100 mm above pipe-crown due to the movement of 1 N surface load along the transverse direction of the pipe. The stress at 100 mm above the pipe crown was considered since stress at that location was measured during the field tests. Soil density has not been taken into consideration in this study. Thus, the stress represents the increase of stress with respect to geostatic stresses due to the surface load. Figure 5.13 reveals that pipe with greater stiffness and backfill soil having lower modulus cause to attract higher loads for the surface. This may be due to negative arching caused by the stiffer pipe. Effects of the surface load do not contribute to create considerable stresses on pipe where the load reaches to 3.0 m away from the pipe along the transverse direction of pipe.

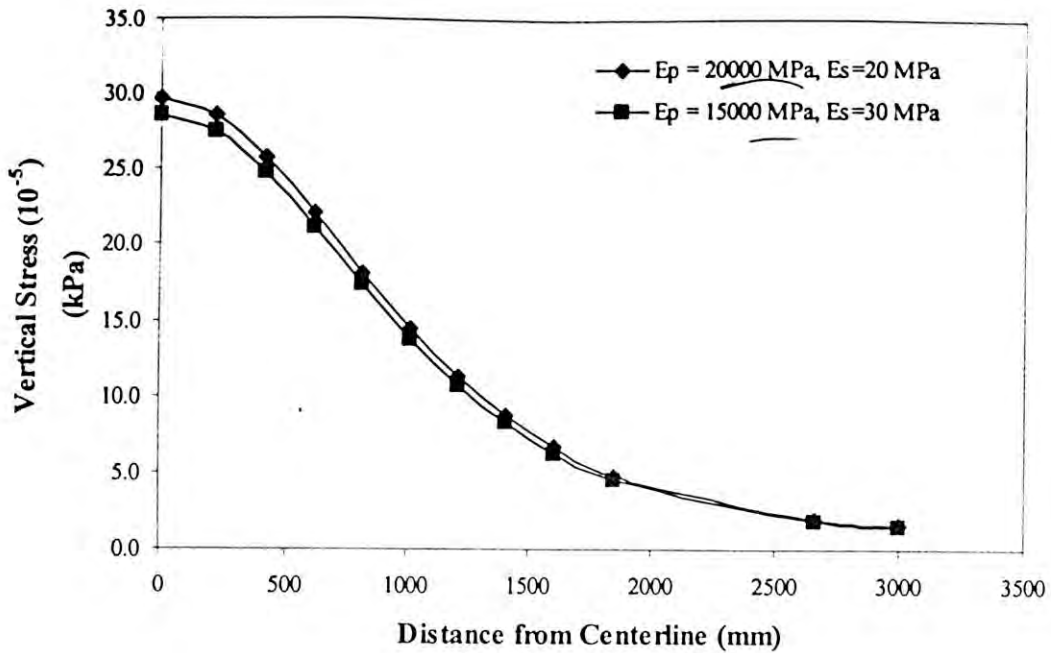


Figure 5.13: Influence Line for Vertical Soil Stress at 100 mm above Pipe-Crown (Transverse Direction, Burial Depth = 2.2D)

Figure 5.14 shows influence line of vertical stresses along the longitudinal direction of pipe. Effects of the surface load of the wheel become insignificant at 2.0 m away from the load along the longitudinal direction of pipe. Thus, stresses reaching to the pipe from the wheel of any side of an axle load may not be affected by the stresses from the wheel of other side of the same axle considering that wheels are located greater than 2.0 m apart. The study also shows that the maximum stress due to surface load reaches to the pipe if the load directly above the pipe crown.

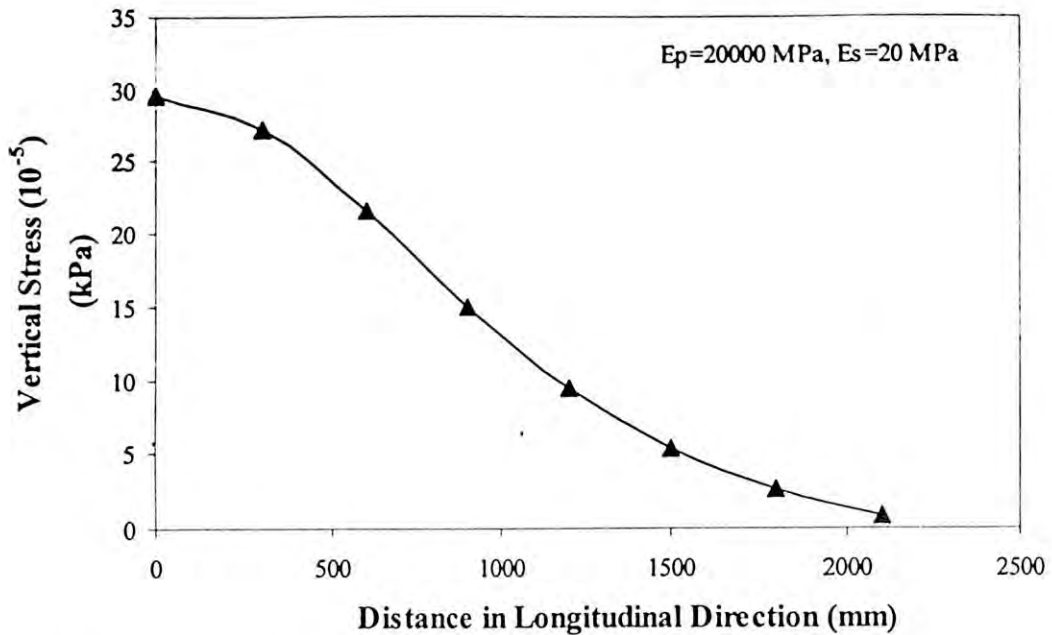


Figure 5.14: Influence Line for Vertical Soil Stress at 100 mm above Pipe-Crown (Longitudinal Direction, Burial Depth = 2.2D)

5.6 COMPARISON WITH MEASUREMENTS

Stress increases due to traffic load (Truck A & F) were calculated using the finite element analysis and compared with field measurements. As discussed earlier, analysis was performed with live load as a unit concentrated load acting vertically on top ground surface. The resulting influence line was used to calculate the stress due to truck load. The stresses due to the truck loads were determined by multiplying wheel loads with the stresses found from the influence line owing to its respective positions.

Table 5.5 and Table 5.6 shows the stresses at pipe crown due to the virtual truck F having each equal wheel load, 1 N. Two different pipe-soil modulus were taken into consideration in tables. The table also reveals how much the effect of other wheels is when one wheel reaches vertically on top of the pipe. Crown stresses are not significantly affected by other axles when Axle-1 is on top of the pipe because Axle-2 is too far away from pipe. Axle-3 affects the stress when Axle-2 is on top of the pipe and vice versa since the axles are very close (1.5 m). Similarly, Axle-5 affects when

Axle-4 is on top of the pipe and vice versa. Crown stress is not significant when the pipe is in between Axle-3 and Axle-4.

Table 5.7 shows stresses increase at crown level due to the presence of Truck F. Unlike field observation, Axle-4 in lieu of Axle-5 has been observed in finite element analysis that produces maximum stress at crown level. It is not surprising as Axle-4 carries the maximum amount of loads. Figure 5.15 shows the stress increase at crown level with different position of axles. The five axles are expressed here with the numbers only. Figure 5.15 also shows that the stress at crown level is increased by 18.6 kPa (and 17.8 kPa) due to the last axle of truck F in the finite element analysis depending upon pipe-soil modulus while it was found to be 17.2 kPa in the field observation. However, the discrepancy in between finite element results and field observations appears large in case of other axles. One of the reasons may be that the loads were not symmetrically placed in the field observation.

Figure 5.15 shows the comparison of the changes in crown stress due to different axles of Truck F on top of the pipe. Crown stress of 5 kPa was increased when Axle-1 was on top of the pipe leaving four other axles of this truck away from pipe. The finite element analysis calculated the stress as 8 kPa. The stress was decreased in both analysis and measurement as the axle moved away from the pipe bringing Axle-2 close to the pipe. The calculated stress matched reasonably well with the measurements for in-between position of the pipe with respect to Axle-1 and Axle-2. The stress increased again when the second axle reached to the pipe crown, which is also predicted by the finite element analysis. However, the analysis showed an overestimation of the crown stress with respect to the measurement. This may be due to the fact that the finite element analysis was based on linear elastic soil model, while non-linear elasto-plastic deformation might have caused stress redistribution, resulting in less crown stress in measurements. Both analysis and measurement continued the stress increase upto when Axle-2 moved forward and Axle-3 came on top of the pipe. The distance between Axle-2 and Axle-3 was less relative to the distance between Axle-1 and Axle-2. Due to the short distance (1.5 m) between Axle-2 and Axle-3 the crown stress was not reduced when Axle-2 move forward from above-the-pipe. However, the crown stress decreased again when Axle-3 moved further, because the distance between Axle-3 and Axle-4 was too long (7 m). Stress increases from

analysis followed the measurements when the vehicles moved further. Thus, the finite element analysis successfully predicted the measured stress due to the truckload during movement of the truck over the pipe bed. The finite element method provided a conservative estimate of the crown stress, may also be due to the consideration of loads placed exactly above the pipe crown while exact location of pipe crown during measurement was not exactly known. In finite element analysis, the magnitude of the stress at the crown level is assumed as the stress increase due to the live load, since the soil density was not considered. FE analysis for crown stress due to Truck A also appeared to overestimate the stress (Figure 5.16)

**Table 5.5: Stress Matrix due to Unit Load ($E_p=20000$ MPa, $E_s=20$ MPa)
(Truck F)**

(Position of Axle) MPa	1	2	3	4	5
1	2.96E-07	0	0	0	0
2	0	2.96E-07	7.75E-08	0	0
3	0	7.75E-08	2.96E-07	0	0
4	0	0	0	2.96E-07	4.79E-08
5	0	0	0	4.79E-08	2.96E-07

**Table 5.6: Stress Matrix due to Unit Load ($E_p=15000$ MPa, $E_s=30$ MPa)
(Truck F)**

(Position of Axle) MPa	1	2	3	4	5
1	2.85E-07	0	0	0	0
2	0	2.85E-07	7.20E-08	0	0
3	0	7.20E-08	2.85E-07	0	0
4	0	0	0	2.85E-07	4.47E-08
5	0	0	0	4.47E-08	2.85E-07

Table 5.7: Crown Stress Increase due to Axle Loads (Truck F)

Axle	Wheel Load (kg)	Wheels per Axle	Wheel Load (kg) (one side of an Axle)	Wheel Load (N) (one side of an Axle)	Stress Increase (kPa) (FEM)		Stress Increase (kPa) (Full Scale Test)
					Ep=20000 MPa, Es=20 MPa	Ep=15000 MPa, Es=30 MPa	
					1	2800	
2	2616	4	5232	51325.92	19.488	18.615	9.5
3	2822	4	5644	55367.64	20.371	19.476	13.8
4	3151	4	6302	61822.62	20.831	19.978	13.9
5	2688	4	5376	52738.56	18.576	17.795	17.2

Table 5.8: Stress Matrix due to Unit Load (Ep=20000 MPa, Es=20 MPa) (Truck A)

(Position of Axle) MPa	2	3	4	5
2	2.96E-07	0	0	0
3	0	2.96E-07	1.97E-08	0
4	0	1.97E-08	2.96E-07	1.65E-08
5	0	0	1.65E-08	2.96E-07

**Table 5.9: Stress Matrix due to Unit Load ($E_p=15000$ MPa,
 $E_s=30$ MPa) (Truck A)**

(Position of Axle) MPa	2	3	4	5
2	2.85E-07	0	0	0
3	0	2.85E-07	1.80E-08	0
4	0	1.80E-08	2.85E-07	1.55E-08
5	0	0	1.55E-08	2.85E-07

Table 5.10: Crown Stress Increase due to Axle Loads (Truck A)

Axle	Wheel Load (kg)	Wheels per Axle	Wheel Load (kg) (one side of an Axle)	Wheel Load (N) (one side of an Axle)	Stress Increase (kPa) (FEM)		Stress Increase (kPa) (Full Scale Test)
					$E_p=20000$ MPa, $E_s=20$ MPa	$E_p=15000$ MPa, $E_s=30$ MPa	
2	3600	4	7200	70632	20.913	20.131	14.8
3	3168	4	6336	62156.16	19.465	18.687	11
4	2752	4	5504	53994.24	18.089	17.335	12.4
5	2720	4	5440	53366.4	16.692	16.047	10.7

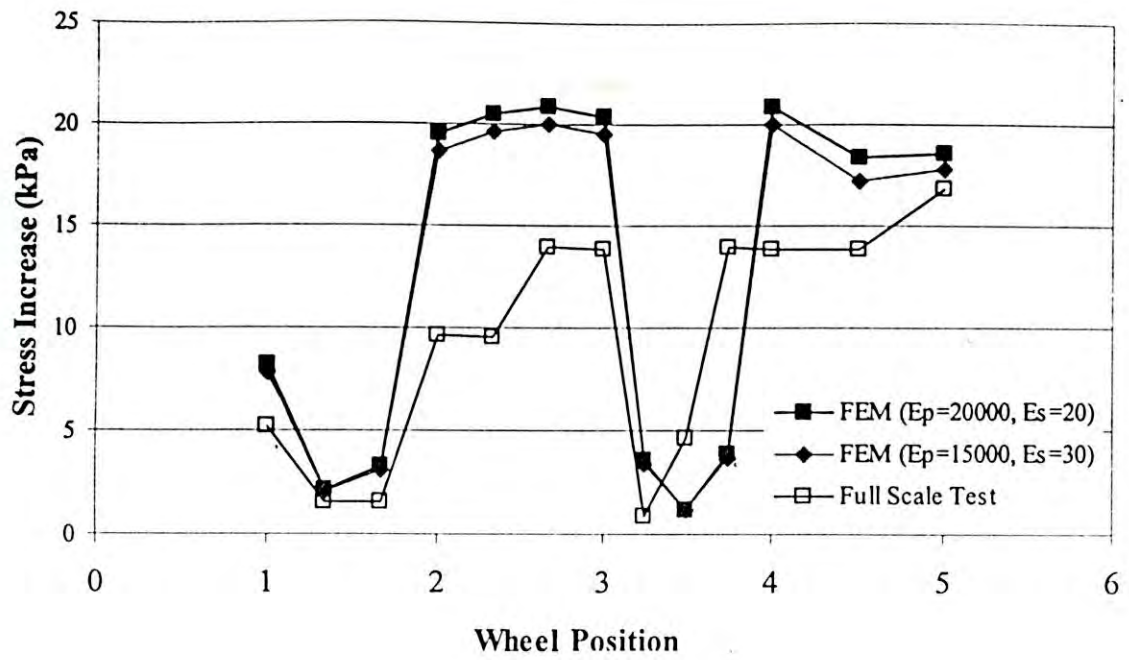


Figure 5.15: Comparison of Crown Stresses due to Truck F

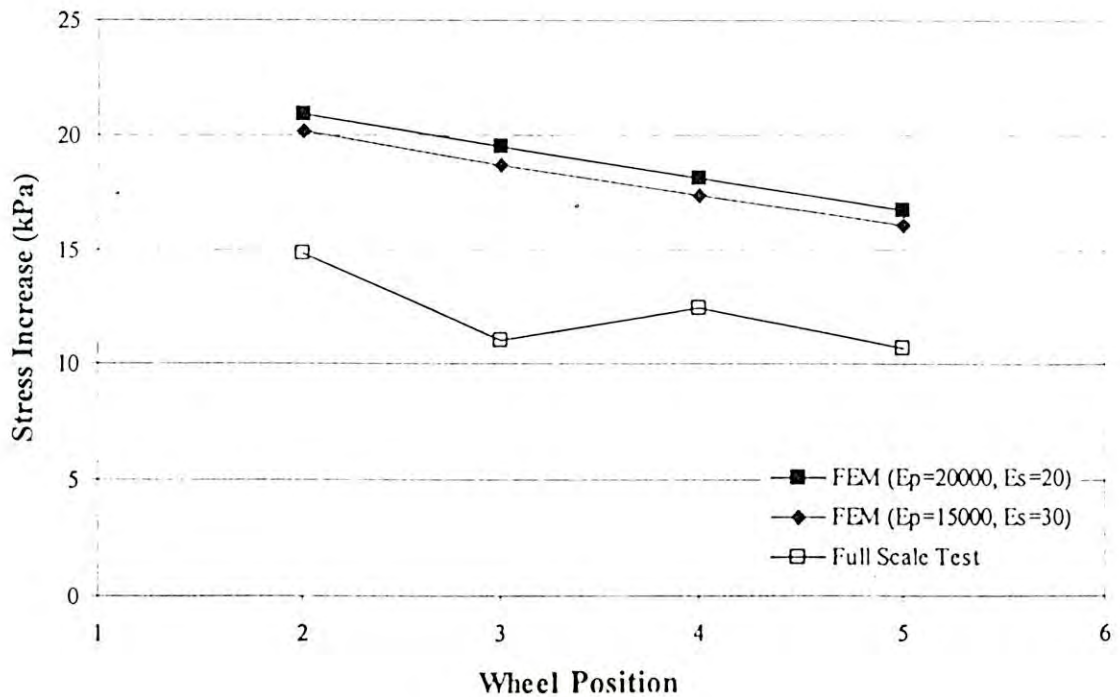


Figure 5.16: Comparison of Crown Stresses due to Truck A

5.7 SUMMARY

Soil stress around a concrete pipe under surface live load was measured in a full-scale test undertaken by Ontario Concrete Pipe Association in Canada. The test bed was consisted of five 2.4 m long segments of 600 mm diameter (inner) pipes buried at an average depth of 1.75 m. Earth pressure cells were installed around the pipe at different points to measure soil stresses. Increase of the soil stress around the pipe was measured in a live load test program due to several trucks/vehicles passing over the test bed. The test bed has been investigated using three-dimensional FE model to interpret some of the test investigation. Influence lines for different stresses have also been developed based on the finite element analysis to determine the stress increase for various positions of wheel loads on ground surface. The study reveals the followings:

- The influence lines of stresses can effectively be used to evaluate the effect of live load around buried rigid pipe.
- Influence line of stress distributions on soil in longitudinal direction of the pipe are suddenly decreases with a short distance away from the point of loading (Figure 5.13 and 5.14). Effects of the surface load of a single wheel were found to be insignificant at 2.0 m away from the load. Thus, stresses reaching to the pipe from any wheel load may not be affected by the stresses from the other wheel of the same axle.
- Finite element method provides a conservative estimate (30 to 50 percent higher stress) of the stress increase at the crown (Figure 5.15). This may be due to the fact that the axle load was not placed exactly vertically above the test pipe section where the stress was measured.
- Measurements showed that crown stress is affected more significantly than springline stress of the pipe due to the live loads, agreeing with the calculated values using finite element method.

CHAPTER 6

INCORPORATION OF SURFACE LOAD IN DESIGN CODE

6.1 INTRODUCTION

The study presented in Chapter 4 and Chapter 5 of this thesis reveals that concentrated surface load causes additional stress on pipe wall, particularly for shallow burial condition. Allouche et al. (2004) indicated stress increase of 10 to 35% of geostatic stress due to surface load around a pipe buried at 2.2 m below ground surface. The concentrated load on ground surface above the pipe results from vehicles moving on the surface. It is also revealed that the stress around the pipe under the surface load is influenced by the position of the moving vehicle. The effect of the surface load is considered in current design codes (ie, AASHTO, ASCE, CSA etc) as a uniformly distributed load at crown level of the pipe. The uniform crown stress is then distributed around the pipe circumference according to Heger earth pressure distribution. The uniformly distributed load is calculated through dividing the wheel load by an area calculated by multiplying effective length in both sides obtained as size of wheel footprint plus 1.75 times the depth to the pipe crown. Thus, the surface load is assumed to be spread at a rate of 1.75 with depth. If the wheels are too close causing overlapping of the area, the combined area of two or more wheels are used. However, comparison of stress around pipe with those calculated using the design methods reveals that the methods underestimate the stress around the pipe. The measurement of soil stress around a rigid concrete pipe also showed similar observation. Allouche et al. (2004) compared the soil stress calculated using ASCE (1993) design method with that of measured in a full-scale test. The design method appeared to underestimate the stress by a factor of two or more, indicating unconservative estimate of the stress. The full-scale test observations have been simulated successfully in this research as discussed in Chapter 5. Thus the finite

element analysis appeared as an effective tool to incorporate the effect of surface load during buried pipe design.

Finite element analysis is the most powerful tool for soil-pipe interaction analysis. It was used successfully in interpreting different aspects of soil stress around buried rigid pipe revealed from the field observation. Chapter 5 described the study of live load using the finite element analysis that simulated the soil stress around pipe reasonably. However, undertaking of the analysis for various position of wheel load during design is tedious. In this regard, influence line of the stresses under different condition can be developed. The influence lines can effectively be used to calculate the soil stresses around the pipe for various position of surface load. In this chapter, a recommendation is made for incorporation of live load in rigid pipe design using the influence lines.

6.2 DEVELOPMENT OF INFLUENCE LINES

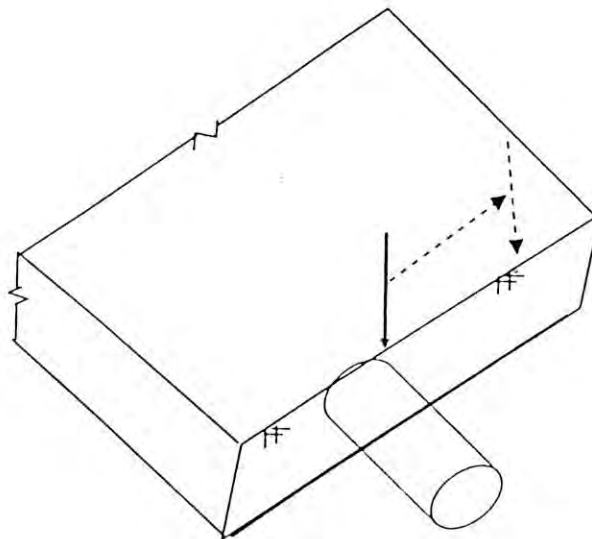


Figure 6.1: Location of Unit Surface Load in Transverse Direction

To develop the influence line of stresses in both transverse and longitudinal direction, a unit surface load with variation of locations was placed in the respective directions during finite element analysis. Figure 6.1 shows the location of unit surface load for developing the influence line of stress in transverse direction. The unit load is placed at different location and the analysis is performed. Then the stress and other quantities

of interests (such as, thrust, moment etc) are obtained for each of the locations. Quantities are then plotted as shown in figure 6.2, where the quantities of interest are plotted in y-axis and distance of the unit load from the centerline of the pipe is plotted in x-axis. Thus figure 6.2 gives a quantity for different location of the unit load. Similar analysis can be performed for different location of unit load in longitudinal direction of the pipe. Figure 6.3 shows the location of unit surface load for developing the influence line of stresses for moving load in longitudinal direction. The influence line of stresses in longitudinal direction is useful to understand how much a pipe is affected by the stresses from the wheel of other side of the same axle.

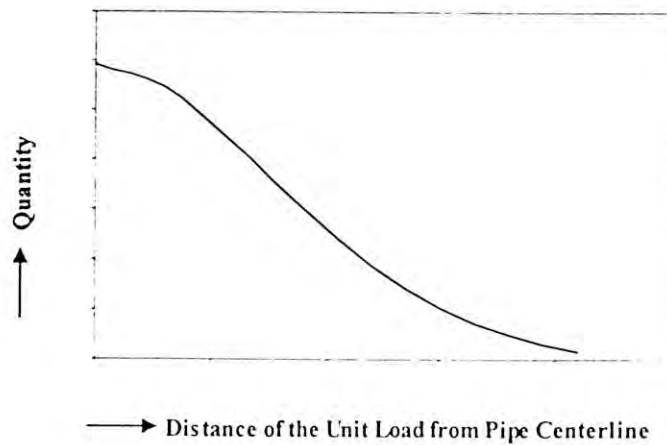


Figure 6.2: Plotting of influence line for a quantity (Schematic)

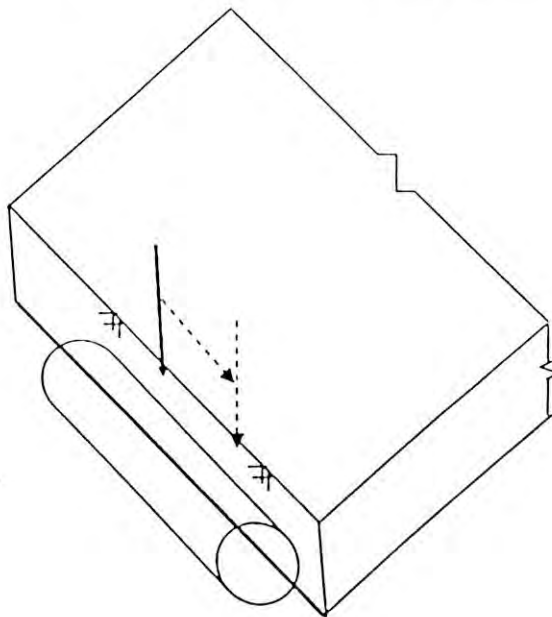


Figure 6.3: Location of Unit Surface Load in Longitudinal Direction

6.3 INFLUENCE LINES FOR SOIL STRESSES

Figure 6.4 shows the influence line for vertical soil stresses above pipe-crown in transverse direction. Soil density has not been taken into consideration in this study. Thus, the stress represents the increase of stress due to the surface load in addition to geostatic stress. Pipe with greater stiffness relative to the soil causes to attract higher loads for the surface due to negative arching caused by the stiffer pipe. Similar study can be performed for a wide range of variation of the pipe to soil modulus for incorporation in the design code. Figure 6.5 shows influence line of vertical stresses along the longitudinal direction of pipe.

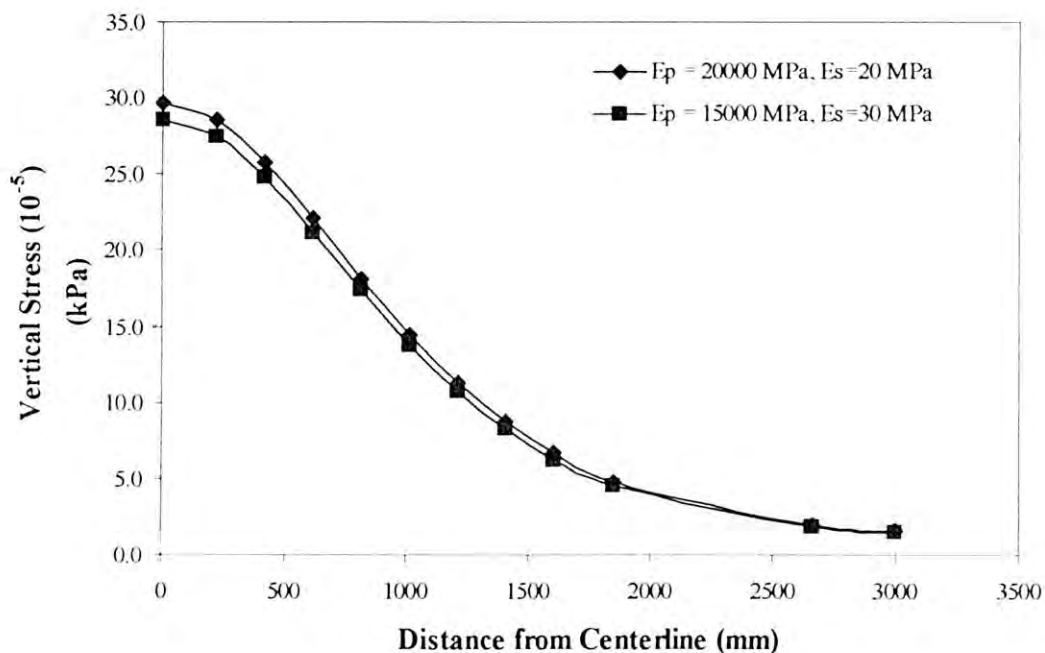


Figure 6.4: Influence Line for Vertical Soil Stress at 100 mm above Pipe-Crown (Transverse Direction, Burial Depth = 2.2D)

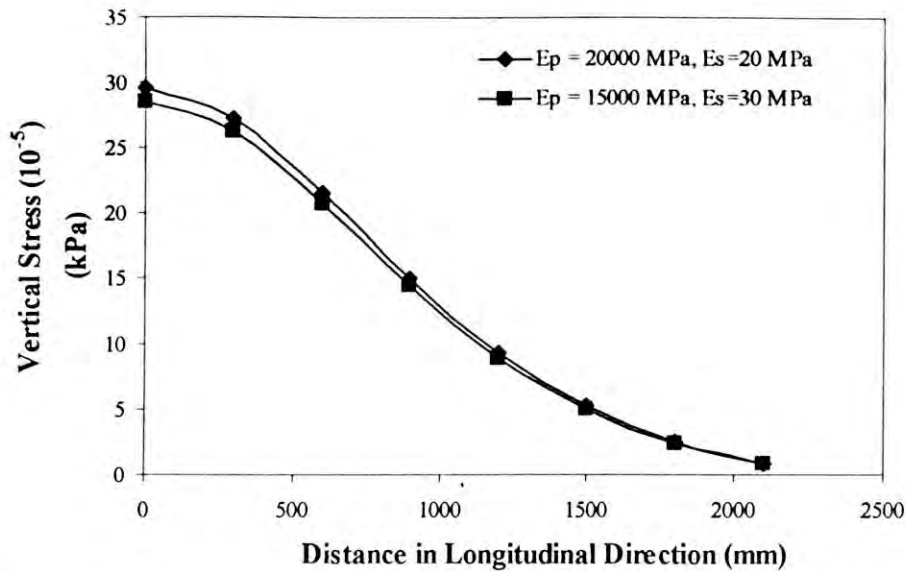


Figure 6.5: Influence Line for Vertical Soil Stress at 100 mm above Pipe-Crown (Longitudinal Direction, Burial Depth = 2.2D)

6.4 CALCULATION OF STRESS USING INFLUENCE LINES

The influence lines of stress can be used to calculate the stress around a pipe for different position of wheel loads. A unit surface load with variation of the location is used to develop the influence line of desired stresses due to the surface load (Figure 6.4 and 6.5). Then the stress induced in the pipe for any wheel can be calculated by multiplying the wheel load with the ordinate of the influence line for the respective position. Figure 6.6 shows ordinates for vertical stress for different wheels of a truck located at a distance of 300 mm from the pipe centerline. Each of the ordinate should be multiplied by the corresponding wheel load and then sum up to obtain the combined effects of all the wheels on the vertical stress. If more than one truck/vehicle exists, the ordinates for the wheels of the other vehicles can be obtained as shown in Figure 6.7 and then be added up to get the effects. Thus, any quantity resulting from many wheels can be obtained as:

$$\text{Quantity of interest} = \sum_{i=1}^n w_i y_i$$

Where,

n = Number of wheels

w_i = Weight of 'i' wheel

y_i = Ordinate of the influence line for the quantity at respective wheel (wheel 'i') position

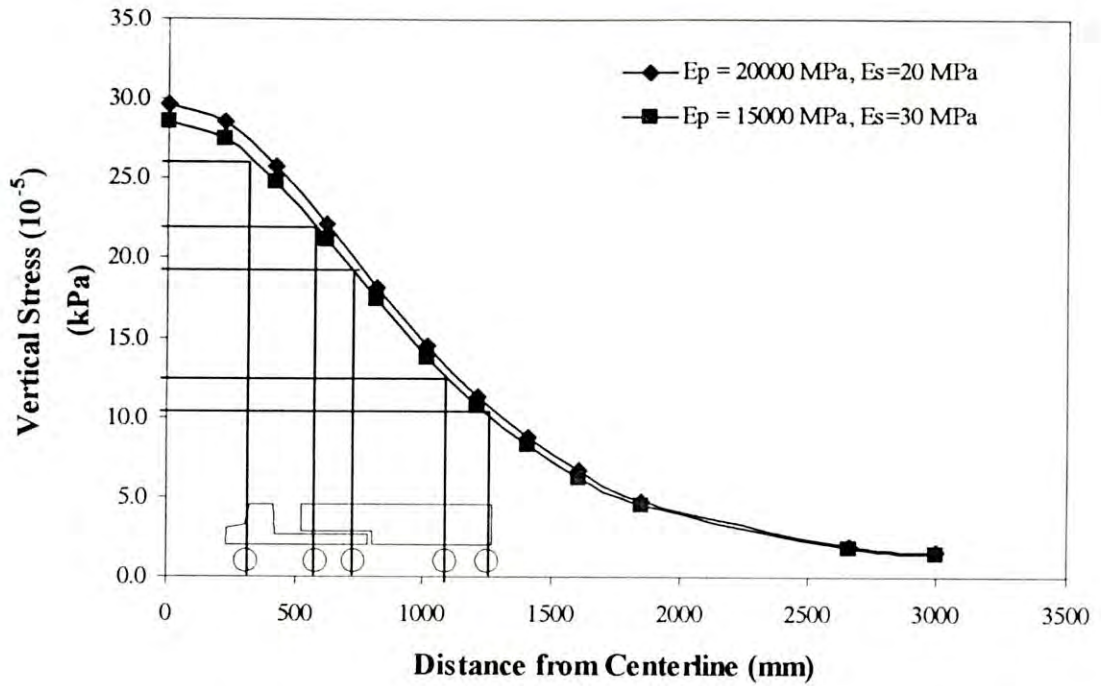


Figure 6.6: Pipe Stress Calculation from Influence Line (one vehicle)

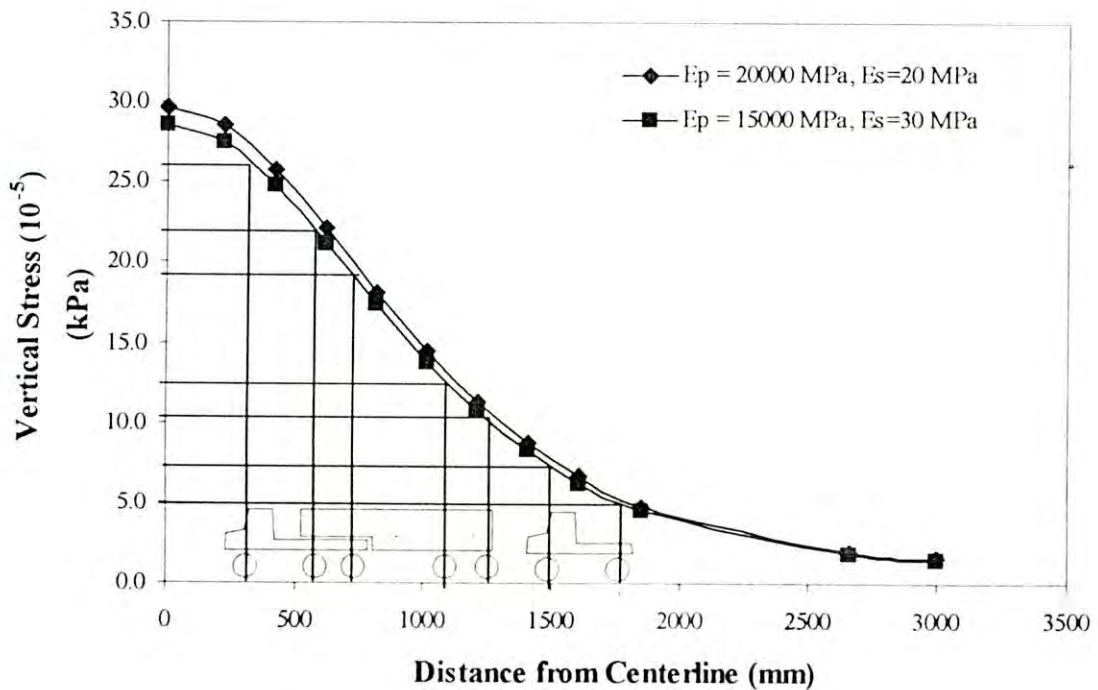


Figure 6.7: Pipe Stress Calculation from Influence Line (two vehicles)

6.5 SUMMARY

This chapter presents a method of incorporating the effect of concentrated surface live loads in the design code. Influence lines of soil stresses around pipe are developed using finite element analysis performed with a various position of a unit load. The influence lines are then used to calculate the stresses resulting from different wheel loads.

The recommendation is made in this chapter for incorporation of the live load effects based on the simulation of a particular condition of rigid pipe installation, i.e. Standard Installation Direct Design (SIDD) Type IV installation specifications. The installation condition represents a pipe in uniform ground condition where the backfill is uniformly compacted around the pipe. Pipe with 800 mm diameter and 100 mm thickness was emphasized in this study. However, similar study can be carried out to develop the influence line for a wide variety of pipe products which could be incorporated in pipe design code for incorporation of live load rationally.

CHAPTER 7

CONCLUSIONS AND RECOMMENDATIONS

7.1 INTRODUCTION

Municipalities in Bangladesh mainly use concrete pipes for storm and wastewater disposal. Concrete pipes are considered to be rigid with minimum or no deflection under load. Based on purpose, use, location and load pattern on it, a wide aspects need to be considered for buried rigid pipe design. Research is therefore warranted to develop a rational basis for optimum design of buried rigid pipe. The objective of this research was to determine the behavior of buried rigid pipe and to contribute to the development of design methods to predict and control for designing buried rigid pipe under surface live load. This Chapter summarizes the research findings reported in this thesis. Recommendations are then made regarding future work required to improve shallow buried rigid pipe design under surface live load.

7.2 CONCLUSIONS

Current design codes of rigid pipe design are studied in this thesis with particular attention to live load effects. The study reveals that a complete three-dimensional analysis is required to represent a more effective design of rigid pipe especially under surface load at shallow burial condition. Three-dimensional finite element analysis was performed in this thesis to study the pipe-soil interaction under vehicle loads. An extensive analysis has been performed to select the finite element mesh before the analysis was started. Finally, a full-scale test observation has been predicted using the finite element analysis. Based on the above study, the following conclusions can be drawn:

- Concentrated surface load may cause significant stress on pipe wall for shallow buried pipe, which is the greatest at crown followed by springline and invert respectively (Figure 4.11 to 4.15).
- The parametric study conducted shows that the ratio of the pipe to soil modulus has an influence on the results from 2D plane strain idealization and 3D idealization. Plane strain idealization appeared very good for pipes with low material modulus, while for pipe with higher modulus results from 2D analysis deviates from 3D analysis by 4 to 6% for the case considered in this study (Figure 3.13-3.16).
- ASCE and AASHTO design standard provides a reasonable estimate of the effects of live load where AASHTO shows more conservative results (Figure 4.18). But at shallow burial condition, the standards provide 30 to 50 percent unconservative estimate with respect to finite element results.
- For pipes buried at depths greater than 3 times the diameter, influence of pipe on the mechanism of wheel/axle load transfer is insignificant (Figure 4.16). Therefore, pipe-soil interaction analysis may not be required to calculate the soil stress. Classical theory (Boussinesq, 1885) can be used to calculate the stresses. However, if the burial depth is less than 3 times the diameter, pipe-soil interaction analysis should be performed to obtain the stresses.
- The pattern of stress distributions in longitudinal and transverse direction of the pipe is very similar (Figure 4.20). But at shallow burial condition, maximum of 5 to 6 percent tensile stress with respect to the highest compressive stress was developed along the longitudinal direction.
- Stress distributions at pipe crown level in both directions (longitudinal/transverse) decreases with a short distance away from the load. Effects of the surface load of a single wheel become insignificant at 1.5 m (2 times the diameter) away from the load. Thus, stresses reaching to the pipe from any wheel load may not be affected by the stresses from the other wheel of the same axle considering the distance between the wheels is greater than 1.5 m (2 times the diameter).

- Evaluation of a field test result indicates that finite element method can provide a useful tool for estimation of soil stresses around the pipe.
- Influence lines of different stresses have been developed based on the FE analysis. The influence lines can effectively be used to calculate the soil stresses around the pipe for various position of surface load. A proposal is made in this thesis for incorporation of live load effect using the influence lines.

7.3 RECOMMENDATIONS FOR FUTURE STUDY

Despite that different direct design tools such as Standard Installation Direct Design (SIDD) was developed for design of buried rigid pipe, the indirect design methods are popularly used in many countries around the world including Bangladesh for design of buried rigid pipe due to limitations of the direct design methods. Researcher's attention is therefore required in the areas of buried rigid pipes to improve direct design method of the pipe. This thesis focuses on the analysis of buried rigid pipes under surface live load. A proposal is made regarding rational incorporation of the live load effects during design of pipe. However, the proposal was based on a limited study of a rigid pipe. The study can further be extended as follow:

- Finite element analysis is may be extended for a wide variety of pipes with different diameter and wall thickness to develop design rationale to incorporate the live load effect.
- A study can be performed for a wide range of variation of the pipe to soil modulus to develop influence lines and to incorporate in the design code.
- Full-scale tests need to be carried out in our locality, using the typical materials and vehicles that are commonly used in Bangladesh. The measured response can be used to evaluate the results of finite element analysis.
- A design chart can be adopted in pipe design codes of Bangladesh based on rigorous studies using finite element analysis and the full-scale test observations.
- Simplified equations can be developed for buried rigid pipe design under surface load.

REFERENCES

- 1) AASHTO (1998) "LRFD Bridge Design Specifications", 2nd ed., AASHTO Washington D.C.
- 2) AASHTO (2002), "Highway Live Loads on Concrete Pipe", Design Data 1, American Concrete Pipe Association, 222 W. Las Colinas Blvd., Suite 641.
- 3) Allouche, E. N. and Freure, P. (2001) "Preventative maintenance of municipal sewers in Canada", proceedings of INFRA 2001, November 27-29, Montreal, Quebec, Canada, Session G1, 17 p., (available on conference CD).
- 4) Allouche, E. N., Wong, L. S. and Dhar, A. S. (2003) "Response of SIDD Type IV Bedding to Live Loads", Technical Report, Ontario Concrete Pipe Association, Ontario.
- 5) Allouche, E.N. and Wong, L.S. (2002) "OCPA Standard Installation Direct Design (SIDD) Type 4 Bedding Study – Final Report Phase I", Ontario Concrete Pipe Association.
- 6) Allouche, E.N., Dhar, A.S. and Wong, L.S. (2004) "Response of SIDD Type IV Bedding to Live Loads", 83rd Annual Meeting of the Transportation Research Board, Washington D.C., USA, Jan 11-15, 2004, CD-ROM.
- 7) Argyris, J. H. and Kelsey, S. (1960) "Energy Theorems and Structural Analysis", Butterworths, London; Part I reprinted from Aircraft Engrg. 26, Oct-Nov 1954 and 27, April-May 1955.
- 8) ASCE (1993), "Standard Practice for Direct Design of Buried Precast Concrete Pipe Using Standard Installation (ASCE93-15)," NY: American Society of Civil Engineers.
- 9) Boussinesq, J.V. (1885) "Application des potentiels a l'etude de l'equilibre et du mouvement des solides elastiques", Paris, Ganthier-Villars.
- 10) Burns, J.Q. and Richard, R.M. (1964) "Attenuation of stresses for Buried Cylinders", Proceedings of Symposium on Soil-Structure Interaction, University of Arizona, pp: 379-392.

- 11) CAN/CSA - S6-00 "Buried Structures" Canadian Highway Bridge Design Code.
- 12) Dhar, A. S., Siddique, M. S. A. and Sinha, A. N. (2004) "Deflection of Polyvinyl Chloride Pipes in Clayey Backfill", Transportation Research Record, No. 1892, pp 221-226.
- 13) Dhar, A. S., Kabir M. A., and Noor M. A., (2005) "The Development of Rational Design Method for Rigid Pipes", Proceeding of the Third Annual Paper Meet and International Conference on Civil Engineering, Institute of Engineers, Bangladesh.
- 14) Dhar, A. S. and Moore, I. D. (2004) "Two-Dimensional Analyses of Thermoplastic Culvert Deformations and Strains", Journal of Geotechnical and Geoenvironmental Engineering, ASCE, Vol. 130, No. 2, PP: 199-208.
- 15) Duncan, J.M. (1979) "Behavior and Design of Long-Span Metal Culverts", Journal of the Geotechnical Division, ASCE, Vol. 105, No. GT3: 399-418.
- 16) Haggag, A. A. (1989) "Structural Backfill Design for Corrugated-Metal Buried Structures", Ph.D. dissertation, Amherst, University of Massachusetts.
- 17) Heger, F. J., Liepins, A. A., and Selig, E. T., (1985) "SPIDA: An Analysis and Design System for Buried Concrete Pipe," Advances in Underground Pipeline Engineering, Proceedings of ASCE, pp. 143-154.
- 18) Hoeg. K. (1968) "Stress Against Underground Cylinder", Journal of Soil Mechanics and Foundation Engineering, ASCE, Vol. 94, SM4, 833-858.
- 19) Janssen, H.A. (1895) "Versuche über Getreidedruck in Silozellen", Zeitschrift des Vereins Deutscher Ingenieure, 39, 1045-1049.
- 20) Jayawickrama P.W., Amarasiri, A.L. and P.E. Regino (2002) "Minimum Cover Requirements for Large Diameter HDPE Pipe Installed with Granular Backfill", 81st Annual Meeting of the Transportation Research Board, Washington D.C., January 13 -17, 2002.
- 21) Katona, M.G. (1978) "CANDE: A Versatile Soil-structure Design and Analysis Computer Program", Journal of Advances in Engineering Software, Vol.1, pp. 3-9.
- 22) Katona, M.G., Smith, J.M., Odello, R.S., and Allgood, J.R. (1976) "CANDE -A Modern Approach for the Structural Design and Analysis of Buried Culverts", Report No. FHWA-RD-77-5, Federal Highway Administration, Washington, D.C., October.

- 23) Katona, M.G., Vittes, P.D., Lee, C.H., and Ho., H.T. (1981) "CANDE - 1980: Box Culverts and Soil Models", Report No. FHWA/RD-80/172, Federal Highway Administration, Washington, D.C., May
- 24) Marston, A. and Anderson, A.O. (1913) "The theory of Loads on Pipes in Ditches and tests of Cement and Clay Drain Tile and Sewer Pipe.", Bulletin 31, Iowa Engineering Experiment Station, Ames, Iowa.
- 25) McGrath, T.J. (1998) "Design method for flexible pipe", A report to the AASHTO Flexible Culvert Liaison Committee, Simpson Gumpertz & Heger Inc., Arlington, MA.
- 26) Moore, I.D. (2000) "Culverts and Buried Pipelines" Chapter 18, Geotechnical and Geoenvironmental Handbook, Edited by R.K. Rowe, Kluwer publisher, pp. 541-568.
- 27) Musser, S. C. (1989) "CANDE-89 user Manual", Report No. FHWA-RD-89-169, Federal Highway Administration, Mclean, VA.
- 28) Noor, M. A. and Dhar, A. S. (2003) "Three Dimensional Response of Buried Pipe Under Vehicle Loads", Proceedings of the ASCE International Conference on Pipeline Division of ASCE, Baltimore, Maryland.
- 29) Olander, H. C. (1950) "Stress Analysis of Concrete Pipe," U.S. Bureau of Reclamation Engineering Monograph No. 6.
- 30) Paris, J. M. (1921) "Stress Coefficients for Large Horizontal Pipes," Engineering News Record, Vol. 87, No. 19, November 10, 1921.
- 31) Selig, E. T., (1990) "Soil Properties for Plastic Pipe Installations", ASTM Special Technical Publication 1093, Buried Plastic Pipe Technology, W. Conshohocken, Pa, pp: 141-158.
- 32) Spangler, M.G. and Handy, R.L. (1973) "Soil Engineering" In text Educational Publishers, New York and London. 10.
- 33) Spangler, M.G. (1941) "The Structural Design of Flexible pipe Culverts." Bulletin 153, Iowa Engineering Experiment Station, Ames, Iowa.
- 34) Taleb, B. and Moore, I.D., (2000) "Three-dimensional bending in long span culverts". Proc. Annual Conference of the Canadian Geotechnical Society, Regina, pp. 305-312.
- 35) Taleb, B., and I.D. Moore. (1999) "Metal Culvert Response to Earth Loading: Performance of Two-Dimensional Analysis". Transportation Research Record: Underground and Other Structural Design Issues 1656: 25-36. Paper No. 99-0532.

- 36) Turner, M. J., Clough, R. W., Martin, H. C., and Topp, L. J., (1956) "Stiffness and Deflection Analysis of Complex Structures," *Journal of Aeronautical Sciences*, Vol. 23, No. 9, pp 805-824, Sept. 1956.
- 37) Wong, L. S. (2002) "Empirical and Finite Element Evaluation of Concrete Pipe Bedding Design Methods" Master of Engineering Science thesis, The University of Western Ontario, London, Ontario.
- 38) Wong, L. S., Allouche, E. N. and Moore, I. D. (2002) "Long-term Monitoring and Analysis of Full Scale Concrete Pipe Test Beds", ASCE Pipeline 2002 Conference, Cleveland, OH, USA.
- 39) Young, O.C. and Trott, J.J (1984) "Buried Rigid Pipes: Structural Design of Pipelines" Elsevier Applied Science Publishers, London and New York.
- 40) Zienkiewicz, O.C. (1994) "R.L. Taylor-Distinguished Researcher and Friend." *Recent Developments in Finite Element Analysis (CIMNE)* 1 - 17, 1994.

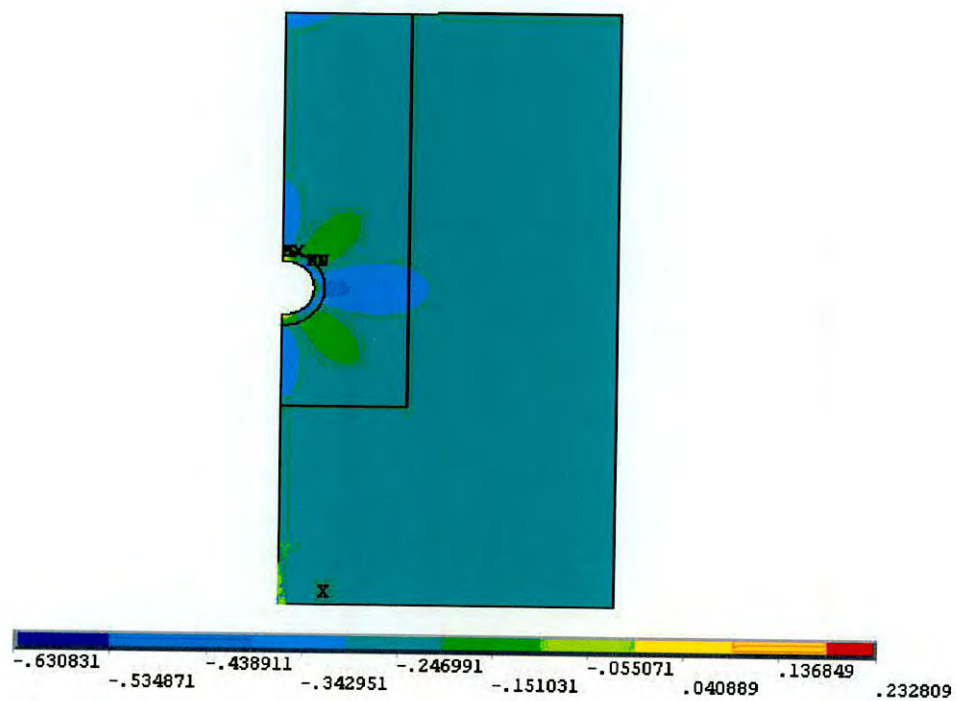
APPENDIX A

STRESS CONTOURS

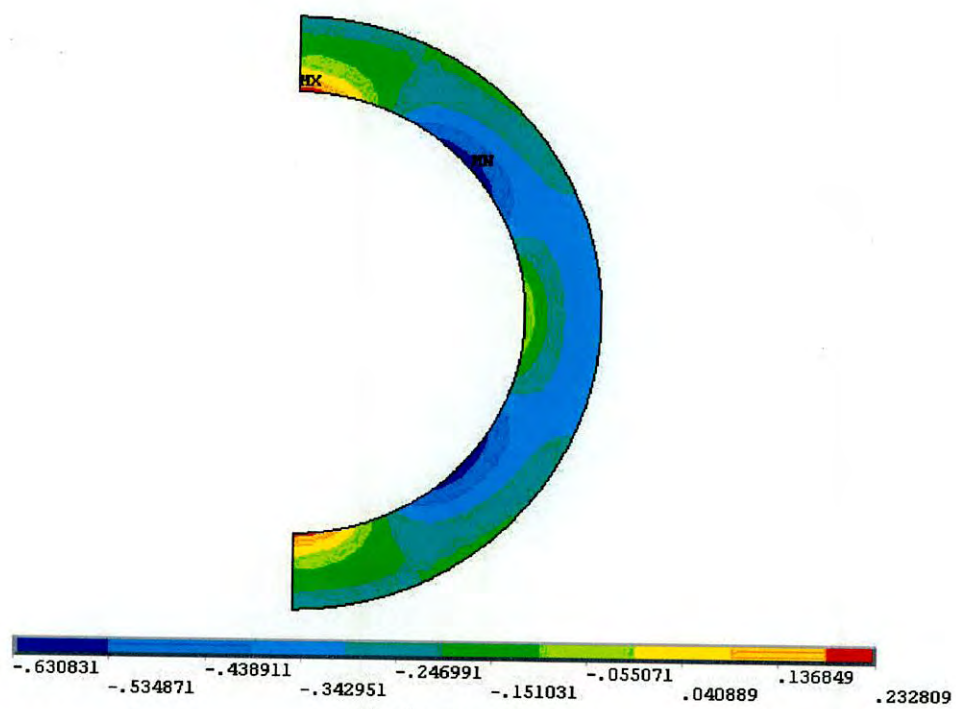
INTRODUCTION

Chapter 3 and Chapter 4 of thesis present an investigation of distribution of stresses in and around buried rigid pipe considering pipe-soil interaction. It has been revealed that interaction between the pipe and soil governed the distribution of stress within the pipe and the surrounding soil. Some contours of stress in the pipe and the surrounding soil under uniform and concentrated surface load are included in this Appendix, which will be helpful to understand the mechanism of stress distribution under pipe-soil interaction.

A-1 Contour of Stress (2-D Model)



(a) Contour for both Soil and Pipe



(b) Contour for Pipe

Figure A-1: Contour of Horizontal Stress under Uniform Surface Load

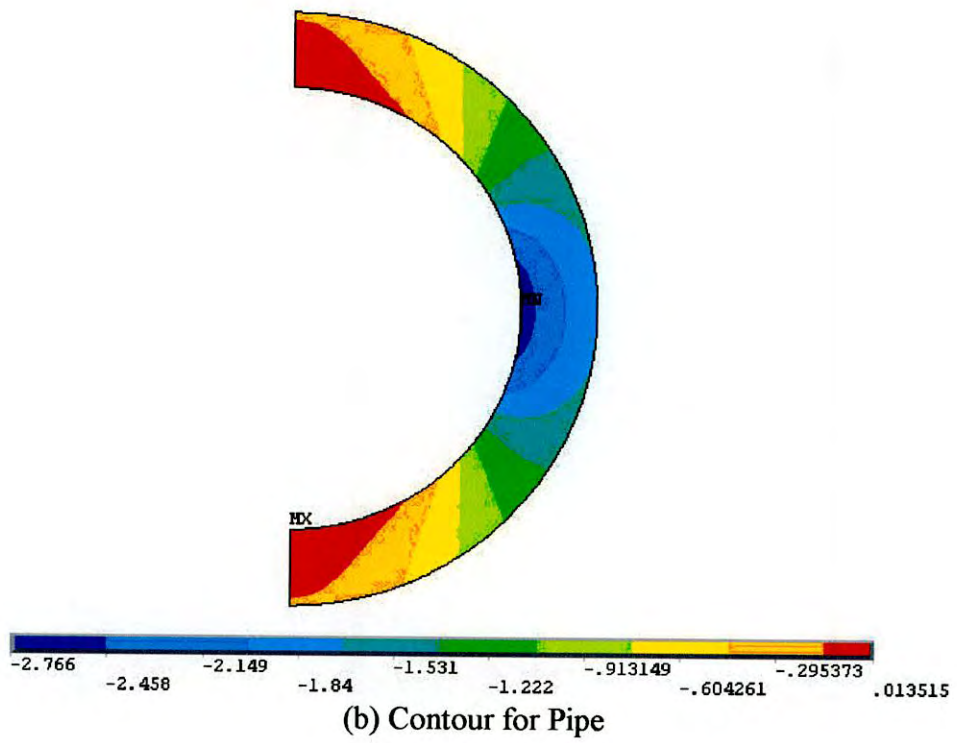
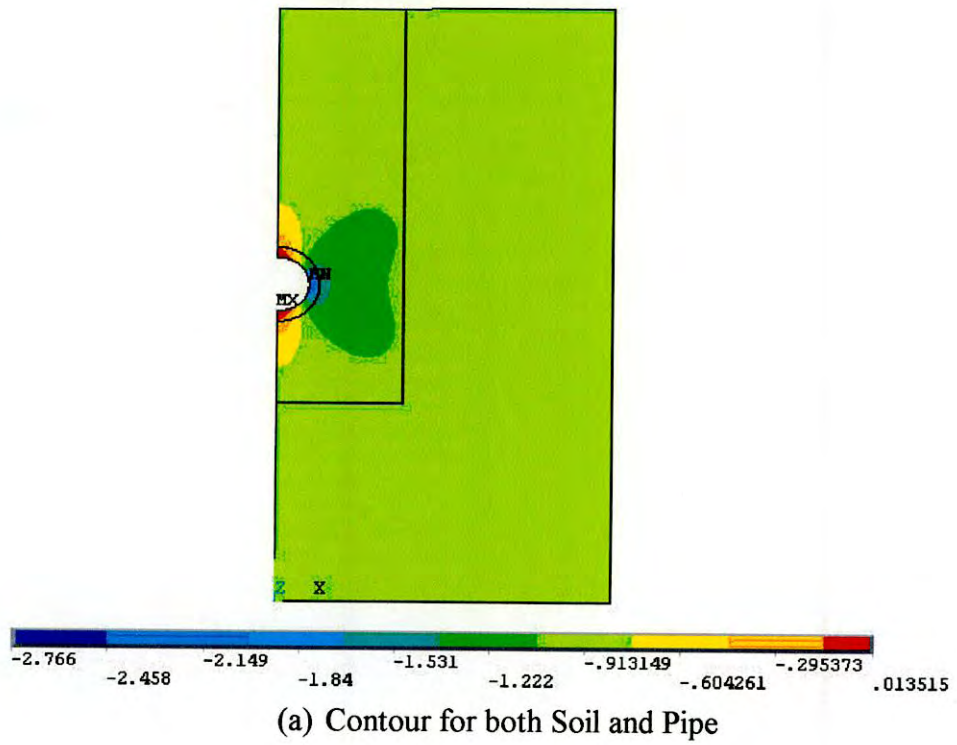


Figure A-2: Contour of Vertical Stress under Uniform Surface Load

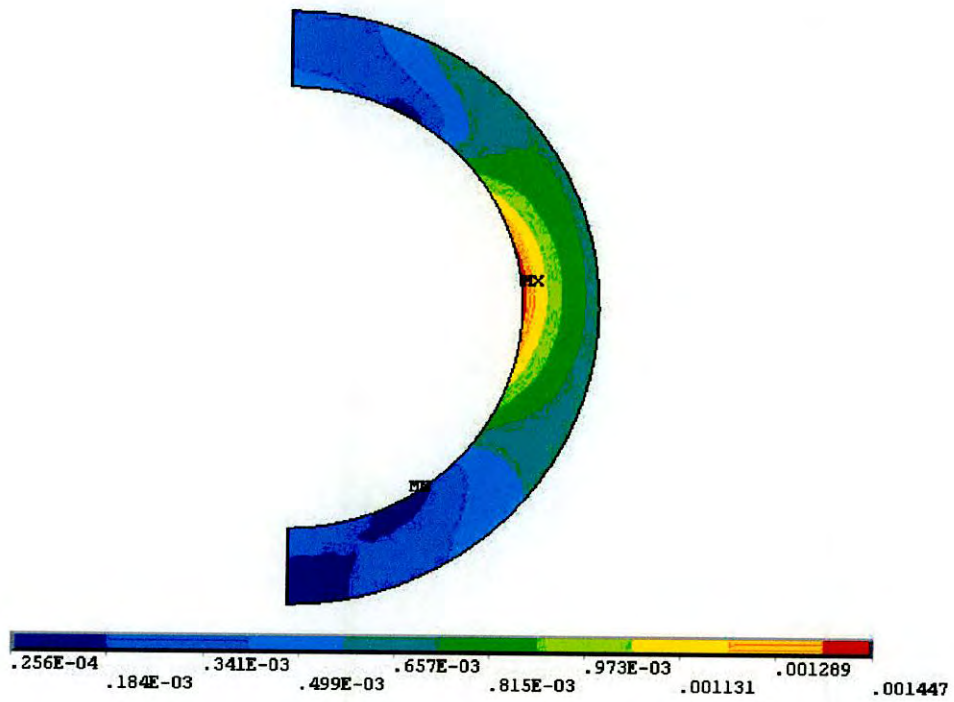
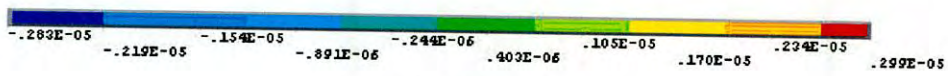
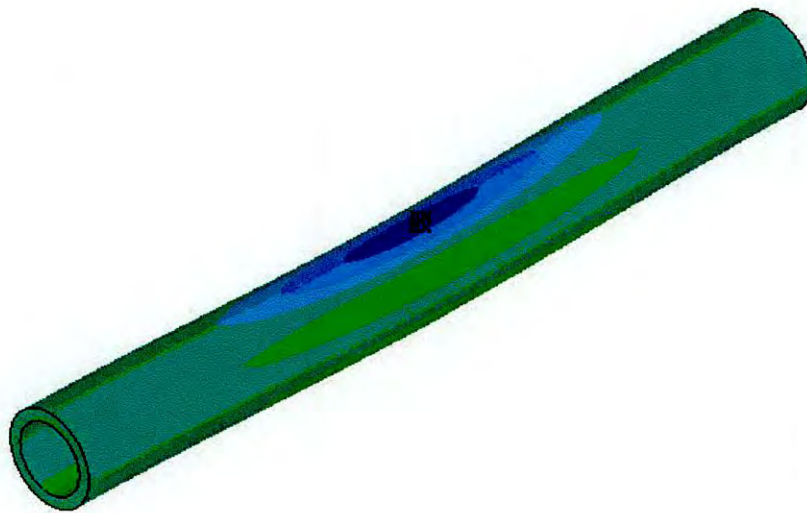
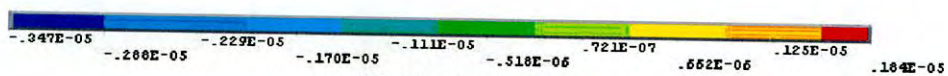
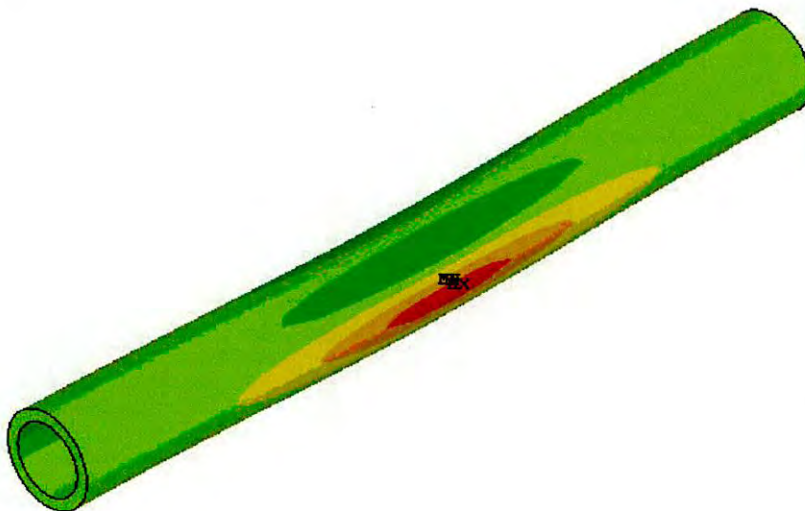


Figure A-3: Contour of Stress Intensity Developed on Pipe Wall under Uniform Surface Load

A-2 Contour of Stress (3-D Model)

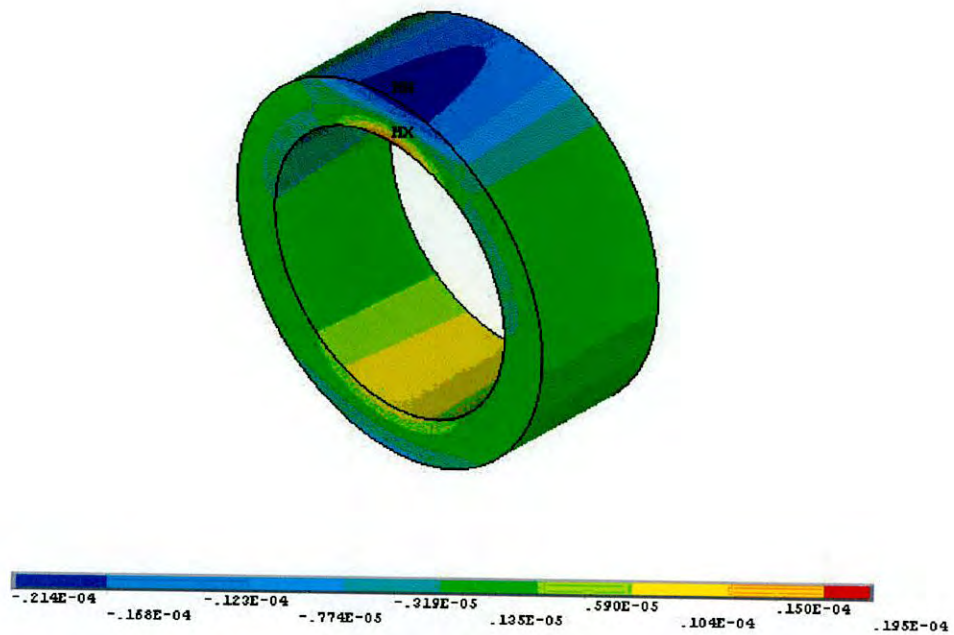


(a) Horizontal Stress

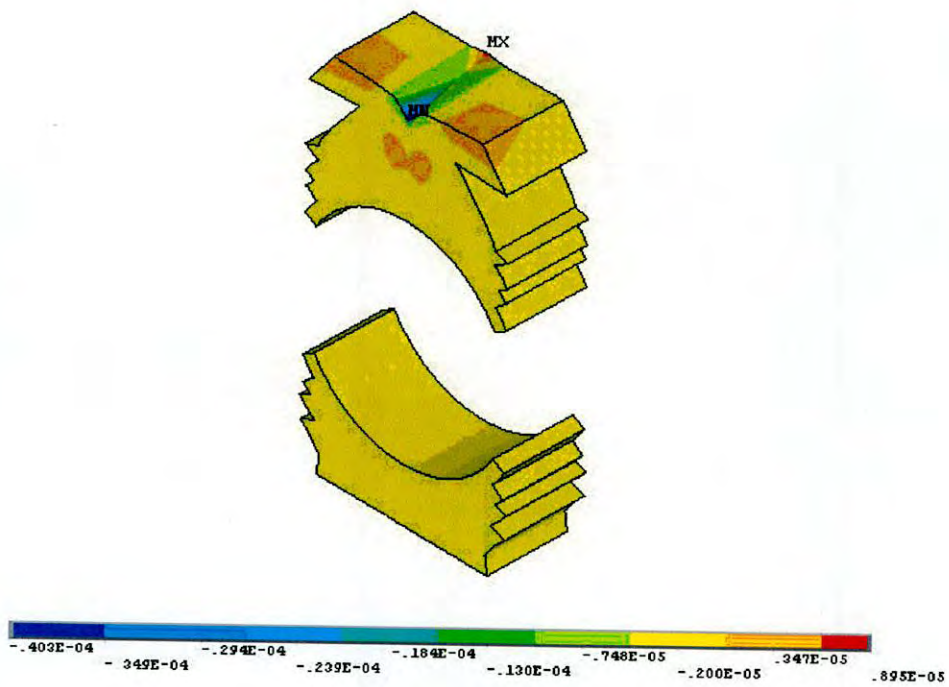


(b) Vertical Stress

Figure A-4: Contour of Stress under Concentrated Surface Load (3-D Model)



(a) Pipe Element



(b) Soil Element

Figure A-5: Contour of Horizontal Stress due to Concentrated Surface Load at Shallow Burial Condition

APPENDIX B

ANSYS CODES USED IN THE ANALYSES

INTRODUCTION

Finite element solution can be done in ANSYS using either graphically user interface or ANSYS coding. The latter one proved the most efficient for performing parametric studies. In this research, the parametric study using the finite element model was done to identify the key parameters contributing significantly to the pipe responses (i.e. thrusts, moments for rigid pipe). This section provides some of the ANSYS coding used in this research work. The codings will be helpful for future researchers using ANSYS for pipe-soil interaction analysis.

B-1 Coding Used in 2-D Simulation

```
!Unit (newton, mm)
/PREP7
!*****DEFINE NECESSARY PARAMETERS TO BE USE TO BUILD THE MODEL*****
DIA=800                ! Pipe diameter in mm
D0=DIA
TCOVER=3*DIA          ! Soil cover above pipe crown
D1=D0+DIA/2
DB=2.5*DIA             ! Soil cover below pipe invert
DS=D1+DB               ! Soil cover beside pipe springline
T=15                  ! Thickness of the interface
RECTHT=TCOVER+DIA+D0+DB ! Height of the whole section
RECTWD=DS              ! Width of the whole section
CIRRAD=DIA/2          ! Pipe radius
CIRCEN=4*CIRRAD/(3*3.14) ! Defining the centroid of the half pipe area

!*****DEFINE ALL THE ELEMENT TYPES TO BE USED*****
PIPE=1                ! Pipe element (PLANE2)
INTFC=2               ! Interface element (PLANE2)
SOIL1=3                ! Smaller meshing type of elements (PLANE2)
SOIL2=4                ! Larger meshing type of elements (PLANE2)
```

```

!*****DEFINE PIPE AS BEAM3 ELEMENT*****
!ET,PIPE,BEAM3
!R,PIPE,100,83333.33,100
!MP,EX,PIPE,20000
!MP,NUXY,PIPE,0.2

```

```

!*****DEFINE PIPE AS PLANE2 ELEMENT*****
ET, PIPE,PLANE2,,,2
MP, EX, PIPE,20
MP,NUXY,pipe,0.2

```

```

!*****DEFINE SOIL AS PLANE2 ELEMENT*****
ET,SOIL1,PLANE2,,,2
MP,EX,SOIL1,20
MP,NUXY,SOIL1,0.2

```

```

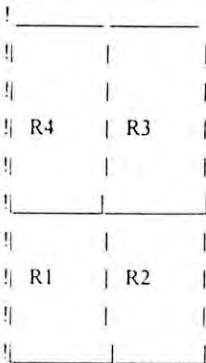
ET,SOIL2,PLANE2,,,2
MP,EX,SOIL2,20
MP,NUXY,SOIL2,0.2

```

```

!*****DEFINING AREAS*****

```



```

RECTNG,0,D1,0,DB          ! Rectangle R1
RECTNG,D1,RECTWD,0,DB     ! Rectangle R2
RECTNG,D1,RECTWD,DB,RECTHT ! Rectangle R3
RECTNG,0,D1,DB,RECTHT     ! Rectangle R4
CYL4,0,DB+D0+CIRRAD,0,-90,CIRRAD,90,0 ! Half Circular area for deduction
ALLSEL
ASEL,S,LOC,X,D1/2,D1/2    ! Select point with X=D1/2
ASEL,R,LOC,Y,DB+(D0+DIA+TCOVER)/2,DB+(D0-DIA+TCOVER)/2 ! Select point with y=DB+D0+DIA/2
*GET,A1,AREA,0,NUM,MIN    ! Get the area number A1 from the selected area
ALLSEL
ASEL,S,LOC,X,CIRCEN-DIA/4,CIRCEN+DIA/4 ! Select point with X=CIRCEN
*GET,A2,AREA,0,NUM,MIN    ! Get the area number A2 from the selected area
ASEL,ALL                  ! Select All Area for operation
ASBA,A1,A2,,DELETE,DELETE ! Delete A2 from A1
CYL4,0,DB+D0+DIA/2,DIA/2-100,-90,DIA/2,90,0 ! Circular RING area

```


ALLSEL

!***** CREATE CONTINUITY: WHEN BOLEAN OPERATION IS PERFORMED*****

NUMMRG,KP ! Merging coincident Items (key point)
NUMCMP,KP ! Compressing item numbers
NUMCMP,LINE ! Compressing item numbers (Line)
NUMCMP,AREA ! Compressing item numbers (Area)

!*****DIVIDING LINES AND THUS MESH GENERATION FOR AREA, INCLUDING MATERIAL
DEFINITION*****

LSEL,S,RADIUS,,DIA/2-100 !Select Inner Boundary line
LESIZE,ALL,,,40 !Specify Line Division Etc. for Element Size (Need)
LSEL,S,RADIUS,,DIA/2 !Select the Line on outer Boundary
LESIZE,ALL,,,40 !Number of Division of that Line
LSEL,S,RADIUS,,DIA/2-100 !Select the Inner Boundary Line
ASLL,S,0 !Select Area Containing the Line
MSHAPE, 0,2D
MSHKEY,0

!*****GENERATE PIPE ELEMENT (BEAM3)*****

TYPE,PIPE !Define element attribute directly or refer to type
REAL,PIPE
MAT,PIPE
AMESH,ALL
ALLSEL

!*****MESH GENERATION FOR AREA (R4) INCLUDING MATERIAL DEFINITION*****

!*****SMALLER MESHING TYPE OF ELEMENTS (PLANE2)*****

KSEL,S,LOC,X,0,D1
KSEL,R,LOC,Y,DB,DB+D0+DIA+TCOVER
KSEL,U,LOC,Y,DB+D0+100,DB+D0+DIA-100
LSLK,S,1
ASLL,S,1
NSLL,S,0
CM,CYLN,NODE
APLOT
SMRTSIZE,3
TYPE,SOIL1
REAL,SOIL1
MAT,SOIL1
AMESH,ALL
ALLSEL

!*****MESH GENERATION FOR AREA (R3) INCLUDING MATERIAL DEFINITION*****

!*****LARGER MESHING TYPE OF ELEMENTS (PLANE2)*****

KSEL,S,LOC,X,D1,DS
KSEL,R,LOC,Y,DB,DB+D0+DIA+TCOVER
LSLK,S,1
ASLL,S,1
NSLL,S,0

```
CM,CYLN,NODE
APLOT
SMRTSIZE,3
TYPE,SOIL2
REAL,SOIL2
MAT,SOIL2
AMESH,ALL
ALLSEL
```

```
!*****MESH GENERATION FOR AREA (R1) INCLUDING MATERIAL DEFINITION*****
```

```
!*****LARGER MESHING TYPE OF ELEMENTS (PLANE2)*****
```

```
KSEL,S,LOC,X,0,D1
KSEL,R,LOC,Y,0,DB
LSLK,S,1
ASLL,S,1
NSLL,S,0
CM,CYLN,NODE
APLOT
SMRTSIZE,3
TYPE,SOIL2
REAL,SOIL2
MAT,SOIL2
AMESH,ALL
ALLSEL
```

```
!*****MESH GENERATION FOR AREA (R2) INCLUDING MATERIAL DEFINITION*****
```

```
!*****LARGER MESHING TYPE OF ELEMENTS (PLANE2)*****
```

```
KSEL,S,LOC,X,D1,DS
KSEL,R,LOC,Y,0,DB
LSLK,S,1
ASLL,S,1
NSLL,S,0
CM,CYLN,NODE
APLOT
SMRTSIZE,3
TYPE,SOIL2
REAL,SOIL2
MAT,SOIL2
AMESH,ALL
ALLSEL
/color,ELEM,0,all
```

```
!*****APPLY BOUNDARY CONDITION (SPECIFY RESTRAINTS)*****
```

```
NSEL,S,LOC,X,0,0           !Select Nodes on Symmetry Line
NSEL,A,LOC,X,RECTWD,RECTWD !Add Selection Node on Right Vertical Line
D,ALL,UX,0                 ! UX =0 for All Node
ALLSEL
NSEL,S,LOC,Y,0,0           !Select Nodes on Bottom Line
D,ALL,UX,0                 ! UX=0 for All Node
D,ALL,UY,0                 ! UY=0 for All Node
```

ALLSEL

```
!*****APPLY LOADS*****  
!*****FOR CONCENTRATED SURFACE LOAD*****  
!LOAD=1  
!LSEL,S,LOC,Y,RECTHT,RECTHT      !SELECT THE LINE FOR LOAD  
!SFL,ALL,PRES,LOAD,LOAD          !SPECIFY SURFACE LOAD ON THAT LINE  
!ALLSEL
```

```
!*****FOR UNIFORM SURFACE LOAD*****  
NSEL,S,LOC,Y,RECTHT,RECTHT  
NSEL,R,LOC,X,0,0  
F,ALL,FY,-1  
ALLSEL
```

```
!*****SOLUTION*****  
/SOLU  
SOLVE  
FINISH
```

B-2 Coding Used in 3-D Simulation

```
!Unit (newton, mm)  
/PREP7  
!*****DEFINE ALL THE ELEMENT TYPES TO BE USED*****  
PIPE=1  
SOILB=2  
SOILO=3  
TMPE=4  
  
!*****DEFINE THE ELEMENT PROPERTIES *****  
!*****DEFINE PIPE AS SOLID45 ELEMENT*****  
ET,PIPE,SOLID45  
KEYOPT,PIPE,4,0  
MP, EX, PIPE, 20000  
MP,NUXY,PIPE,0.2  
MP,NUYZ,PIPE,0.2  
MP,NUXZ,PIPE,0.2  
  
!*****DEFINE SOIL AS SOLID45 ELEMENT*****  
ET,SOILB,SOLID45  
KEYOPT,SOILB,4,0  
MP, EX, SOILB,20  
MP,NUXY,SOILB,0.2  
MP,NUYZ,SOILB,0.2  
MP,NUXZ,SOILB,0.2  
!MP,DENS,STP,STDENS
```



```

ET,SOILO,SOLID45
KEYOPT,SOILO,4,0
MP,EX,SOILO,20
MP,NUXY,SOILO,0.2
MP,NUYZ,SOILO,0.2
MP,NUXZ,SOILO,0.2
!MP,DENS,STP,STDENS

```

```

!*****DEFINE SHELL ELEMENT*****
ET,TMPE,SHELL143
R,TMPE,0.5

```

```

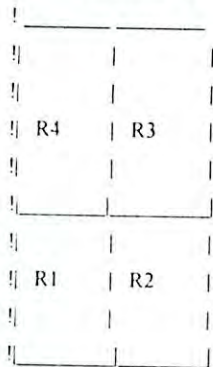
!*****DEFINE NECESSARY PARAMETERS TO BE USE TO BUILD THE MODEL*****
PDIA=800 ! Pipe outer diameter
PTHK=100 ! Pipe thickness
PIDIA=PDIA-2*PTHK ! Pipe inner diameter
W1=1850 ! Width of inner core symmetric soil model
W2=3200 ! Total width of the symmetric model
H1=2650 ! Height of inner core soil model
H2=5350 ! Height of total soil model
Z=2400 ! Model width along the longitudinal direction
TWIDTH=W2 ! Total width of the symmetric model
THT=H2 ! Height of total soil model

```

```

!*****DEFINING AREAS*****

```



```

RECTNG,0,W1,0,H2-H1 !Rectangle R1
RECTNG,W1,TWIDTH,0,H2-H1 !Rectangle R2
RECTNG,W1,TWIDTH,H2-H1,THT !Rectangle R3
RECTNG,0,W1,H2-H1,THT !Rectangle R4

```

```

CYL4,0,H2-H1+100+PDIA/2,0,-90,PDIA/2,90,0 !Half Circular area for deduction

```

```

KSEL,S,LOC,X,0,W1
KSEL,R,LOC,Y,H2-H1,H2
KSEL,U,LOC,Y,H2-H1+100,H2-H1+100+PDIA
LSLK,S,1
ASLL,S,1

```

```

*GET,A1,AREA,0,NUM,MIN ! Get the area number A1 from the selected area
KSEL,S,LOC,X,0,0

```

```

KSEL,R,LOC,Y,H2-H1+100,H2-H1+100+PDIA
LSLK,S,1
ASLL,S,1
*GET,A2,AREA,0,NUM,MIN           ! Get the area number A2 from the selected area
ASEL,ALL                         ! Delete A2 from A1
ASBA,A1,A2,,DELETE,DELETE       ! Delete A2 from A1
ALLSEL
CYL4,0,H2-H1+100+PDIA/2,PIDIA/2,-90,PDIA/2,90 !Add pipe as circular ring area
ALLSEL

```

!***** CREATE CONTINUITY: WHEN BOLEAN OPERATION IS PERFORMED*****

```

NUMMRG,KP                        ! Merging coincident Items (key point)
NUMCMP,KP                        ! Compressing item numbers
NUMCMP,LINE                       ! Compressing item numbers (Line)
NUMCMP,AREA                       ! Compressing item numbers (Area)

```

!*****DIVIDING LINES AND THUS MESH GENERATION FOR AREA, INCLUDING MATERIAL

DEFINITION*****

```

KSEL,S,LOC,Y,H2-H1+100+PDIA,H2
KSEL,R,LOC,Z,0,0
KSEL,R,LOC,X,0,0
LSLK,S,1
LESIZE,ALL,,,20
ALLSEL

```

```

KSEL,S,LOC,X,0,0
KSEL,R,LOC,Y,0,H2-H1
KSEL,R,LOC,Z,0,0
LSLK,S,1
LESIZE,ALL,,,20
ALLSEL

```

```

KSEL,S,LOC,Y,H2-H1,H2-H1
KSEL,R,LOC,Z,0,0,0
KSEL,R,LOC,X,0,W1
LSLK,S,1
LESIZE,ALL,,,20,-3
ALLSEL

```

```

KSEL,S,LOC,X,0,0
KSEL,R,LOC,Y,H2-H1,H2-H1+100
KSEL,R,LOC,Z,0,0
LSLK,S,1
LESIZE,ALL,,,2
ALLSEL

```

```

KSEL,S,LOC,X,0,0
KSEL,R,LOC,Y,H2-H1+100,H2-H1+PDIA+100
LSLK,S,1
*GET,LMIN,LINE,0,NUM,MIN

```

```

*GET,LMAX,LINE,0,NUM,MAX
*GET,LCNT,LINE,0,COUNT
*DIM,LLNTH,,LCNT
*DIM,LNO,,LCNT
LNO(1)=LMIN
*DO,I,1,LCNT
*IF,I,EQ,LCNT,EXIT
*GET,LLNTH(I),LINE,LNO(I),LENG
LNO(I+1)=LSNEXT(LNO(I))
*ENDDO
ASLL,S,1
APLOT
*DO,I,1,LCNT
*IF,I,EQ,LCNT,THEN
*IF,LLNTH(I),LT,LLNTH(I-1),THEN
LESIZE,LNO(I),,2
*ELSE
LESIZE,LNO(I),,20
*ENDIF
*ELSE
*IF,LLNTH(I),LT,LLNTH(I+1),THEN
LESIZE,LNO(I),,2
*ELSE
LESIZE,LNO(I),,20
*ENDIF
*ENDIF
*ENDDO
MSHAPE,0,2D
MSHKEY,0
TYPE,TMPE
MAT,TMPE
REAL,TMPE
AMESH,ALL
ALLSEL

NUMMRG,KP                ! Merging coincident Items (key point)
NUMCMP,KP                ! Compressing item numbers
NUMCMP,LINE              ! Compressing item numbers (Line)
NUMCMP,AREA              ! Compressing item numbers (Area)

KSEL,S,LOC,X,0,W1
KSEL,R,LOC,Y,H2-H1,H2
KSEL,U,LOC,Y,H2-H1+100+PTHK,H2-H1+100+PDIA-PTHK
LSLK,S,1
ASLL,S,1
NSLL,S,0
CM,CYLN,NODE
APLOT
SMRTSIZE,5                ! Meshing parameters for automatic (smart) element sizing
TYPE,TMPE

```


MAT,TMPE
REAL,TMPE
MSHAPE,0,2D
MSHKEY,0
AMESH,ALL
ALLSEL

NSEL,ALL
*GET,NMAX,NODE,0,NUM,MAX
CMSEL,S,CYLN
LOCAL,11,1,0,H2-H1+PDIA/2,0
CSYS,11
CSYS,0
TYPE,TMPE
MAT,TMPE
REAL,TMPE
ASEL,ALL
KSEL,S,LOC,X,0,W1
KSEL,R,LOC,Y,0,H2-H1
CM,LOWKP,KP
CM,HACKP,KP
LSLK,S,1
ASLL,S,1
SMRTSIZE,5
TYPE,TMPE
MAT,TMPE
REAL,TMPE
MSHKEY,0
MSHAPE,0,2D
AMESH,ALL
ALLSEL

! Meshing parameters for automatic (smart) element sizing

KSEL,S,LOC,X,W1,W2
KSEL,R,LOC,Y,0,H2-H1
CM,LOWKP,KP
CM,HACKP,KP
LSLK,S,1
ASLL,S,1
SMRTSIZE,5
TYPE,TMPE
MAT,TMPE
REAL,TMPE
MSHKEY,0
MSHAPE,0,2D
AMESH,ALL
ALLSEL

! Meshing parameters for automatic (smart) element sizing

KSEL,S,LOC,X,W1,W2
KSEL,R,LOC,Y,H2-H1,H2
LSLK,S,1

ASLL,S,1	
SMRTSIZE,5	
TYPE,TMPE	! Meshing parameters for automatic (smart) element sizing
MAT,TMPE	
REAL,TMPE	
MSHKEY,0	
MSHAPE,0,2D	
AMESH,ALL	
ALLSEL	
NUMMRG,KP	! Merging coincident Items (key point)
NUMCMP,KP	! Compressing item numbers
NUMCMP,LINE	! Compressing item numbers (Line)
NUMCMP,AREA	! Compressing item numbers (Area)
NUMMRG,NODE	
NUMMRG,ELEM	
NUMCMP,NODE	
NUMCMP,ELEM	
KSEL,S,LOC,X,0,W2	
KSEL,R,LOC,Y,0,H2	
LSLK,S,1	
ASLL,S,1	
TYPE,SOILB	
MAT,SOILB	
ESIZE,,8	
VEXT,ALL,,,,-2400	! Generates additional volumes by extruding areas.
NVGEN=3	
VSEL,ALL	
VGEN,NVGEN,ALL,,,,-2400	
KSEL,S,LOC,X,0,W2	
KSEL,R,LOC,Y,0,H2-H1	
KSEL,A,LOC,X,W1,W2	
LSLK,S,1	
ASLL,S,1	
VSLA,S,1	
CM,STVOL,VOLU	
ESLV,S	
EMODIF,ALL,TYPE,SOILO	
EMODIF,ALL,MAT,SOILO	
ALLSEL	
KSEL,S,LOC,X,0,0	
KSEL,R,LOC,Y,H2-H1+100,H2-H1+100+PDIA	
LSLK,S,1	
ASLL,S,1	
VSLA,S,1	

CM,STVOLI,VOLU
ESLV,S
EMODIF,ALL,TYPE,PIPE
EMODIF,ALL,MAT,PIPE
ALLSEL

ESEL,S,TYPE,,TMPE
EDELE,ALL
ALLSEL
ESEL,S,TYPE,,TMPE
ACLEAR,ALL
ALLSEL
VSYMM,X,ALL
ALLSEL

NUMMRG,KP
NUMCMP,KP
NUMMRG,NODE
NUMMRG,ELEM
NUMCMP,NODE
NUMCMP,ELEM
ALLSEL

/SOLU
NSEL,S,LOC,X,-W2,W2
NSEL,R,LOC,Y,0,0
D,ALL,ALL
ALLSEL
NSEL,S,LOC,Z,-2400*3,-2400*3
D,ALL,UZ
ALLSEL
NSEL,S,LOC,Z,0,0
D,ALL,UZ
ALLSEL
NSEL,S,LOC,X,-W2,-W2
NSEL,A,LOC,X,W2,W2
D,ALL,UX
ALLSEL

!/color,ELEM,0,all
/ESHAPE,1
EPLOT
/VIEW,1,1,1,1
/ANG,1
/REP,FAST

NSEL,S,LOC,Y,H2,H2,H2
NSEL,R,LOC,X,0,0,0
NSEL,R,LOC,Z,-3600,-3600,-3600
F,ALL,FY,-1

ALLSEL
SOLVE

/POST1

!*****CIRCUMFERENTIAL STRESS EXTRACTION*****

ALLSEL

NSEL,S,LOC,Z,-3600,-3600,-3600

NSEL,R,LOC,X,0,400

NSEL,R,LOC,Y,2800,3600

/PNUM,NODE,1

NPLOT

!*****VERTICAL STRESS ON SOIL OVER CROWN*****

ALLSEL

NSEL,S,LOC,Z,-3600,-3600,-3600

NSEL,R,LOC,X,0,0

NSEL,R,LOC,Y,3600,3600+800

/PNUM,NODE,1

NPLOT

!*****HORIZONTAL STRESS DISTRIBUTION ALONG CROWN LEVEL IN TRANSVERSE DIRECTION*****

ALLSEL

NSEL,S,LOC,Z,-3600,-3600,-3600

NSEL,R,LOC,Y,3600,3600

/PNUM,NODE,1

NPLOT

!*****HORIZONTAL STRESS DISTRIBUTION ALONG CROWN LEVEL IN LONGITUDINAL DIRECTION*****

ALLSEL

NSEL,S,LOC,Z,0,-7200

NSEL,R,LOC,Y,3600,3600

NSEL,R,LOC,X,0,0

/PNUM,NODE,1

NPLOT

